

A BRIGHTER METHOD TO ILLUMINATE THE DARK SIDE OF  
ADHESION G PROTEIN-COUPLED RECEPTORS:  
DETECTION OF THE ADGRG1 DIMERS BY  
BIOLUMINESCENCE RESONANCE ENERGY TRANSFER (BRET)

A THESIS SUBMITTED TO  
THE GRADUATE SCHOOL OF NATURAL AND APPLIED SCIENCES  
OF  
MIDDLE EAST TECHNICAL UNIVERSITY

BY

MERVE MURAT

IN PARTIAL FULFILLMENT OF THE REQUIREMENTS  
FOR  
THE DEGREE OF MASTER OF SCIENCE  
IN  
MOLECULAR BIOLOGY AND GENETICS

SEPTEMBER 2021



Approval of the thesis:

**A BRIGHTER METHOD TO ILLUMINATE THE DARK SIDE OF  
ADHESION G PROTEIN-COUPLED RECEPTORS:  
DETECTION OF THE ADGRG1 DIMERS BY  
BIOLUMINESCENCE RESONANCE ENERGY TRANSFER (BRET)**

submitted by **MERVE MURAT** in partial fulfillment of the requirements for the degree of **Master of Science in Molecular Biology and Genetics, Middle East Technical University** by,

Prof. Dr. Halil Kalıpçılar  
Dean, Graduate School of **Natural and Applied Sciences**

Prof. Dr. Ayşe Gül Gözen  
Head of the Department, **Biological Sciences**

Assoc. Prof. Dr. Çağdaş Devrim Son  
Supervisor, **Biological Sciences, METU**

Dr. Orkun Cevheroğlu  
Co-Supervisor, **Stem Cell Institute, Ankara University**

**Examining Committee Members:**

Assoc. Prof. Dr. Tülin Yanık  
Biological sciences, METU

Assoc. Prof. Dr. Çağdaş Devrim Son  
Biological Sciences, METU

Assoc. Prof. Dr. Pınar Baydın  
Stem Cell Institute, Ankara University

Date: 07.09.2021

**I hereby declare that all information in this document has been obtained and presented in accordance with academic rules and ethical conduct. I also declare that, as required by these rules and conduct, I have fully cited and referenced all material and results that are not original to this work.**

Name, Last name : Merve Murat

Signature :

## ABSTRACT

### **A BRIGHTER METHOD TO ILLUMINATE THE DARK SIDE OF ADHESION G PROTEIN-COUPLED RECEPTORS: DETECTION OF THE ADGRG1 DIMERS BY BIOLUMINESCENCE RESONANCE ENERGY TRANSFER (BRET)**

Murat, Merve  
Master of Science, Molecular Biology and Genetics  
Supervisor: Assoc. Prof. Dr. Çağdaş Devrim Son  
Co-Supervisor: Dr. Orkun Cevheroğlu

September 2021, 104 pages

G protein-coupled receptors (GPCRs) form oligomeric complexes in living cells, and these complex structures affect the receptor maturation, trafficking, and signaling processes. Adhesion G protein-coupled receptors (aGPCRs), the second-largest sub-family of GPCRs, interact with extracellular matrix and ligands on the adjacent cell surface to modulate tissue and organ development. However, it is still unclear whether aGPCRs interact with each other. In this study, ADGRG1 was used as a model aGPCR to investigate the aGPCR dimerization in living cells using Bioluminescence Resonance Energy Transfer (BRET). BRET donor (NLuc) or acceptor (EGFP) tagged ADGRG1 receptors at various positions at C-terminus were expressed in HEK 293 cells. The cellular localizations of tagged receptors verified by laser scanning confocal imaging. The expression of C-terminally tagged constructs were determined using Western blot technique and their function was assessed with a bioluminescence based Serum Response Element (SRE) assay. The EGFP-tagged ADGRG1 constructs were all functional with elevated SRE activity as in the case for WT, and N-terminally truncated receptors. Since both NanoLuc

(NLuc) and *Renilla luciferase* (RLuc) oxidize coelenterazine, NLuc-tagged ADGRG1 receptors could not be tested for the function using this method. However, as the tagging position was same and the tag NLuc was smaller in size these constructs were assumed to be functional. Various constructs of ADGRG1 tagged with NLuc were co-transfected with ADGRG1 EGFP constructs to determine the *in vivo* dimerization of ADGRG1. BRET resulting from the interacting receptor dimers was measured. Observed BRET increased in constructs tagged after 667<sup>th</sup> amino acid at C-terminus compared to the constructs with NLuc and EGFP appended at the end of C-terminus. The results given herein, suggest for the first time the homodimerization and may be oligomerization of ADGRG1, an aGPCR.

Keywords: Adhesion GPCR, ADGRG1, GPR56, Dimerization, BRET

## ÖZ

### **ADEZYON G PROTEİNE KENETLİ RESEPTÖRLERİN KARANLIK TARAFINI AYDINLATACAK PARLAK METOT: BİYOLÜMİNESANS REZONANS ENERJİ TRANSFERİ (BRET) İLE ADGRG1 DİMERLERİNİN GÖSTERİLMESİ**

Murat, Merve  
Yüksek Lisans, Moleküler Biyoloji ve Genetik  
Tez Yöneticisi: Doç. Dr. Çağdaş Devrim Son  
Ortak Tez Yöneticisi: Dr. Orkun Cevheroğlu

Eylül 2021, 104 sayfa

G proteine kenetli reseptörler (GPKR), canlı hücrelerde oligomerik yapılar oluşturur ve bu kompleks yapılar reseptörün matürasyonu, trafiği ve sinyalizasyon mekanizmalarını etkiler. GPKR'lerin en büyük ikinci alt-ailesi olan adezyon G proteine kenetli reseptörler de (aGPKR), hücreler arası matriks ve komşu hücre yüzeyinde bulunan ligandlarla doku ve organ gelişimine etki etmek için etkileşime girerler. Fakat, aGPKR'lerin birbirleri ile etkileşime girip girmediği hala belirsizdir. Bu çalışmada, aGPKR'lerin dimerizasyonun canlı hücrelerde Biyoluminesan Rezonans Enerji Transferi (BRET) ile araştırılması için model bir aGPKR olan ADGRG1 kullanılmıştır. BRET donörü (NLuc) ya da akseptörü (EGFP) ile C-terminalindeki çeşitli pozisyonlardan işaretlenmiş ADGRG1 reseptörlerinin HEK 293 hücrelerinde ifade edilmesi sağlanmıştır. İşaretli reseptörlerin hücre içi lokalizasyonları lazer taramalı konfokal mikroskop ile doğrulanmıştır. C-terminalinden işaretli konstraktların hücre içi ifadeleri Western blotlama yöntemi ile belirlenmiş ve konstraktların işlevselliği biyoluminesans temelli Serum Response Element (SRE) Assay ile belirlenmiştir. EGFP ile işaretli bütün ADGRG1

konstraktlarının, WT ve N-terminalinden kesilmiş reseptörlerde olduğu gibi fonksiyonel oldukları gösterilmiştir. NanoLuc (NLuc) ve *Renilla luciferase* (RLuc)'in ikisi de coelenterazine'i okside ettikleri için, NLuc işaretli ADGRG1 reseptörleri SRE yöntemi ile test edilememiş ancak işaretlemeler aynı bölgeden yapıldığı için daha küçük bir tag olan NLuc ile işaretli reseptörler de fonksiyonel olarak sayılmıştır. ADGRG1 reseptörünün *in vivo* dimerizasyonunun saptanması için NLuc ile işaretli ADGRG1 konstraktları, EGFP ile işaretli ADGRG1 konstraktları ile birlikte transfekte edilmişlerdir. Etkileşime giren reseptörlerden dolayı meydana gelen BRET ölçülmüştür. C-terminalinden işaretli reseptörler ile karşılaştırıldığında, C-terminalindeki 667'inci amino asiti ardından işaretlenmiş ADGRG1 reseptörlerinde BRET artmıştır. Bu çalışmada belirtilen sonuçlar, aGPKR'lerden biri olan ADGRG1'in homodimerizasyonuna hatta oligomerizasyonuna ilişkin ilk kez bilgi sağlamaktadır.

Anahtar Kelimeler: Adezyon GPKR, ADGRG1, GPR56, Dimerizasyon, BRET

To Uğur, who is my other part and serves as the driving force behind me.

## ACKNOWLEDGMENTS

I would like to show my special regards to my supervisor Assoc. Prof. Dr. Çağdaş Devrim Son and co-supervisor Dr. Orkun Cevheroğlu, who guided me to be a professional in academia throughout my research. I am deeply grateful for their priceless advice, patience and our friendly conversation and meetings during my Master study which force me to think unconventionally. Dr. Son's office door was always open whenever I had a trouble spot about my research, and I would also like to express my thanks to him for his empathy and great sense of humor during our meetings. Without Dr. Cevheroğlu's dedicated involvement and assistance in every step, this thesis would have never been finalized.

Many thanks to Assoc. Prof. Dr. Pınar Baydın for her advice, comments, and suggestions. It gives me a great pleasure in acknowledging her patient support which improves the thesis.

I am indebted to my colleagues in Dr. Son's lab, particularly to Sara Mingu, Nil Demir, Dilara Öğütçü and Berkay Demirbaş for their support, fellowship and wonderful collaboration. Each of them has provided me professional and personal assistance over these past three years. I also appreciate for a cherished time spent together in and outside the lab. I consider it an honor to work with them.

I am thankful to Scientific and Technological Research Council of Turkey (TUBITAK, grant no. 118Z590) for the financial assistance, and my gratitude extend to Ankara University Stem Cell Institute and all its staff to give me the opportunity to work in there.

Most importantly, the person with a remarkable indirect contribution to the thesis is my lovely partner Uğur Aydoğan whose love and continuing support are with me in whatever I need. I could not go on this adventure without he and our family members, Sütlaç, Cheddar and Mari. I would also like to express my thanks his and my family

members, Yeter Demirtuđ, Anıl Murat, Döndü Aydođan, Metin Aydođan and Burcu Soylu for their constant encouragement and unwavering love.

## TABLE OF CONTENTS

ABSTRACT .....	v
ÖZ.....	vii
ACKNOWLEDGMENTS .....	x
TABLE OF CONTENTS .....	xii
LIST OF TABLES .....	xv
LIST OF FIGURES .....	xvii
LIST OF ABBREVIATIONS .....	xxii
CHAPTERS	
1 INTRODUCTION .....	1
1.1 G protein-coupled receptors.....	1
1.2 Adhesion G protein-coupled receptors .....	2
1.2.1 Classification and nomenclature of adhesion G protein-coupled receptors .....	2
1.2.2 The general structure of adhesion G protein-coupled receptors.....	4
1.2.3 Activation and signaling mechanisms of adhesion G protein-coupled receptors .....	6
1.2.4 Overview of adhesion G protein-coupled Receptor 56 (ADGRG1/GPR56) .....	8
1.3 G protein-coupled receptor oligomerization.....	18
1.4 Bioluminescence resonance energy transfer (BRET).....	19
1.4.1 The theory behind BRET.....	24

1.4.2	NanoBRET system.....	26
1.4.3	Quantitative BRET assays: BRET saturation assay.....	27
1.5	Aim of the thesis .....	29
2	MATERIALS AND METHODS.....	31
2.1	Construction of fluorescent or bioluminescent-tagged ADGRG1 .....	31
2.2	Truncation of ADGRG1 .....	38
2.3	Cell culture .....	41
2.3.1	HEK 293 maintenance, passage, seeding into culture vessels.....	41
2.3.2	Transient plasmid transfection of HEK 293 cells .....	42
2.4	Laser scanning confocal imaging.....	43
2.5	Western blotting .....	44
2.5.1	Sample preparation: cell lysis and protein harvesting .....	44
2.5.2	Cell loading and running.....	44
2.5.3	Protein transfer .....	44
2.5.4	Blocking and antibody probing.....	45
2.6	Serum Response Element (SRE)-dual-luciferase reporter assay .....	46
2.7	NanoBRET assay .....	47
2.8	BRET saturation assay .....	48
3	RESULTS .....	49
3.1	Construction of fluorescent or bioluminescent-tagged receptors.....	49
3.2	Truncation of ADGRG1 .....	52
3.3	Laser scanning confocal microscopy .....	53
3.4	Western blotting .....	54
3.5	SRE-dual luciferase reporter assay.....	56

3.6	NanoBRET assay .....	58
3.7	BRET saturation assay .....	60
4	DISCUSSION.....	63
4.1	Construction of fluorescent or bioluminescent-tagged receptors .....	63
4.2	Truncation of ADGRG1 .....	64
4.3	Laser scanning confocal microscopy .....	64
4.4	Western blotting.....	65
4.5	SRE-dual luciferase reporter assay .....	65
4.6	NanoBRET assay .....	66
4.7	BRET saturation assay.....	67
5	CONCLUSION .....	69
	REFERENCES .....	73
	APPENDICES	
A.	Bacterial medium preparation.....	93
B.	Solutions and buffers for Western blotting.....	94
C.	Coding sequences of ADGRG1 constructs.....	96

## LIST OF TABLES

### TABLES

Table 1.1. The comparison of different BRET techniques with donor and acceptor pairs and corresponding emission peaks. (Created using BioRender.com.).....	23
Table 2.1 Primer pair used for amplification of EGFP and NLuc cDNAs. Each primer is extended in a 5' to 3' direction. EGFP or NLuc sequences are denoted by upper-case letters, and ADGRG1 homologous sequence is indicated by lower-case letters. Forward primers lack stop codon not to hamper the expression of EGFP or NLuc protein which was positioned right after the ADGRG1. Reverse primers for EGFP or NLuc protein positioned between amino acids 667-668 lack stop codon. ....	32
Table 2.2. The first PCR components and conditions for the amplification of EGFP and NLuc cDNAs.....	33
Table 2.3. Insertional PCR components and conditions to fuse amplified EGFP or Nluc cDNAs into ADGRG1 cDNA in pcDNA3.1(+). The PCR was set as the molar ratio of ADGRG1 plasmid to amplified EGFP, or Nluc is 1:20.....	34
Table 2.4. DpnI digestion protocol. ....	34
Table 2.5. Primer pair used for colony PCR. Each primer is extended in a 5' to 3' direction. ....	35
Table 2.6. Colony PCR components and conditions. ....	35
Table 2.7. Double restriction enzyme digestion protocol for confirmation of the positive inserts. ....	36
Table 2.8. Primer pair used in PCR for truncation of ADGRG1 at position 342. Each primer extended in a 5' to 3' direction.....	39
Table 2.9. PCR components and conditions to truncate ADGRG1 at position 342. ....	39
Table 2.10. Double restriction enzyme digestion protocol. ....	40
Table 2.11. Ligation reaction conditions. ....	40
Table 2.12. HEK 293 seeding density into cell culture vessels used.....	42

Table 2.13. Reagents used in transient transfection of HEK 293 cells according to culture vessels.....	43
Table 2.14. Substrate preparation for luciferase reporter assay. ....	47

## LIST OF FIGURES

### FIGURES

- Figure 1.1. Illustration of the aGPCR subfamilies with the latest terminology, classified according to their characteristic extracellular termini architecture. Calx, calnexin; CUB, Cs1 and Csr/Uegf/BMP1; EGF\_CA, calcium-binding EGF; EPTP, epitempin; HRM, hormone receptor motif; I-set, immunoglobulin I-set domain; LRR, leucine-rich repeat; PTX, pentraxin; RBL, rhamnose-binding lectin; SEA, sperm protein, enterokinase, agrin module; TSP, thrombospondin. Adapted from [17]. ..... 3
- Figure 1.2. Representation of an adhesion G protein-coupled Receptor structure. (A) aGPCR is generally composed of three main parts, ECD, 7-TM, and ICD. After the GPS autoproteolysis of receptors, they are divided into two parts, including CTF and NTF. (B) The GAIN domain is highly sophisticated and unique for aGPCRs. It contains an N-terminal subdomain A and a subdomain B that has both N-terminal and C-terminal portions. Adapted from [16]. ..... 5
- Figure 1.3. Activation mechanisms of aGPCRs. (A) An aGPCR interaction with a soluble ligand or proteins in the extracellular matrix acting as ligand leads to ECD-mediated receptor activation. (B) The Shedding model involves the release of NFT and subsequent receptor activation by the *Stachel* peptide sequence. (C) Cell-to-cell interaction between other membrane proteins or aGPCRs, resulting in NFT dissociation. (Created using BioRender.com.) ..... 7
- Figure 1.4. Representation of ADGRG1 receptor structure. ICR, intracellular region/domain. Adapted from [50]. ..... 9
- Figure 1.5. ADGRG1 signaling in different physiological systems. (A) ADGRG1 signaling via collagen III in neurons. (B) ADGRG1 signaling via apigenin in skeletal muscle cells. (C) ADGRG1 signaling via TG2 and laminin-111 in OPCs. (D) ADGRG1 signaling via dystroglycan and lectin in Schwann cells. (E) ADGRG1 signaling via Hobit in natural killer (NK) cells. The dotted lines and the solid lines indicate indirect and direct pathways, respectively. Adapted from [87]. ..... 12

Figure 1.6. ADGRG1 signaling in different pathological conditions. (A) ADGRG1 signaling in colorectal cancer cells. (B) ADGRG1 signaling in melanoma cells. (C) ADGRG1 signaling in fibrosarcoma cells. (D) ADGRG1 signaling in glioblastoma cells. The dotted lines and the solid lines indicate indirect and direct pathways, respectively. Adapted from [87]. ..... 16

Figure 1.7. A brief representation of native BRET. (A) Luciferase catalyzes substrate oxidation and emits light if the fluorescent protein is far enough. (B) Luciferase transfers its energy to the fluorescent protein if it is in close proximity. (Created using BioRender.com.) ..... 20

Figure 1.8. Emission wavelengths of NanoLuc, Renilla, and Firefly luciferases. The maximum emission wavelength of NanoLuc is 460 nm; the maximum emission wavelength of *Renilla* luciferase is 480 nm; the maximum emission wavelength of Firefly luciferase is 565 nm. Adapted from promega.com. .... 21

Figure 1.9. Excitation and emission wavelengths of enhanced GFP. The maximum excitation wavelength of EGFP is 488 nm; the maximum emission wavelength of *EGFP* is 507 nm. (FPbase ID: R9NL8) Adapted from fpbase.org. .... 22

Figure 1.10. Simplified Jablonski Diagram. Adapted from leica-microsystems.com. .... 24

Figure 1.11. Stoke's shift. It indicates the difference between the excitation and the emission wavelength maxima of a fluorophore. Adapted from leica-microsystems.com. .... 25

Figure 1.12. Cartoon of the NanoBRET method. Acceptor (fluorescent) protein cannot be excited through furimazine oxidation catalyzed by NLuc if two proteins do not interact with each other. In the case of interaction, photons released after oxidation reaction excite the acceptor, resulting in a NanoBRET signal. (Created using BioRender.com.) ..... 26

Figure 1.13. Theoretical saturation curves.  $BRET_{50}$ , a ratio of the receptor concentration where the curve reaches half-maximum. Adapted from [167]. ..... 28

Figure 2.1. The pcDNA3.1(+) plasmid carrying full-length human ADGRG1 (GPR56) between KpnI and XbaI restriction enzymes. .... 31

Figure 2.2. Representation of insertional PCR method. EGFP insertion into the C-terminus of the ADGRG1 cDNA is given as an example. (Created using BioRender.com.) ..... 32

Figure 2.3. The representation of ADGRG1-Ct-EGFP or -Ct-NLuc fusion cDNAs in pcDNA3.1(+). (A) EGFP cDNA was amplified by PCR, then cloned into pcDNA3.1(+), right after ADGRG1 C-terminus. (B) Nluc cDNA was amplified by PCR, then cloned into pcDNA3.1(+), right after ADGRG1 C-terminus. (Created using BioRender.com.) ..... 37

Figure 2.4. The representation of ADGRG1-Ct-L-EGFP or -Ct-L-NLuc fusion cDNAs in pcDNA3.1(+). (A) L-EGFP cDNA was amplified by PCR, then cloned into pcDNA3.1(+), right after ADGRG1 C-terminus. (B) L-Nluc cDNA was amplified by PCR, then cloned into pcDNA3.1(+), right after ADGRG1 C-terminus. (Created using BioRender.com.)..... 37

Figure 2.5. The representation of ADGRG1-667EGFP or -667Nluc fusion cDNAs in pcDNA3.1(+). (A) EGFP cDNA was amplified by PCR, then cloned into pcDNA3.1(+), between ADGRG1 amino acids 667-668. (B) Nluc cDNA was amplified by PCR, then cloned into pcDNA3.1(+), between ADGRG1 amino acids 667-668. (Created using BioRender.com.) ..... 38

Figure 2.6. Representation of PCR run for truncation of ADGRG1. (Created using BioRender.com.) ..... 38

Figure 2.7. Assembly of a protein transfer pack. Adapted from Bio-Rad.com. .... 45

Figure 2.8. Serum Response Element (SRE) in pmirGLO plasmid. SRE is located upstream of FLuc, which is the experimental reporter. RLuc is constitutively expressed and acts as a control reporter..... 46

Figure 3.1. Agarose gel image of insertional PCR products after restriction enzyme (KpnI-XbaI) digestion to control the size of the EGFP tagged ADGRG1 on C-terminus. The size of EGFP tagged ADGRG1 cDNAs is 2799 bp. Red boxes indicate the plasmid and insert with the correct size. DNA ladder is Invitrogen™ 1 kb Plus DNA Ladder..... 49

Figure 3.2. Agarose gel image of insertional PCR products after restriction enzyme (KpnI-XbaI) digestion to control the size of the NLuc tagged ADGRG1 on C-terminus. The size of NLuc tagged ADGRG1 cDNAs is 2595 bp. Red boxes indicate the plasmid and insert with the correct size. DNA ladder is Invitrogen™ 1 kb Plus DNA Ladder. .... 50

Figure 3.3. Agarose gel electrophoresis image of colony PCR for C-terminally tagged ADGRG1 cDNAs with EGFP carrying linker (2811 bp) or NLuc carrying linker (2607 bp). Red boxes indicate the plasmid and insert with the correct size. DNA ladder is Invitrogen™ 1 kb Plus DNA Ladder. .... 50

Figure 3.4. Agarose gel electrophoresis image of colony PCR for ADGRG1 cDNAs tagged with EGFP carrying linker (2799 bp) or NLuc carrying linker (2595 bp) between amino acids 667-668. Red boxes indicate the plasmid and insert with the correct size. DNA ladder is Invitrogen™ 1 kb Plus DNA Ladder. .... 51

Figure 3.5. Agarose gel image of restriction enzyme (KpnI-XbaI) digestion products of the NLuc with linker or EGFP with linker tagged ADGRG1 on C-terminus. Red boxes indicate the plasmid and insert with the correct size. DNA ladder is Invitrogen™ 1 kb Plus DNA Ladder. .... 51

Figure 3.6. Agarose gel image of restriction enzyme (KpnI-XbaI) digestion products of the NLuc with linker or EGFP with linker tagged ADGRG1 on C-terminus. Red boxes indicate the plasmid and insert with the correct size. DNA ladder is Invitrogen™ 1 kb Plus DNA Ladder. .... 51

Figure 3.7. Agarose gel image of restriction enzyme (KpnI-XbaI) digestion products of the truncated ADGRG1 (1062 bp). Red box indicates the plasmid and inserts with the correct size. DNA ladder is Invitrogen™ 1 kb Plus DNA Ladder. FlhGPR56, full-length human GPR56 (ADGRG1). .... 52

Figure 3.8. Schematic illustration of image generation in a confocal microscope. Adapted from ptglab.com. .... 53

Figure 3.9. Laser scanning confocal images of ADGRG1-EGFP (A), ADGRG1-L-EGFP (B), and ADGRG1-667-EGFP (C). Scale bar corresponds to 2 μm. .... 54

Figure 3.10. Before transfer, stain-free precast SDS gel image. The size of ADGRG-WT is 77.7 kDa; ADGRG1-CtE is 104.6 kDa; ADGRG1-CtN is 96.8 kDa. Precision Plus Protein™ Unstained Protein standard (Bio-Rad, USA) was used as a protein ladder..... 55

Figure 3.11. After transfer, stain-free precast SDS gel image (A) and PVDF membrane image (B)..... 55

Figure 3.12. The immunoblot image. (A) The size of ADGRG1-WT is 77.7 kDa; ADGRG1-Ct-E is 104.6 kDa; ADGRG1-Ct-N is 96.8 kDa. (B) The immunoblot image of ADGRG1 (GPR56) detected by GPR56 Antibody (G-6) 200 µg/ml was taken from Santa Cruz Biotechnology. .... 56

Figure 3.13. Dual Luciferase reporter assay in HEK 293 cells. The bars indicate ADGR1-WT, ADGRG1-Δ1-342, ADGRG1-EGFP, ADGRG1-L-EGFP, and ADGRG1-667-EGFP, respectively. Error bars denote the standard deviation among readings. # p<0.05. \* p<0.001. n=3. .... 58

Figure 3.14. The net BRET ratio of ADGRG1 fusion proteins, including ADGRG1-EGFP and ADGRG1-NLuc; ADGRG1-Ct-L-EGFP and ADGRG1-L-NLuc; ADGRG1-667-EGFP and ADGRG1-NLuc. Error bars denote the standard deviation among readings. p<0.05. n=3..... 60

Figure 3.15. BRET saturation assay for ADGRG1 constructs. The ratio of EGFP tagged ADGRG1 receptor concentration to NLuc tagged ADGRG1 receptor concentration ([EGFP] / [NLuc]) is 0, 1, 2, 5, 20, 50, respectively..... 61

## LIST OF ABBREVIATIONS

### ABBREVIATIONS

7-TM	7-transmembrane
ADGRG1	Adhesion G protein-coupled Receptor, G subfamily, 1
aGPCR	Adhesion G protein-coupled receptor
BFPP	Bilateral frontoparietal polymicrogyria
CNS	Central nervous system
CTF	C-terminal fragment
ECD	Extracellular domain
ECM	Extracellular matrix
EGFP	Enhanced green fluorescent protein
FLuc	Firefly luciferase
G protein	Guanine nucleotide-binding protein
GAIN	GPCR autoproteolysis-inducing
GPCR	G protein-coupled Receptor
GPS	GPCR proteolysis site
ICD	Intracellular domain
NLuc	Nanoluciferase
NPC	Neuronal progenitor cell
NTF	N-terminal fragment
OL	Oligodendrocyte

OPC	Oligodendrocyte precursor cell
PNS	Peripheral nervous system
QD	Quantum dots
RLuc	Renilla luciferase
SC	Schwann cell
SRE	Serum response element
WT	Wild-type



## CHAPTER 1

### INTRODUCTION

#### 1.1 G protein-coupled receptors

In light of the pioneering electron diffraction study on bacteriorhodopsin, bacterial G protein-coupled receptor (GPCR), characteristic seven  $\alpha$ -helical structure of the GPCRs was elucidated for the first time [1]. Thenceforth GPCRs are known as 7-transmembrane (7-TM) domain receptors or heptahelical receptors. They belong to the largest receptor superfamily in mammals and are coupled with plasma membrane-anchored heterotrimeric guanine nucleotide-binding proteins (G proteins) to induce cellular signaling. Upon agonist or antagonist-induced GPCR activation, 7-TM helices of receptor undergo conformational changes, transduce the extracellular signal to various effectors [2], and result in a series of physiological reactions such as taste, vision, smell, neurotransmission, secretion, metabolism, growth, immune response and cellular differentiation [3-6].

G protein-coupled receptors can be classified according to ligand-binding criteria [7, 8] and sequence-based similarity [9-11] or their phylogenetic sequence relations [12, 13]. According to ligand-binding/sequence homology-based classification constituted by The Nomenclature Committee of the International Union of Basic and Clinical Pharmacology (NC-IUPHAR), GPCRs possess six classes:

- Class A (Rhodopsin-like)
- Class B (Secretin receptor-like)
- Class C (Metabotropic glutamate receptor-like)
- Class D (Fungal mating pheromone receptor-like)

- Class E (Cyclic AMP receptor-like)
- Class F (Frizzled/smoothed-like)

On the other hand, phylogenetic analysis-based classification, a more current system for GPCR categorization and named by the acronym GRAFS, has five classes:

- **G**lutamate
- **R**hodopsin
- **A**dhesion
- **F**rizzled
- **S**ecretin receptor

In 2009, genomic analysis of nine different species showed that adhesion GPCRs (aGPCRs) have the same splice setup with the Secretin family, and they share highly conserved domains [14]. *D. melanogaster* and *C. elegans* genomes provided remarkable evidence that aGPCRs might be the ancestor of Secretin family [14]. Therefore, in the GRAFS nomenclature system, class B receptors are subdivided into the Secretin and the Adhesion families, which is the fundamental difference between phylogenetic and sequence homology-based classification systems.

## **1.2 Adhesion G protein-coupled receptors**

### **1.2.1 Classification and nomenclature of adhesion G protein-coupled receptors**

With 33 members, adhesion GPCRs (aGPCRs) are the second-largest GPCR subfamily in humans. When the size of the family is considered, it is highly remarkable that most of these members are still orphan receptors and not well understood. aGPCRs further branched into nine subfamilies, designated using Roman numerals I-IX, based on the phylogenetic similarity of their conserved 7-TM and extracellular termini [8, 15, 16]. In 2015, a prefix ADGR (**A**dhesion **G** protein-coupled **R**eceptor) was recommended to identify any aGPCR homolog. **L**, **E**, **C**, **B**, and **V** letters were

then assigned to **L**atrophilins, **E**GF-TM7 receptors, **C**ELSRs, **B**AI, and **V**LGR subfamilies, respectively. In contrast, **A**, **D**, **F**, and **G** letters have been given in alphabetical order to the remaining subfamilies with GPR# names (Figure 1.1) [17]. ADGRG1, formerly known as GPR56, is a member of Group VIII according to phylogenetic classification.

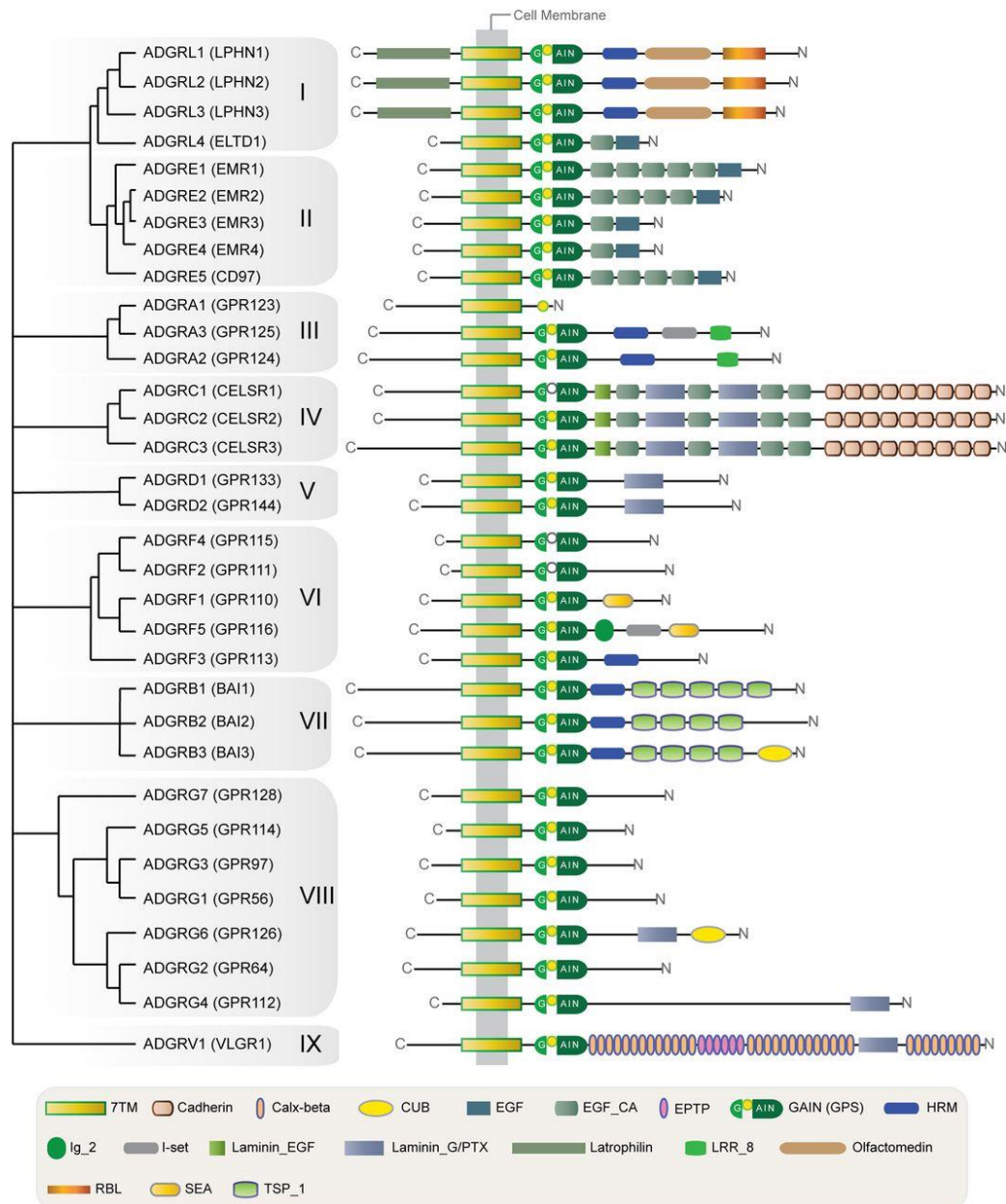


Figure 1.1. Illustration of the aGPCR subfamilies with the latest terminology, classified according to their characteristic extracellular termini architecture. Calx,

calnexin; CUB, Cs1 and Csr/Uegf/BMP1; EGF\_CA, calcium-binding EGF; EPTP, epitempin; HRM, hormone receptor motif; I-set, immunoglobulin I-set domain; LRR, leucine-rich repeat; PTX, pentraxin; RBL, rhamnose-binding lectin; SEA, sperm protein, enterokinase, agrin module; TSP, thrombospondin. Adapted from [17].

### 1.2.2 The general structure of adhesion G protein-coupled receptors

All proteins of aGPCRs coded from multiple protein-coding exons occupying large genomic regions. This fragmented coding region structure provides a basis for alternative splicing, enabling the synthesis of multiple mRNA isoforms from a single gene. In databases, there are several transcript variants reported for aGPCRs [18-22]. It has been shown that some of these variant transcripts are considerably different from constitutive splicing transcripts in terms of function and structure [18, 23, 24].

Considering the topology of aGPCRs, they are mainly composed of three main compartments, including the extracellular domain (ECD), the 7-transmembrane (7-TM) domain, and the intracellular domain (ICD). Unlike other GPCRs, ECDs of aGPCRs are much longer and carry at least one domain, generally unique for adhesion family, and promote cell-to-cell and cell-to-matrix adhesion [25]. One of the most important examples of these unique domains is the GPCR autoproteolysis-inducing (GAIN) domain, approximately 320 residues long in mammalian cells [26]. The conserved GPCR proteolysis site (GPS; 40 amino acid long) motif in the GAIN domain acts as a spacer and facilitate autoproteolysis to divide the receptor into two:

- N-terminal fragment (NTF; composed of N-terminus,  $\alpha$  subunit, and  $\alpha$  chain)
- C-terminal fragment (CTF; composed of a 7-TM domain,  $\beta$  subunit,  $\beta$  chain, and C-terminus) [16, 27-30] (Figure 1.2).

The GPS motif was previously considered as a “stalk” or “mucin-like” region [31, 32]. The structural features of this region initially remained unclear until obtaining crystallographic data from two aGPCRs, Latrophilin 1 (ADGRL1) and Brain Angiogenesis Inhibitor 3 (BAI3) [26]. In the light of these research findings, it was shown that the GPS motif is not a separate domain but is part of a much larger domain

called the GAIN domain. It was further proven that the “*Stachel*” or “stalk” sequence, the hydrophobic  $\beta$ -13 strand, is different from the GPS motif and acts as a tethered agonist to activate the 7-TM after NTF autoproteolysis [33-39].

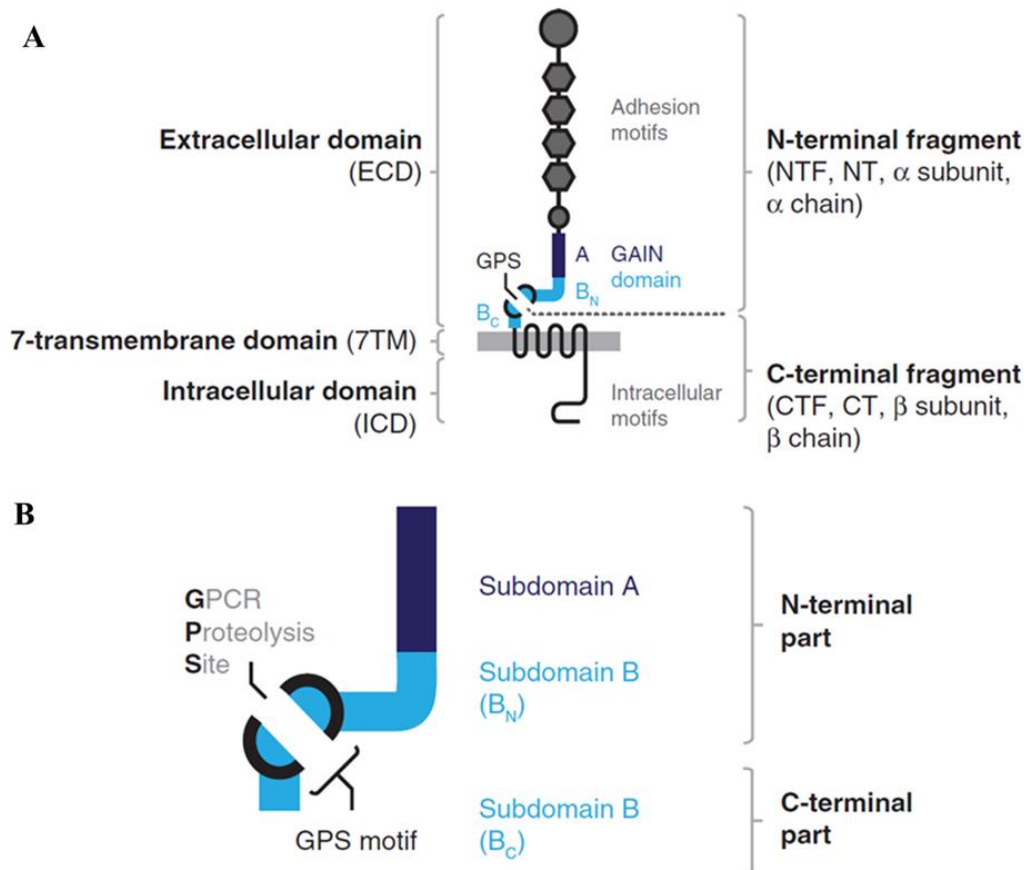


Figure 1.2. Representation of an adhesion G protein-coupled Receptor structure. (A) aGPCR is generally composed of three main parts, ECD, 7-TM, and ICD. After the GPS autoproteolysis of receptors, they are divided into two parts, including CTF and NTF. (B) The GAIN domain is highly sophisticated and unique for aGPCRs. It contains an N-terminal subdomain A and a subdomain B that has both N-terminal and C-terminal portions. Adapted from [16].

The GAIN domain is composed of subdomain A, which includes six  $\alpha$ -helices, and subdomain B that consists of 13  $\beta$ -strands and two small  $\alpha$ -helices. The last five  $\beta$ -strands of subdomain B constitutes the GPS motif, and it also includes some part of subdomain A [16, 40]. Except for ADGRA1 (GPR123), all aGPCRs have a GAIN domain; however, not all aGPCRs undergo the autoproteolysis process. The possible

reason can be the absence of an ideal GPS consensus sequence [41]. Autoproteolysis of the GAIN domain occurs via N-terminal nucleophile hydrolyze (Ntn-hydrolyse), and it has similar mechanistic features with the autoproteolytic process of the thyroid-stimulating hormone receptor (TSHR) [30, 42]. This process takes place by N-glycosylation of a specific site at the GAIN-GPS sequence of the receptor [43] in the endoplasmic reticulum (ER) [29, 44]. Although numerous studies have revealed that GPS autoproteolysis is needed for membrane localization for some aGPCRs [29, 45], other studies have also shown that autoproteolysis-deficient mutant receptors do not fail to localize to the cellular membrane [30, 46-48]. Therefore, it can be concluded that GPS autoproteolysis is not a general mechanism for receptor trafficking of aGPCRs.

aGPCRs also possess conserved motifs such as DRY in TM3 (transmembrane 3), GWGxP in TM4, CWxP in TM6, and NPxxY in TM7 at their 7-TM, which mainly plays a role in ligand-induced activation [49, 50]. When comparing GPCRs, the 7-TM domains of both aGPCRs and the secretin family are more open to peptide hormone ligand binding [51], supporting that the secretin family could be evolved from aGPCRs [14].

### **1.2.3 Activation and signaling mechanisms of adhesion G protein-coupled receptors**

It is known that aGPCRs and the Secretin family share several structural and functional features. Thus, their activation mechanisms are expected to be similar. Until now, various models have been suggested to explain aGPCR activation, including the *Stachel*-dependent or *Stachel*-independent and ECD mediated mechanisms [38, 39, 52-54] (Figure 1.3).

In the *Stachel*-dependent model, also called the “shedding model”, where irreversible dissociation of the NTF from the membrane-anchored CTF, the shedding is induced upon ligand binding to the ECD. This process is called shedding. The ligand can be

a soluble molecule or a membrane protein on a distant cell. The *Stachel* sequence at the newly formed N-terminus of the 7-TM domain becomes exposed and works as a tethered agonist to activate the receptor [17, 33-37].

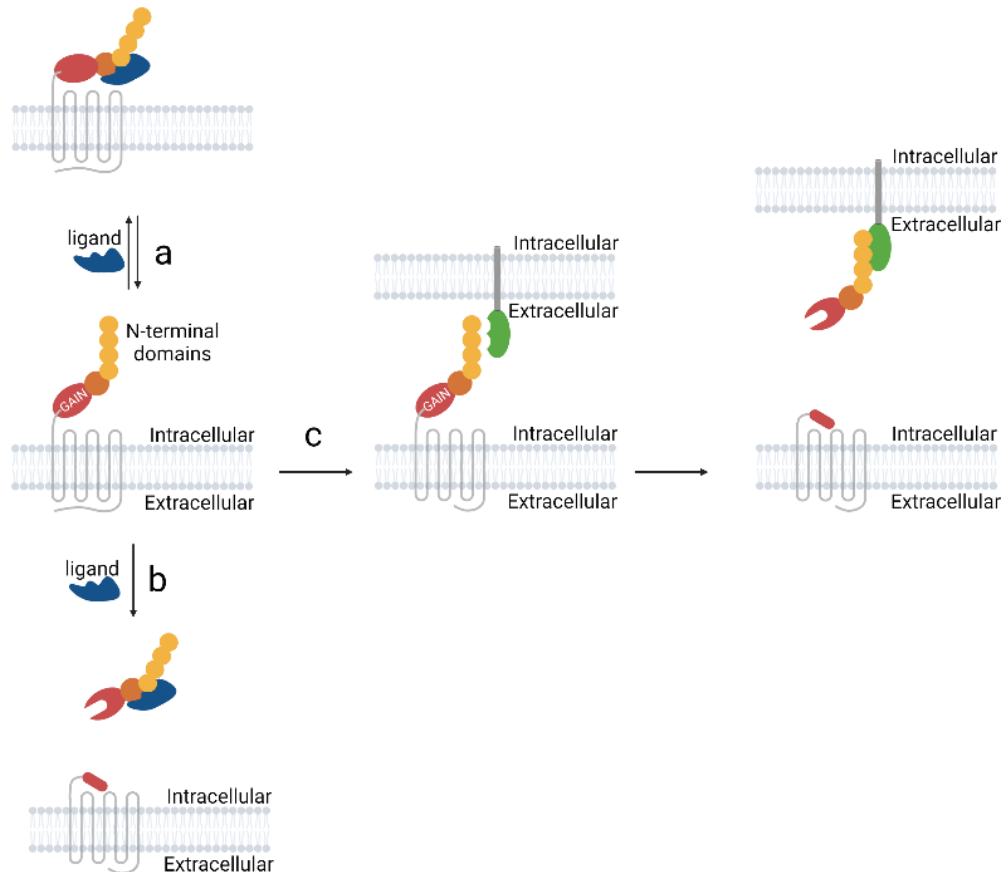


Figure 1.3. Activation mechanisms of aGPCRs. (A) An aGPCR interaction with a soluble ligand or proteins in the extracellular matrix acting as ligand leads to ECD-mediated receptor activation. (B) The Shedding model involves the release of NFT and subsequent receptor activation by the *Stachel* peptide sequence. (C) Cell-to-cell interaction between other membrane proteins or aGPCRs, resulting in NFT dissociation. (Created using BioRender.com.)

ECD-mediated activation model proposes that ECD, including NTF and GAIN domain of an aGPCRs, can contribute to the receptor activation via interacting with the 7-TM domain in a ligand-dependent and *Stachel*-independent manner [16, 39, 55]. It is suggested that some aGPCRs do not need autoproteolysis for activation, such as ADGRL1 (Lphn1) in *C. elegans* [48]. In addition, there are autoproteolysis

deficient aGPCRs due to the lack of their autoproteolysis specific conserved residues in the GPS motif [26, 56]. Additionally, recent studies showed that ECD and 7-TM domain directly interact via transient interactions and ligand binding, leading to conformational changes in the ECD. This interaction may inhibit or activate receptor signaling [39, 53]. These findings point out that *Stachel*-independent and ECD mediated activation is also an essential mechanism for aGPCR activation and receptor signaling.

#### **1.2.4 Overview of adhesion G protein-coupled Receptor 56 (ADGRG1/GPR56)**

ADGRG1 undergoes alternative splicing that could rearrange the pattern of the gene's coding and non-coding regions [57, 58]. Human-specific cerebral cortical patterning is affected by alternative splicing in the upstream non-coding region of ADGRG1 [58]. Alternative splicing in the coding region of ADGRG1 produces four isoforms in humans, two of which lead to partial ECD deletion [57]. However, the effects of alternative splicing in the architecture and function of ADGRG1 are not fully understood.

Considering the topology of ADGRG1, its NTF mainly comprises of GAIN domain and Pentraxin/Laminin/neurexin/sex-hormone-binding globulin-like (PLL) domain which is unique for ADGRG1 [20] (Figure 1.4). The previously unknown PLL domain was revealed after the crystal structure of the ADGRG1 ECD, the first fully resolved aGPCR ECD structure [20], and it is formed by two  $\beta$ -sandwiches called  $\beta$ -sheet A, and  $\beta$ -sheet B. PLL domain contains a fold diverged from Pentraxin (PTX) and Laminin/neurexin/sex-hormone-binding globulin-like (LNS) domains, and conserved motif (H $\Phi$ C<sup>91</sup>xxWxxxxG) [20]. It was further elucidated that the PLL domain also regulates the function of the receptor. The deletion of this domain increases the basal activity of ADGRG1 and mediates the alternative splice variant formation [20].

ADGRG1 is activated *in vitro* in a *Stachel*-mediated manner [38]. Interestingly, the truncation of NTF from amino acid 382 [53] and amino acid 342 (up to GPS domain) [55] increases the activity of ADGRG1. ADGRG1 receptor activation and its downstream elements,  $G\alpha_{12/13}$ -RhoA [59] triggered by the binding of receptor activating antibodies or activating ligands. The NTF of the receptor is irreversibly removed from the CTF and exposed *Stachel* region then acts as a tethered agonist to activate subsequent signaling elements [38, 39, 52, 53, 60]. RhoA signaling cascade activated through  $G\alpha_{12/13}$ , and calcium-ion channel activation through  $G\beta\gamma$  [39, 53]. Autoproteolysis deficient ADGRG1 mutants can be triggered by an agonist, 3- $\alpha$ -DOG [52, 61], and a panel of human GPR56-specific monobodies [54].

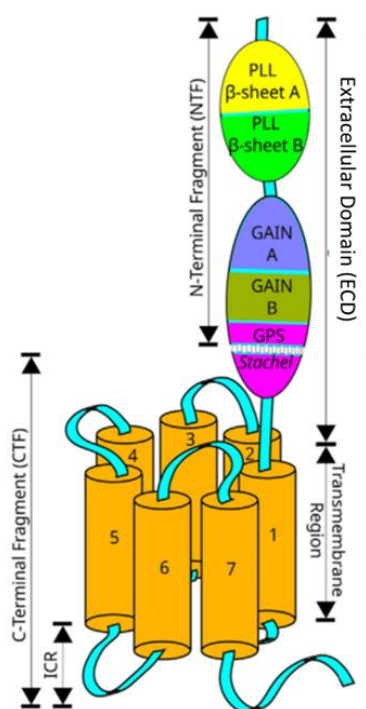


Figure 1.4. Representation of ADGRG1 receptor structure. ICR, intracellular region/domain. Adapted from [50].

Interestingly, ADGRG1 constructs with different ECD truncations can show basal activity. According to SRE luciferase reporter assay results, ADGRG1 truncated from NTF (up to *Stachel*) showed robust activity, but ECD (NTF and *Stachel* peptide) truncated constructs showed the lowest receptor activity [39]. The full-

length ADGRG1 constructs of both the wildtype and the autoproteolysis-deficient mutants revealed a moderate level of receptor activity [54], verifying that *Stachel* acts as a tethered agonist. Together, these results suggest that ECD is one of the critical controllers to modulate 7-TM domain signaling in aGPCRs (Figure 1.5 and 1.6).

In multicellular organisms, cellular adhesion and subsequent cellular signaling are critical processes in organ development. Disruption in these mechanisms affects almost every organ system and leads to the formation of several different diseases. The importance of the aGPCRs in complex human systems was first revealed by discovering the mutations in the ADGRG1 locus, which cause bilateral frontoparietal polymicrogyria (*BFPP*) [16, 62]. *BFPP* is a recessively inherited rare genetic disorder that involves cortical malformation affecting brain development [63]. The brain of the *BFPP* patients suffers from morphological abnormalities in multiple regions. One of these regions is the cerebral cortex which controls divergent functions like controlling motor functions and touch sensation or determining personality and intelligence. The importance of ADGRG1 expression in ventricular and subventricular zones of the cerebral cortex and neuronal progenitor cells (NPCs) was also indicated many times with *in situ* hybridization and immunocytochemistry, referring to its role in cortical lamination [59, 62, 64, 65]. Migration of the NPCs along radial glial fibers is a critical process for lamination during cortical development. In 2008, Iguchi *et al.* reported the negative regulation of ADGRG1 overexpression on NPC migration. Later, in 2014, it was further revealed that ADGRG1 expression and its splice variants affect the formation of the neocortex, proliferation of the NPC, and cerebral cortical patterning [58]. Recently, fascinating findings have revealed the expression of human ADGRG1 on cerebral cortex GABAergic neurons in the transgenic marmoset model [66]. *In situ* hybridization and immunohistochemistry data suggest that ADGRG1 is predominantly expressed in GABAergic neurons of the developing marmoset fetus brain. Other brain regions affected by *BFPP* are the cerebellum and pons [67]. *Gpr56*-knockout mice model combined with molecular and histological approaches demonstrated that loss of

ADGRG1 is responsible for both granule cell abnormalities in the rostral part of the cerebellum and loss of neurons in the pontine gray nuclei [68]. In 2011, collagen type III, alpha-1 (Col3a1) was identified as a ligand of the neuronal ADGRG1, which couples to the  $G\alpha_{12/13}$  to activate the RhoA pathway [69] (Figure 1.5A). Inactive ADGRG1 mainly locates in particular membrane regions occupied with detergent-soluble non-lipid rafts [70]. Interaction between the NTF of ADGRG1 and collagen III results in the NTF dissociation from the rest of the receptor [71]. The agonistic tethered *Stachel* is exposed after NTF shedding [52], followed by a translocation of the receptor CTF to the lipid rafts [71]. GDP bound- $G\alpha_{12/13}$  heterotrimeric G protein activated upon conformational changes in the CTF of the receptor, and  $G\alpha_{12/13}$  protein complex dissociation occurs via GDP-GTP exchange to activate RhoA, inhibiting neuronal migration [69]. The synergism of integrin  $\alpha3\beta$ , which works together with laminin-511 [72] and ADGRG1 in cerebral cortical development, was also suggested [73] (Figure 1.5A). Nevertheless, details of this interaction are still unclear. All these data reveal that ADGRG1 is essential for proper morphogenesis of the specific brain regions.

ADGRG1 has also been linked to impaired myelination due to decreased white matter volume and signal changes in MRIs in *BFPP* patients [62, 74, 75]. Myelin is the multilayered fatty material that is formed by Schwann cells (SCs) in the peripheral nervous system (PNS) and oligodendrocytes (OLs) in the central nervous system (CNS) to insulate nerve cell axons. In light of several studies, it has been shown that extracellular matrix (ECM) proteins, ECM receptors such as aGPCRs [76-78], and other glial cells such as microglia and astrocytes [79-81] are crucial regulators of OL development and subsequent myelination during embryonic brain development. In CNS myelination, the role of ADGRG1, affecting OL precursor cells (OPCs) proliferation, is pointed out using the cerebral white matter and the brain of *Gpr56*-knockout mice [82]. In 2015, Ackerman *et al.* showed that ADGRG1 is expressed in OLs during the early stages of the developmental process and reported a remarkable decrease in the number of OL and myelinated axons using both *Gpr56*<sup>-</sup> mouse and zebrafish mutants [83]. A complex composed of ADGRG1

on OPC surface, laminin-111 in ECM and microglia derived-tissue transglutaminase 2 (TG2), promotes myelination and myelin repair by assisting OPC proliferation and inhibiting OPC differentiation through  $G\alpha_{12/13}$ -RhoA pathway [82-85] (Figure 1.5C). The effect of ADGRG1 on PNS development and maintenance in *Gpr56*-knockout rodents and mutant zebrafishes was also indicated [86]. Transmembrane and cytoskeletal linker proteins, dystroglycan and plectin, also interact with the ADGRG1 found in the Schwann cells to enhance PNS myelination via cytoskeletal remodeling through the RhoA pathway [86] (Figure 1.5D). In other words, ADGRG1 arranges the number of myelinating glia in the CNS; it is also responsible for the radial sorting of axons in developing SCs and regulation of myelin sheath thickness in mature PNS.

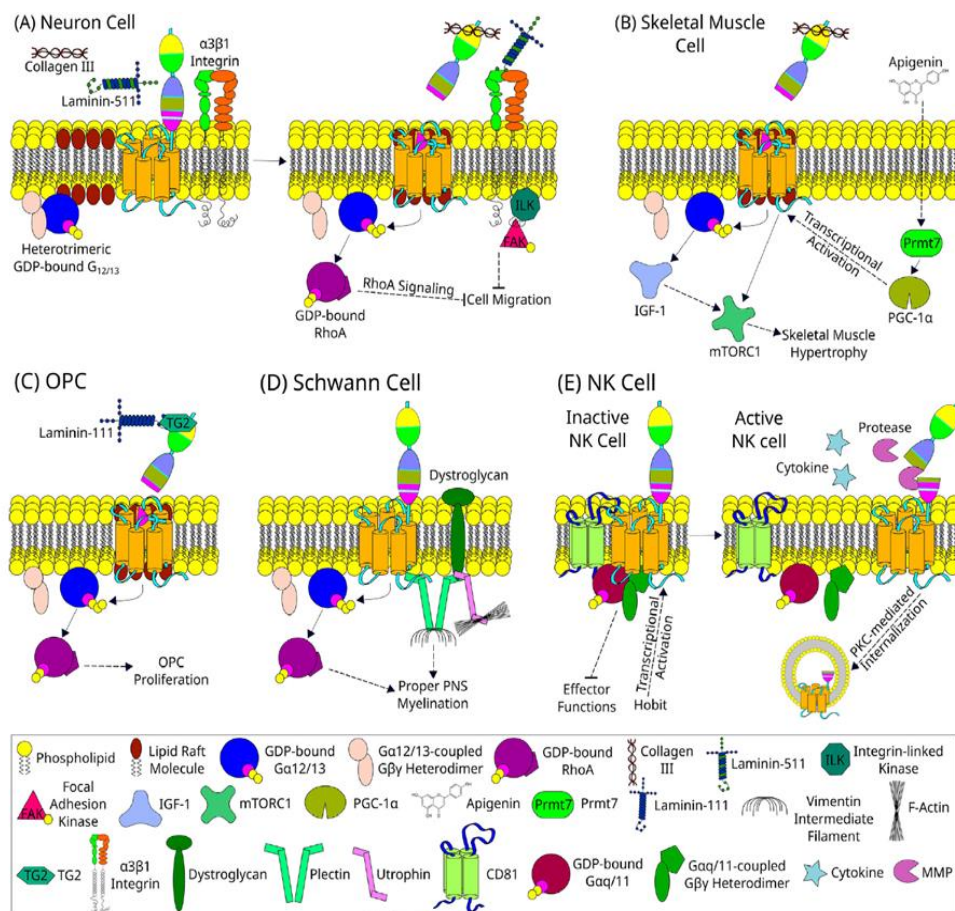


Figure 1.5. ADGRG1 signaling in different physiological systems. (A) ADGRG1 signaling via collagen III in neurons. (B) ADGRG1 signaling via apigenin in skeletal

muscle cells. (C) ADGRG1 signaling via TG2 and laminin-111 in OPCs. (D) ADGRG1 signaling via dystroglycan and lectin in Schwann cells. (E) ADGRG1 signaling via Hobit in natural killer (NK) cells. The dotted lines and the solid lines indicate indirect and direct pathways, respectively. Adapted from [87].

Due to microglial immune activation, demyelination is one of the characteristic symptoms of Multiple Sclerosis (MS). Microglia is responsible for maintaining brain homeostasis and acts as phagocytes in the MS demyelination process. Transcriptional profile analysis of human microglia isolated from control donors and MS patient brain donors provide evidence to reveal regional alteration in gene expression for microglia in both control and patients [88]. They showed that ADGRG1 is downregulated in white matter microglia during the early stages of MS. Another interesting finding of this study is the transcriptional difference for ADGRG1 in grey and white matter microglia, compared to microglia in choroid plexus. Thus, it could be argued that ADGRG1 is one of the critical elements for maintaining microglial homeostatic functions.

ADGRG1 can also be linked to other nervous system-associated pathologies besides *BFPP*. A severe cortical disruption mainly in the Broca's region, resulting in a defect of speech, has been reported as a consequence of a 15-bp deletion in a regulatory element of the ADGRG1 gene [58]. A recent study argued that ADGRG1 could be a biomarker for major depressive disorder (MDD) patients treated with antidepressants and chronic stress [89]. Anti-depressant treatment induced an increase in the level of ADGRG1 mRNA in the blood of the responder cohort. In contrast, chronic stress in mice and MDD in humans led to reduced mRNA levels, mainly in the brain's prefrontal cortex. Such a decrease in ADGRG1 expression could be related to depressive-like behaviors in mice, which is reversed after the anti-depressant treatment.

In addition to CNS development, ADGRG1 is also involved in developmental processes in various other tissues. The negative effect of *in vitro* loss of ADGRG1 on the muscle cell differentiation process was shown, especially in the early stage of myotube fusion and myoblast differentiation. Even so, this loss interestingly did not

affect the development or regeneration of the muscle in knockout mice models due to unknown compensatory regulators [90]. It is also demonstrated that resistance/loading-type exercise and apigenin, a natural flavone, regulates muscle hypertrophy by enhancing the ADGRG1 and collagen III expressions [91, 92] (Figure 1.5B). Entrance of apigenin in the cell induces the activation of protein arginine methyltransferase 7 (Prmt7) and subsequent peroxisome proliferator-activated receptor-gamma coactivator (PGC-1 $\alpha$ ) [92], which acts as a transcriptional factor for ADGRG1 and collagen III expression to induce muscle hypertrophy upon insulin-like growth factor-1 (IGF-1) - mammalian target of rapamycin complex 1 (mTORC1) pathway [91, 92]. In 2015, ADGRG1 was associated as a positive factor for hypertrophy of cardiomyocytes together with Poly(C)-binding protein 2 (PCBP2), which is a negative factor [93]. This is the first study to reveal the inhibitory effect of PCBP2, which is down-regulated in hypertrophy, and the promotive effect of ADGRG1 in angiotensin II induced-hypertrophic heart. The same study showed that ADGRG1 mRNA stability and degradation are regulated by PCBP2, indicating the role of PCBP2 for ADGRG1 regulation at the transcriptional level in hypertrophic growth of cardiomyocytes. Recently, it has been reported that extracellular transglutaminase-2 secreted by  $\beta$ -carotene-stimulated or all-trans-retinoic-acid-induced myotubes and the soleus muscles enhance Akt, ribosomal p70S6K, and mTOR via ADGRG1, resulting in hypertrophy [94]. In the reproductive system, *in situ* hybridization and immunohistochemical analysis provide evidence for the critical function of ADGRG1 on cell polarity regulation [95]. *Gpr56* knockout mice exhibit asymmetry in the testis cord during embryogenesis, resulting in defects in seminiferous tubule formation of the male mice and fertility. RNA-seq analysis of chicken embryonic gonads also represented the differentially expressed genes during sexual differentiation [96]. ADGRG1 is primarily expressed in the ovary's cortex of chickens during ovarian development. In a recent report, the contribution of ADGRG1 to Mullerian duct development through regulation of duct elongation in an avian model was for the first time identified [97].

In the immune system, the restricted expression of ADGRG1 in cytotoxic natural killer (NK) cells [98, 99] and cytotoxic T cells [99, 100] is elicited using ADGRG1-specific antibodies, indicating that ADGRG1 can be utilized as a cytotoxic lymphocyte marker. The receptor, together with CD81, is found to prevent migration and cytotoxicity of the NK cells [98, 100]. Hobit, which is a homolog of Blimp-1 in T cells, controls the expression of ADGRG1 in cytotoxic NK cells, and ADGRG1 inhibits the effector functions of resting NK cells, like degranulation, production of cytolytic proteins and inflammatory cytokines, upon CD81 association [100, 101] (Figure 1.5E). On the other hand, NK cell activation via cytokines leads to downregulation of ADGRG1 expression by shedding the NTF [101]. In addition to lymphocytes, it is also expressed in platelets to respond to collagen and subsequently induce platelet adhesion and plug formation [102]. It was proposed that the PLL domain of the ADGRG1 on circulating platelets interacts with the collagen matrix, and this interaction creates a force, resulting in dissociation of the receptor N-terminal fragment (NTF) from membrane-associated C-terminal fragment (CTF). The receptor CTF is then immediately activated via its tethered agonist to initiate  $G\alpha_{13}$  signaling, which modulates changes in the platelet shape through cytoskeletal reorganization. Furthermore, a novel classification system for  $CD4^+$  memory cells is recently suggested based on the surface expression of NK cell-associated proteins, including ADGRG1 [103]. According to the novel system,  $CD4^+$  cells can be divided into four subgroups: high, medium, low, and exhausted surface expression patterns.

It has been shown that different types of tumors express ADGRG1. The expression ADGRG1 increases in colorectal cancer and this upregulated expression is associated with drug resistance [104, 105], malignant tumor progression, and migration of colorectal cancer cells by activating PI3K/ACT [105, 106]. Progastrin (PG), a colonic growth factor, promotes colonic stem cell proliferation and mediates tumorigenesis in human and mouse colons [107]. PG binding to ADGRG1 receptor on colorectal cancer cells activates PI3K/Akt signaling pathway, resulting in epithelial-mesenchymal transition and metastasis [106] (Figure 1.6A). It was also reported that activated ADGRG1 in colorectal cancer tumors contributes to drug

resistance via the RhoA pathway and regulating multidrug resistance protein 1 (MDR1) expression [104] (Figure 1.6A). Similarly, ADGRG1 is significantly expressed in epithelial ovarian cancer cells [108]. It was reported that ADGRG1 knockdown in the SKOV3 ovarian cell line resulted in an increase in E-cadherin level and a decrease in RhoA-GTP, negatively affecting the cancer cell proliferation, migration, and invasion [108].

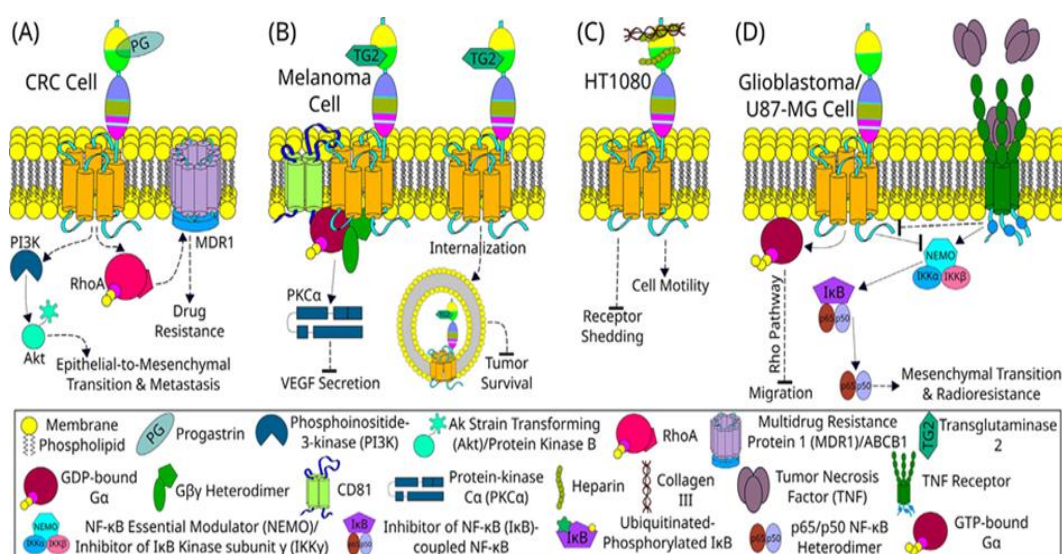


Figure 1.6. ADGRG1 signaling in different pathological conditions. (A) ADGRG1 signaling in colorectal cancer cells. (B) ADGRG1 signaling in melanoma cells. (C) ADGRG1 signaling in fibrosarcoma cells. (D) ADGRG1 signaling in glioblastoma cells. The dotted lines and the solid lines indicate indirect and direct pathways, respectively. Adapted from [87].

It is also described as a player both for inhibiting or promoting cancer growth in the context of the tumorigenic state and cell type [105]. In 1999, gene expression analysis showed that ADGRG1 is poorly expressed in human metastatic melanoma cell lines [109]. It is further proved that ADGRG1 splicing variants also contribute to inhibition or enhancing tumor formation by modulating the activity of cancer related-transcription factors [57]. In addition to these findings, the role of ADGRG1 in metastatic melanoma tumorigenesis was further explored. ADGRG1 blocks the tumor formation in multiple ways: (i) inhibiting vascular endothelial growth factor

(VEGF) secretion, hampering the blood vessels formation around the tumor site [110], and (ii) inhibiting the accumulation of a major ECM protein, fibronectin, and the phosphorylation of its downstream effector, focal adhesion kinase (FAK), indicating the causative relation between cell adhesion and metastatic growth [111]. ADGRG1 keeps melanoma metastasis under control by assisting the TG-2-bound ADGRG1 internalization to reduce the TG2 level in ECM [112, 113] (Figure 1.6B). ADGRG1 also interact with tetraspanins, like CD 81, to inhibit angiogenesis through  $G\alpha_{q/11}$  and  $PKC\alpha$  signaling pathway [110, 113] (Figure 1.6B). Heparin acts as a ligand of ADGRG1 in the HT1080 fibrosarcoma cell line [113]. It binds to the NTF of the receptor, corresponding to the collagen III binding sites, in order to inhibit NFT shedding and enhance cellular adhesion [114] (Figure 1.6C).

Many studies have also shown that ADGRG1 is a reliable biomarker for  $CD34^+$  acute myeloid leukemia cells and  $CD34^-$  leukemia stem cells [115-117] and could be used as a therapeutic agent, especially for chemo-resistant acute myeloid leukemia [118]. High expression [119] and activation of ADGRG1 hamper U87-MG human glioma cell migration upon  $G\alpha_q$  and its downstream elements, Rho [120] (Figure 1.6D). Upregulated expression level is not observed during the mesenchymal transition of glioblastoma, suggesting ADGRG1 could be an inhibitor of this process via tumor necrosis factor (TNF) and  $NF-\kappa B$  [121] (Figure 1.6D).

Taken together, ADGRG1 is required to maintain the homeostatic state, and it has a variety of therapeutic roles. Thus, it has the potential to be used as a distinctive marker for different pathological conditions. Unfortunately, ADGRG1 is still unexplored in aGPCR pharmacology. However, it seems that ADGRG1 will be a commonly employed target for a significant fraction of marketed drugs in years to come. With the growing interest, the potential of ADGRG1 in the field will be harvested as the mystery of its activation and signal transduction mechanisms is puzzled out.

### 1.3 G protein-coupled receptor oligomerization

It has been documented that oligomerization modulates processes that play an essential role in the lifetime of a receptor, such as maturation, trafficking, signaling, and internalization [122]. G protein-coupled receptors, which have been thought to work as monomers for a long time, make interconnections with other GPCRs and form heteromer, homomer, tetramer, or higher-order complexes [123]. Quantitative Förster Resonance Energy Transfer (FRET) showed that metabotropic glutamate receptors (mGluRs), class C receptor family members, can be found as a heterodimer [124] as well as a homodimer [125]. On the other hand, it was demonstrated that the  $\beta_2$ -adrenergic receptor ( $\beta_2$ AR), class A member, can be functional both as a monomer in a high-density lipoprotein reconstitution system [126] and as a higher oligomer [127]. Additionally, secretin receptor (SCTR), in class B, have provided clues to support G protein-coupled receptor oligomerization with the help of bioluminescence resonance energy transfer (BRET) and confocal imaging [128].

Although there are GPCRs, fully functional and highly stable in monomeric form, oligomerization provides some advantages to these more complex units. Sometimes, it might be mandatory for their function, particularly for class C GPCRs. In the brain, heterodimerization is required for the maturation and membrane localization of the GABA<sub>B</sub> receptor [129]. Similarly,  $\alpha_{1D}$ -AR's trafficking to the cellular membrane controlled by heterodimerization with  $\alpha_{1B}$ -ARs [130], and  $\beta_2$ AR enhances membrane localization of  $\alpha_{1D}$ AR [131]. Also, several studies have argued that most of the GPCRs, including GABA<sub>B</sub> [129, 132, 133], rhodopsin [134], and leukotriene B4 receptor [135] require oligomerization to activate G proteins. It was also reported that the homodimerization of the Glucagon-like-1 receptor regulates G protein-dependent high-affinity binding of agonists, like GLP-1(7-36)NH<sub>2</sub>, to the receptor [136]. A combination of confocal microscopy, BRET, and bimolecular fluorescence complementation methods show us that GPCRs initially dimerize in the ER, affecting the receptor-G protein association [137]. The oligomer-based complexes, including the receptor homo- or heteromers, G protein, and other effector proteins,

are localized to the cellular membrane to signal and provide more coordinated signaling machinery [138]. Moreover, many studies support the relationship between GPCR oligomerization and the functional state of the receptor. Single-molecule imaging data revealed that CXCR4 oligomerization enhances G protein-mediated signal transduction [139, 140]. Another comprehensive study utilized rhodopsin to investigate the positive contribution of oligomerization toward receptor stability and G protein signaling [140, 141].

#### **1.4 Bioluminescence resonance energy transfer (BRET)**

To better understand how the cellular machinery works, detecting and measuring the protein-protein interactions in living cells is one of the critical steps. There are many different biophysical and biochemical methods, such as radiation inactivation analysis [142], X-ray crystallography [143], NMR spectroscopy [144], and fluorescence and bioluminescence methods (fluorescence anisotropy [145], fluorescence correlation spectroscopy [146], Förster resonance energy transfer [147], fluorescence recovery after photobleaching [148] and bioluminescence resonance energy transfer (BRET) [149]) to detect oligomerization and stoichiometry of the oligomeric complexes.

Resonance energy transfer (RET) techniques have become a popular strategy for screening protein oligomerization in the last decade. RET methods are mainly based on the same principle. When non-radiative energy is transferred from a “donor” molecule, the energy is then captured by an “acceptor” molecule [150]. If the donor's emission spectrum overlaps with the acceptor's excitation spectrum to some extent, resonance energy will be transferred efficiently.

BRET is one of the straightforward and valuable techniques to provide robust evidence for molecular interactions. The method is a natural phenomenon first discovered in some marine species. Non-radiative energy released during the oxidation of a substrate by a light-emitting enzyme, such as luciferase, is donated to

an “acceptor,” such as a fluorescent protein that can capture this energy and resulting in light emission [151] (Figure 1.7).

Although BRET and FRET occur through the same physical mechanisms, in the former it is not necessary to excite the donor via an external light source. Due to the absence of a light-generating enzyme in mammalian cells, a high signal-to-noise ratio (low background) could be achieved in BRET compared to FRET. BRET also overcomes the problems associated with FRET-like light scattering or photobleaching. Additionally, BRET is a ratiometric method, enabling to hamper interferences from experimental conditions.



Figure 1.7. A brief representation of native BRET. (A) Luciferase catalyzes substrate oxidation and emits light if the fluorescent protein is far enough. (B) Luciferase transfers its energy to the fluorescent protein if it is in close proximity. (Created using BioRender.com.)

In artificial BRET systems, *Renilla luciferases* (RLucs) are commonly preferred as the donor. Hydrophobic and cell-permeable coelenterazine oxidized by RLuc, resulting in a light emission maximum at 480 nm with a short lifetime (Figure 1.7). Synthetic analogs of coelenterazine, such as coelenterazine-400a (DeepBlueC™), can be utilized to obtain emission profiles with different brightness and wavelength intervals. Choice of a donor with a suitable emission spectrum provides the spectral separation between donor and acceptor, thereby enhancing the BRET sensitivity [152].

Another bioluminescent protein, *Firefly luciferase* (FLuc), has been used as a donor in the BRET systems. D-luciferin oxidized by FLuc in the presence of Mg<sup>2+</sup>, O<sub>2</sub>, and

ATP, resulting in emission spectra maximum at 565 nm [153] (Figure 1.8). In this BRET system, lower cellular autofluorescence is obtained; however, the signal is weak, and acceptor emission spectrums can overlap with the FLuc's emission [152].

*NanoLuc luciferase* (NLuc) is much brighter than RLuc and FLuc with a narrower emission spectrum and superior stability [154]. Furimazine, a coelenterazine analog, is oxidized by NLuc to generate light emission at 460 nm (Figure 1.8). Brighter NLuc can detect low prevalence dimerizations, meaning a more sensitive assay [155]. Another advantage is that NLuc is also smaller than other luciferases, leading to less function-altering steric hindrance when fused in the proteins of interest [155].

Green fluorescent protein (GFP) is a widely used acceptor in BRET experiments. Its chromophore region, responsible for the fluorescence, is caged in the center of a  $\beta$ -barrel structure, thus protected from quenching. *Wild-type* (WT) GFP possessed significant disadvantages, such as prolonged maturation time, two excitation peaks, strong aggregation tendency, and low fluorescent signal at a physiologically relevant temperature [156]. On the other hand, engineered enhanced GFP (EGFP) was constructed to solve these problems [157]. EGFP with two mutations F64L and S65T has a single excitation maximum at 488 nm (Figure 1.9) and has improved fluorescence signal at 37°C due to enhanced folding efficiency at this temperature [156].

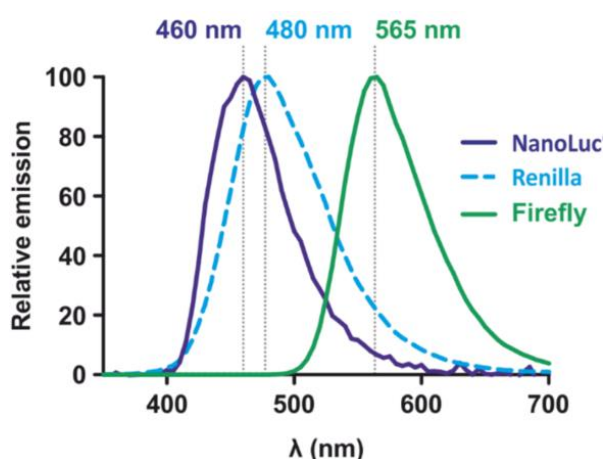


Figure 1.8. Emission wavelengths of NanoLuc, Renilla, and Firefly luciferases. The maximum emission wavelength of NanoLuc is 460 nm; the maximum emission

wavelength of *Renilla* luciferase is 480 nm; the maximum emission wavelength of Firefly luciferase is 565 nm. Adapted from promega.com.

BRET was used for the first time to investigate protein-protein interactions in 1999 [158]. Xu *et al.* detected the interactions of proteins in living cyanobacteria using RLuc as the donor and its substrate coelenterazine h to excite enhanced yellow fluorescent protein (EYFP). This method was later called BRET<sup>1</sup>, and since then, it has been widely used in standard overexpression systems with approximately 1-hour assay duration [155]. The same study also highlighted that any appropriate pair of luminescent donor and fluorescent acceptor could be utilized in this technique. However, BRET<sup>1</sup> is unsuitable for systems requiring genome-edited proteins since this method is less sensitive [155].

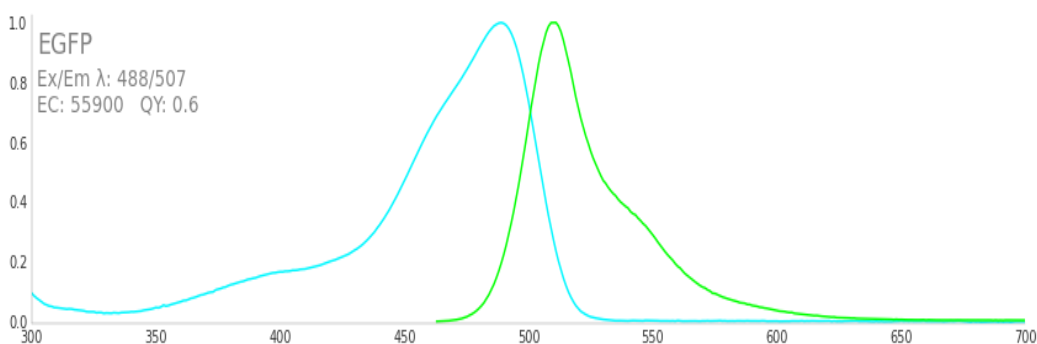


Figure 1.9. Excitation and emission wavelengths of enhanced GFP. The maximum excitation wavelength of EGFP is 488 nm; the maximum emission wavelength of EGFP is 507 nm. (FPbase ID: R9NL8) Adapted from fpbase.org.

Over the last years, the BRET method has been diversified with multiple developments (Table 1.1). Each method has benefits and limitations. BRET<sup>2</sup> uses GFP and RLuc with DeepBlueC™, resulting in a bioluminescence emission peak with the maximum located at 400 nm, resulting in a better separation with the donor emission hence a lower background signal. Thus, it can be preferred in cases where a high signal-to-noise ratio is required. However, the drawback for the BRET<sup>2</sup> assay is that the duration is limited to seconds as a result of the rapid substrate decay [159]. In 2008, enhanced BRET<sup>2</sup> (eBRET) was derived from BRET<sup>2</sup> by mutating RLuc

(RLuc8) to increase the BRET signal [160]. RLuc8, containing eight amino acid substitutions leading to a 5 - 30-fold increased signal compared to RLuc, allows to conduct the assay for more than six hours. However, as a drawback, the substrate needed pre-incubation [155]. The BRET<sup>3</sup> method consists of a combination of FLuc with D-Luciferin as a donor and Red fluorescent protein (DsRed) as an acceptor [161]. More sustained emission by FLuc and lower cellular autofluorescence are the significant enhancements for this method.

On the other hand, the limitation of BRET<sup>3</sup> is the overlap between donor and acceptor emissions peaks and weak light signals. Additionally, the oligomerization tendency of DsRed is another drawback of the BRET<sup>3</sup> [159]. In Quantum Dot-BRET (QD-BRET), semiconductor nanocrystals, quantum dots (QD), and RLuc8 with coelenterazine combined, offering clear separated emission spectrums as a result of the QDs flexible emission profiles [162]. QD-BRET also provides high sensitivity, photostability, and brightness, which makes it valuable for deep tissue imaging [162]. However, QDs are quite big molecules and cannot be expressed in living cells [159].

Table 1.1. The comparison of different BRET techniques with donor and acceptor pairs and corresponding emission peaks. (Created using BioRender.com.)

	<b>BRET<sup>1</sup></b>	<b>BRET<sup>2</sup></b>	<b>eBRET</b>	<b>BRET<sup>3</sup></b>	<b>QD-BRET</b>	<b>NanoBRET</b>
<b>Donor</b>	RLuc	RLuc	RLuc8	FLuc	RLuc8	NLuc
<b>Substrate</b>	Coelenterazine	DeepBlueC	DeepBlueC	Luciferin	Coelenterazine	Furimazine
<b>Donor Emission (nm)</b>	480	395	395	565	480	460
<b>Acceptor</b>	EYFP	GFP	GFP	DsRed	QDot	HaloTag Ligand
<b>Acceptor Emission (nm)</b>	530	510	510	583	605	618

### 1.4.1 The theory behind BRET

In the BRET technique, ligands are oxidized by bioluminescent enzymes, and the released energy from the reaction is converted to bioluminescence emission. The electron state of the donor (enzyme) is transformed from the ground state to the excited ( $S_1$ ) state by the reaction energy. The vibrational energy of the  $S_1$  state electrons is emitted as a photon at a longer wavelength; as a result, they return to the ground ( $S_0$ ) state. The energy of the  $S_1$  state electrons could also undergo RET to acceptor protein if the bioluminescence spectrum of the NLuc overlaps the excitation spectrum of the acceptor. Excited electrons interact with the electron cloud of the acceptor (fluorescent protein) with a certain probability, resulting in excitation of the acceptor (Figure 1.10). BRET requires proximity ( $\leq 10$  nm) between the donor and the acceptor to transfer resonance energy efficiently [163], and it is highly efficient when NLuc and the acceptor are positioned within the distance at which 50% of the excitation energy has transferred the acceptor, called the Förster distance [164].

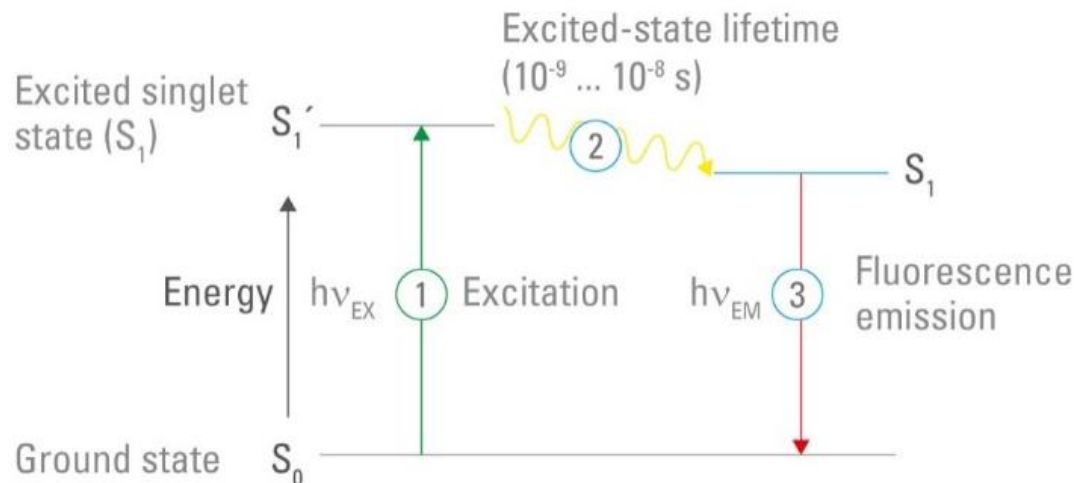


Figure 1.10. Simplified Jablonski Diagram. Adapted from leica-microsystems.com.

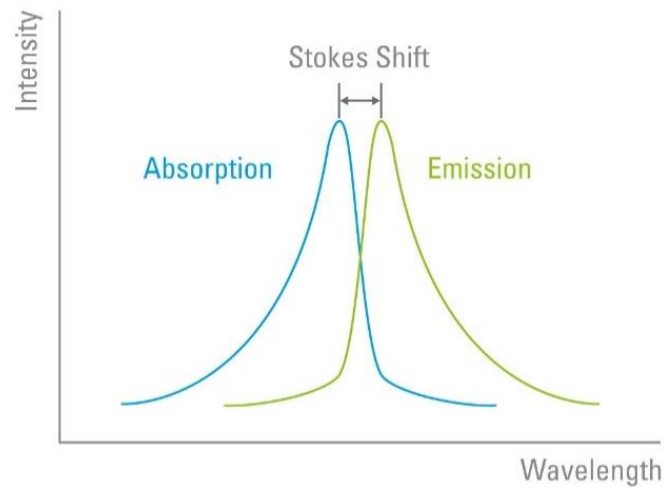


Figure 1.11. Stoke's shift. It indicates the difference between the excitation and the emission wavelength maxima of a fluorophore. Adapted from leica-microsystems.com.

Proximity is not the only criteria for RET. It also depends on the relative orientations of donor and acceptor and the stability of dimerization [165]. Additionally, the emission spectrum of the donor should overlap the excitation spectrum of the acceptor [165] (Figure 1.11). Furthermore, Stoke's shift of the acceptor should be large enough to resolve the acceptor emission and the NLuc emission spectra [166].

BRET is formulized as the ratio between transferred ( $T$ ) and not-transferred energy ( $Q$ ):

$$BRET = \frac{T}{Q} \text{ [167, 168]}$$

The energy transfer efficiency ( $E$ ) affects the probability of RET in a single pair:

$$T = E \times Q_o, \text{ where } Q_o \text{ is total energy } Q_o = T + Q \text{ [167].}$$

According to the Förster equation,  $E$  is inversely proportional to the sixth power of the distance ( $R$ ) between the donor and the acceptor [169]. Förster radius ( $R_o$ ) determined by the dipole orientation and the spectral overlap between the donor and the acceptor:

$$E = \frac{R_o^6}{R_o^6 + R^6} \text{ [167].}$$

The energy transfer efficiency is calculated using maximum BRET ( $BRET_{max}$ ). The occupation of all donor molecules by acceptor molecules gives maximum BRET:

$$E = \frac{BRET_{max}}{BRET_{max}+1} [167].$$

Furthermore, quantitative BRET calculations are simplified with the following formula:

$$BRET_{E \ll 1} = \frac{T}{Q_o} [170].$$

### 1.4.2 NanoBRET system

The deep-sea shrimp, *Oplophorus*, produces a luciferase, which catalyzes the coelenterazine oxidation to emit blue light. This native enzyme consists of four subunits, two of them are 35 kDa, and the others are 19 kDa; however, only the smaller subunit exhibits bioluminescence activity (Oluc-19) [171]. Oluc-19 is also unstable and dependent on its 35 kDa partner for the expression [171]. In 2012, this native luciferase and coelenterazine were engineered to generate an improved bioluminescence system [154]. This system, called NanoBRET, is based on the combination of an engineered luciferase (NLuc) and a coelenterazine analog, furimazine [154].

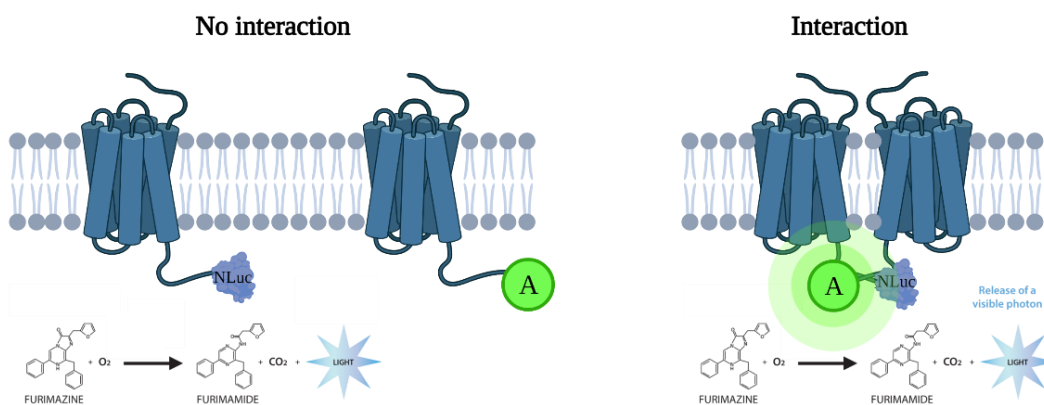


Figure 1.12. Cartoon of the NanoBRET method. Acceptor (fluorescent) protein cannot be excited through furimazine oxidation catalyzed by NLuc if two proteins

do not interact with each other. In the case of interaction, photons released after oxidation reaction excite the acceptor, resulting in a NanoBRET signal. (Created using BioRender.com.)

In NanoBRET systems, two sets of proteins of interest are constructed by genetically fusing NLuc (donor) or fluorescent protein (acceptor). The co-expression of donor- and acceptor-fused constructs in living cells allow us to evaluate the oligomerization quantitatively in real-time [172]. When the proteins of interest form oligomers, the interaction brings the Nanoluc and fluorescent protein in close proximity, resulting in non-radiative dipole-dipole coupling (Figure 1.12).

### **1.4.3 Quantitative BRET assays: BRET saturation assay**

Interpretation of BRET data is the most critical point, even though measuring the signal is relatively straightforward. Random collisions can occur through non-specific binding of the donor and the acceptor molecules in a biological system, resulting in misinterpretations of the BRET data. Identification of a stable and specific binding among random collisions is essential if the expression of the proteins is in the physiological range. An increase in the protein concentration can increase random collisions resulting in an increased probability that two proteins are within the range of Förster radius. This phenomenon is called “bystander” BRET. To overcome these problems, various quantitative BRET assays have been developed, including dilution, competition, and saturation assays [168, 173].

In the BRET dilution assay, the bystander BRET is excluded by simultaneously decreasing the donor and the acceptor concentrations, keeping the donor and the acceptor ratio constant [168]. This dilution results in a decrease in the measured BRET signal towards the actual oligomerization BRET signal since RET occurs independently of the concentration. In the BRET competition assay, the untagged protein concentration increased, and the concentrations of the donor- and the acceptor-tagged proteins were kept constant [174, 175]. If a specific oligomerization is present, a decrease in the BRET signal is expected due to the competition of

untagged receptors with tagged receptors. In the BRET saturation assay, the concentration of the donor remains constant while the acceptor concentration increases [176, 177]. In theory, an increase in the acceptor concentration increases the signal until all donor molecules are occupied with acceptor molecules. Saturation of all donor molecules makes the BRET signal reach a maximum value ( $BRET_{max}$ ); after which increasing acceptor concentration any further does not affect the measured BRET signal. Theoretical BRET saturation curves plotted as a function of the ratio of tagged proteins are given in Figure 1.13.

BRET signal measured from the random collisions of monomers is non-specific. High protein concentration generates a quasi-linear curve due to random collision; however, oligomers are saturated faster. The theoretical  $BRET_{50}$  value of homodimers is 1, which is related to the oligomerization affinity of the proteins. Except for  $MT_2$ -  $MT_1$  and  $MT_2$ -  $MT_2$  melatonin receptor pairs [178], the saturation curve shifts to the right if the receptor is less likely to form a heterodimer, meaning a high  $BRET_{50}$  value [168, 179].

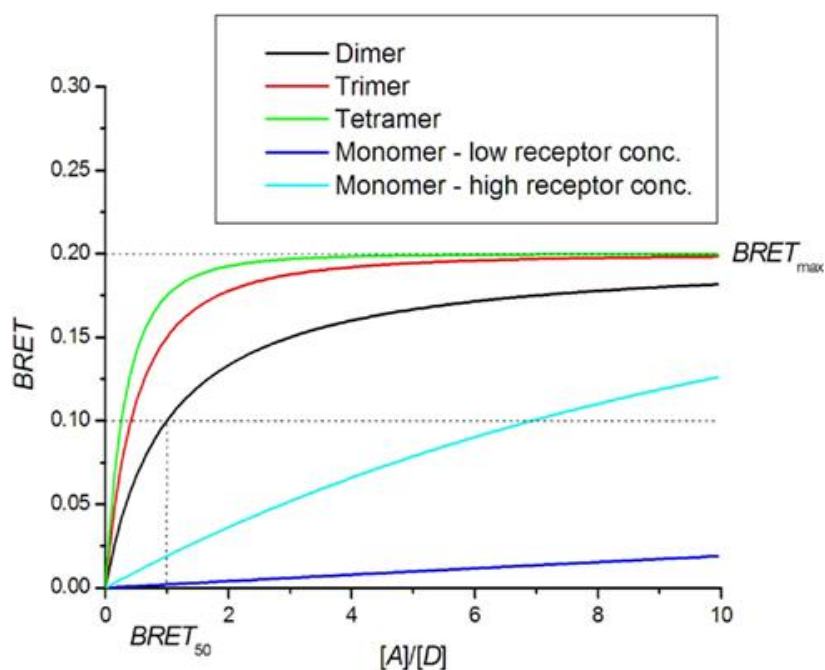


Figure 1.13. Theoretical saturation curves.  $BRET_{50}$ , a ratio of the receptor concentration where the curve reaches half-maximum. Adapted from [167].

## **1.5 Aim of the thesis**

This thesis aims to investigate the ADGRG1 receptor oligomerization utilizing the NanoBRET method in live cells. For this purpose, constructs were made by tagging ADGRG1 with NLuc, EGFP, or linker (GSSG) added-versions of these tags at various positions at the C-terminal domain of the receptor. Mammalian cells were co-transfected with these constructs, and NanoBRET was measured to determine receptor dimerization.



## CHAPTER 2

### MATERIALS AND METHODS

#### 2.1 Construction of fluorescent or bioluminescent-tagged ADGRG1

EGFP, NLuc from pEGFP-N2, pNL-1, and linker (GSSG) “cassettes” of these proteins constructed in pcDNA3.1(+) were used for the tagging of human ADGRG1 receptors using insertional polymerase chain reaction (PCR) protocol. The ADGRG1 receptor plasmid is a kind gift from Dr. Demet Araç (University of Chicago). The plasmid map is depicted in Figure 2.1.

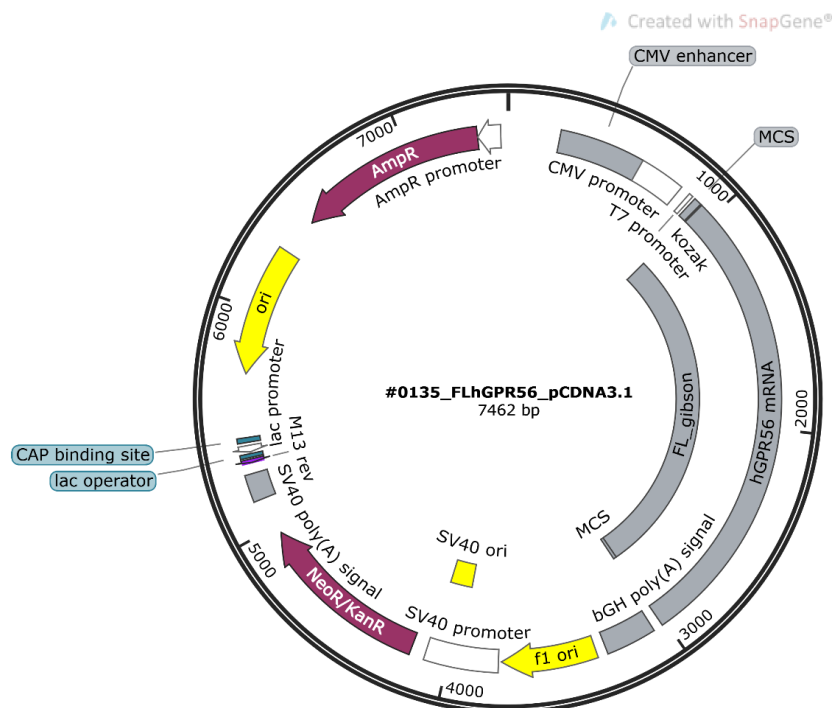


Figure 2.1. The pcDNA3.1(+) plasmid carrying full-length human ADGRG1 (GPR56) between KpnI and XbaI restriction enzymes.

The insertional PCR protocol consists of two sequential PCR. In the first PCR, EGFP or NLuc are amplified using primer pairs carrying homologous sequences from 5' and 3' of the EGFP or NLuc, flanked by the bases from directed positions ADGRG1 cDNA sequence (C-terminus and between the amino acids 667-668). The PCR products are then used as a primer in the following insertional PCR to fuse EGFP or NLuc into the ADGRG1 cDNA. In this PCR, the whole plasmid is amplified. The cartoon of the brief insertional PCR protocol is shown in Figure 2.2.

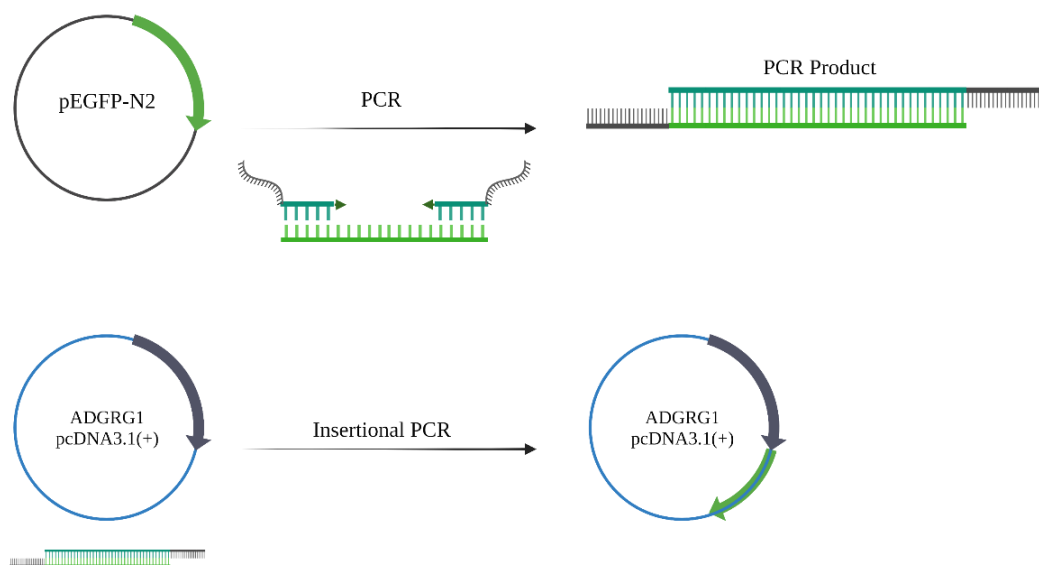


Figure 2.2. Representation of insertional PCR method. EGFP insertion into the C-terminus of the ADGRG1 cDNA is given as an example. (Created using BioRender.com.)

The primer pair used in the first PCR to obtain EGFP, NLuc, and GSSG added-versions (hereafter referred to as GSSG-EGFP and GSSG-NLuc) with ADGRG1 homologous sequences is given in Table 2.1.

Table 2.1 Primer pair used for amplification of EGFP and NLuc cDNAs. Each primer is extended in a 5' to 3' direction. EGFP or NLuc sequences are denoted by upper-case letters, and ADGRG1 homologous sequence is indicated by lower-case letters. Forward primers lack stop codon not to hamper the expression of EGFP or NLuc

protein which was positioned right after the ADGRG1. Reverse primers for EGFP or NLuc protein positioned between amino acids 667-668 lack stop codon.

Primer	Sequence
ADGRG1-Ct-EGFP-F	cccatcagctcgggcagcacctcgtccagccgcatcATGGTGAGCAAGGGCG AGGAG
ADGRG1-Ct-EGFP-R	cagcgggtttaaacgggcctctagactcgagcctaCTTGTACAGCTCGTCCA TGCCG
ADGRG1-Ct-L-EGFP-F	cccatcagctcgggcagcacctcgtccagccgcatcGGCAGCAGCGGCGTGA GCAAGGGC
ADGRG1-Ct-EGFP-R	cagcgggtttaaacgggcctctagactcgagcctaCTTGTACAGCTCGTCCA TGCCG
ADGRG1-667-EGFP-F	ctgtactggtccatcgggtcgcaggccggggtGTGAGCAAGGGCGAGGA G
ADGRG1-667-EGFP-R	ggcgctgtctgagttgctcttcagagggggggccCTTGTACAGCTCGTCCA TGCCG

Table 2.2. The first PCR components and conditions for the amplification of EGFP and NLuc cDNAs.

Component	Volume (µl)	Final Concentration
Nuclease-free water	12.6-x	
5X Phire High Fidelity Buffer	4	1X
2 mM dNTPs	2	200 µM each
Primer forward	0.5	0.5 µM
Reverse Primer	0.5	0.5 µM
Template*	x	100 ng
Phire Hot Start DNA Polymerase	0.4	0.02 U/µl

98°C 30 s

**98°C 10 s**

**54°C 30 s**

**35 cycle**

**72°C 15-30 s/kb**

72°C 1 m

\* pEGFP-N1 for EGFP, pNL-1 for NLuc, L-EGFP-L cassette in pcDNA3.1(+) for constructs with GSSG.

PCR products, carrying ADGRG1 homolog sequences, purified using Thermo Scientific™ GeneJET PCR Purification Kit and used in the insertional PCR. The PCR conditions are as follows:

Table 2.3. Insertional PCR components and conditions to fuse amplified EGFP or Nluc cDNAs into ADGRG1 cDNA in pcDNA3.1(+). The PCR was set as the molar ratio of ADGRG1 plasmid to amplified EGFP, or Nluc is 1:20.

Component	Volume (μl)	Final Concentration
Nuclease-free water	9.8-(x+y)	
5X Q5 Reaction Buffer	4	1X
5X Q5 High GC Enhancer	4	1X
2 mM dNTPs	2	200 μM each
PCR product	y	
ADGRG1 in pcDNA3.1(+)	x	200 ng
Q5 High-Fidelity DNA Polymerase	0.2	0.02 U/μl

98°C 30 s

**98°C 10 s**

**50-60°C 30 s 35 cycle**

**72°C 30 s/kb**

72°C 2 m

After PCR, the product was digested with Thermo Scientific™ FastDigest DpnI enzyme to get rid of the methylated template plasmid, thereby leaving only the newly amplified plasmid. DpnI recognizes 5'-G<sup>m6</sup>A/TC-3' and cleaves only when the site is methylated. The template, isolated from the DH5α strain (*E. coli*), has already been methylated; thus, it is cleaved in the presence of DpnI. The digestion conditions are given in Table 2.4.

Table 2.4. DpnI digestion protocol.

Component	Volume (μl)
10X FastDigest Buffer	2.3
FastDigest DpnI	1
PCR mixture	20

incubation at 37°C for 3h

At the end of digestion, the mixture was directly transformed using DH5α competent *E. coli* strain. Under aseptic conditions, competent cells were thawed on ice for 5 minutes and, 2 μl of digestion mixture was added to 50 μl of competent cells; then

mixed gently by tapping the tube. The cells were incubated on ice for 30 minutes, followed by a heat shock at 42°C for 45 seconds. Afterward, cells were placed on ice for 5 minutes. The volume was completed to 1 ml with Super Optimal Broth with catabolite repression (SOB, see Appendix A), and cells were grown with constant shaking at 37°C for 1 hour. Cells were centrifuged at 6000 rpm for 3 minutes, and 800 µl of supernatant was discarded. The pellet was resuspended with the remaining medium, and cells were seeded onto Ampicillin selective agar plate using glass beads. Plates were incubated at 37°C for 16 hours. The following day, four colonies were selected on the plate, and half of a colony was transferred in 12 µl of nuclease-free water and denatured at 98°C for 3 minutes for colony PCR. The primer pairs and conditions were utilized in colony PCR are as follows:

Table 2.5. Primer pair used for colony PCR. Each primer is extended in a 5' to 3' direction.

Primer	Sequence
KpnI-ADGRG1-F	GTTGTTGTTggtaccatgactccccagtcgctgctgcagacgacactg
EGFP-XbaI-R	GTTGTTGTTtctagaTACTTGTACAGCTCGTCCATGC
ADGRG1-XbaI-R	GTTGTTGTTtctagactagatgcggtggacgaggtgctgcc

Table 2.6. Colony PCR components and conditions.

Component	Volume (µl)	Final Concentration
Nuclease-free water	12	
5X Phire High Fidelity Buffer	4	1X
2 mM dNTPs	2	200 µM each
Forward primer	0.5	0.5 µM
Reverse primer	0.5	0.5 µM
Phire Hot Start II DNA Polymerase	0.4	0.02 U/µl
DMSO	0.6	3%

98°C 30 s

**98°C 5 s**

**54°C 5 s      35 cycle**

**72°C 30 s/kb**

72°C 1 m

PCR products run on 1% agarose gel, and plasmids with correct inserts were inoculated to Ampicillin selective Luria-Bertani (LB, see Appendix A) broth and grown with constant shaking at 37°C for 16 hours. Plasmids isolated using Thermo Scientific™ GeneJET Plasmid Miniprep kit. The plasmids with the desired insert were determined on 1% agarose gel following double restriction enzyme digestion (Table 2.7).

Table 2.7. Double restriction enzyme digestion protocol for confirmation of the positive inserts.

<b>Component</b>	<b>Volume (µl)</b>
Nuclease-free water	9.1
10X FastDigest Green Buffer	2
FastDigest KpnI	0.2
FastDigest XbaI	0.2
Plasmid	4

incubation at 37°C for 3h

C-terminally EGFP tagged ADGRG1 cDNAs in pcDNA3.1(+) (hereafter referred to as ADGRG1-EGFP) and C-terminally Nluc tagged ADGRG1 cDNAs in pcDNA3.1(+) (hereafter referred to as ADGRG1-NLuc) is depicted in Figure 2.3. C-terminally L-EGFP tagged ADGRG1 cDNAs in pcDNA3.1(+) (hereafter referred to as ADGRG1-L-EGFP) and C-terminally L-Nluc tagged ADGRG1 cDNAs in pcDNA3.1(+) (hereafter referred to as ADGRG1-L-NLuc) is represented in Figure 2.4.

EGFP tagged ADGRG1 cDNAs between amino acids 667-668 in pcDNA3.1(+) (hereafter referred to as ADGRG1-667-EGFP) and Nluc tagged ADGRG1 cDNAs between amino acids 667-668 in pcDNA3.1(+) (hereafter referred to as ADGRG1-667-NLuc) is represented in Figure 2.5.



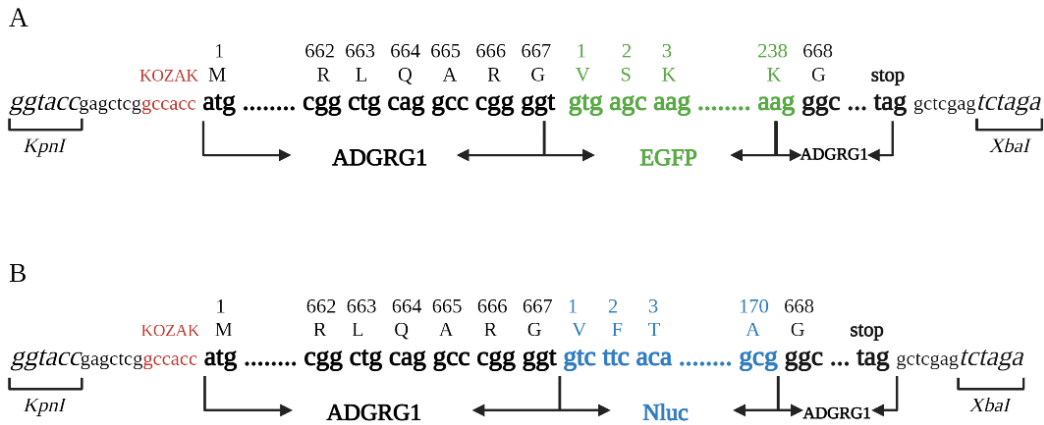


Figure 2.5. The representation of ADGRG1-667EGFP or -667Nluc fusion cDNAs in pcDNA3.1(+). (A) EGFP cDNA was amplified by PCR, then cloned into pcDNA3.1(+), between ADGRG1 amino acids 667-668. (B) Nluc cDNA was amplified by PCR, then cloned into pcDNA3.1(+), between ADGRG1 amino acids 667-668. (Created using BioRender.com.)

Positive constructs were sent to MCLAB (USA) for sequencing, and the constructs with correct sequence were used in further experiments.

## 2.2 Truncation of ADGRG1

Truncated constructs were created from WT ADGRG1 receptors using PCR and ligation methods. The first step was to run PCR to truncate ADGRG1 (Figure 2.6).

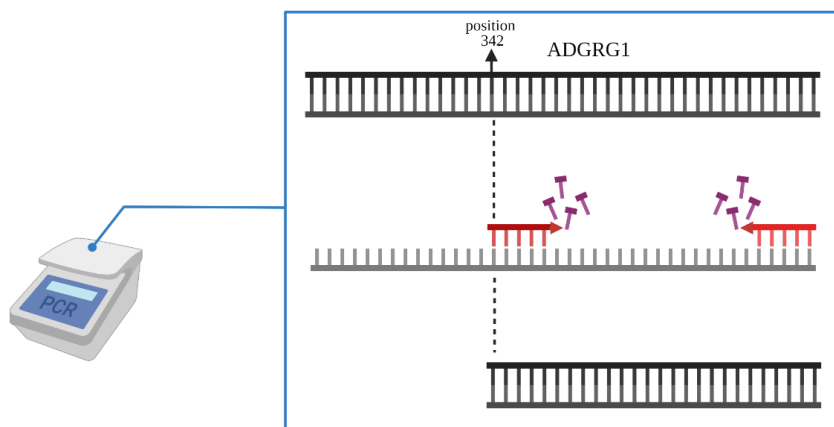


Figure 2.6. Representation of PCR run for truncation of ADGRG1. (Created using BioRender.com.)

The forward primer was designed to carry ADGRG1 homologous region at position 342 and downstream bases and KOZAK consensus sequence accompanied with the start codon “ATG”. Forward and reverse primers were also flanked by KpnI and XbaI restriction sites, respectively (Table 2.8). The PCR conditions are given in Table 2.9.

Table 2.8. Primer pair used in PCR for truncation of ADGRG1 at position 342. Each primer extended in a 5' to 3' direction.

<b>Primer</b>	<b>Sequence</b>
KpnI-K-atg-ADGRG1 Δ1-342-F	gttggtgttggtaccgccaccatgactctgcaatgtgtgttctgggtgaagac
ADGRG1-XbaI-R	gttggtgttctagactagatgctggctggacgaggtgctgcc

Table 2.9. PCR components and conditions to truncate ADGRG1 at position 342.

<b>Component</b>	<b>Volume (μl)</b>	<b>Final Concentration</b>
Nuclease-free water	12.6-x	
5X Phusion High Fidelity Buffer	4	1X
2 mM dNTPs	2	200 μM each
Primer forward	0.5	0.5 μM
Reverse Primer	0.5	0.5 μM
ADGRG1-WT	x	100 ng
Phusion Hot Start II DNA Polymerase	0.4	0.02 U/μl

98°C 30 s  
**98°C 10 s**  
**54°C 30 s**            **35 cycle**  
**72°C 15-30 s/kb**  
72°C 10 m

PCR products, carrying KpnI and XbaI restriction sites, were purified by Thermo Scientific™ GeneJET PCR Purification Kit and double digested using these enzymes. pcDNA3.1(+) mammalian expression vector was also digested with the same enzyme pairs for the ligation reaction. The digestion protocol is given in the following table:

Table 2.10. Double restriction enzyme digestion protocol.

Component	Volume (μl)
10X FastDigest Green Buffer	4
FastDigest KpnI	1
FastDigest XbaI	1
PCR product or vector	35

incubation at 37°C for 3h

Digested PCR products and vector were run on 1% SeaPlaque™ low melting temperature agarose gel (Lonza Biosciences, USA) and extracted from the gel using QIAquick gel extraction kit (Qiagen, USA). Truncated ADGRG1 constructs ligated between KpnI and XbaI restriction sites in multiple cloning sites of pcDNA3.1(+) (Figure 2.1). The ligation reaction set as 1:5 molar ratio of linearized pcDNA3.1(+) vector to truncated ADGRG1, and 200 ng of the vector used for the ligation reaction outlined in Table 2.11.

Table 2.11. Ligation reaction conditions.

Component	Volume (μl)
Nuclease-free water	17-(x+y)
10X T4 DNA Ligase Buffer	2
T4 DNA Ligase	1
Linearized vector	x
Insert	y

incubation at 22°C for 3h

The ligation reaction mixture was directly used in the bacterial (DH5α) transformation, and positive inserts were determined on 1% agarose gel after digestion control. The protocol was given earlier in Section 2.1.2.

## **2.3 Cell culture**

### **2.3.1 HEK 293 maintenance, passage, seeding into culture vessels**

HEK 293 cells were grown complete medium containing 90% Dulbecco's Modified Eagle Medium (DMEM; ThermoFisher Scientific, USA), 10% Fetal Bovine Serum (FBS; ThermoFisher Scientific, USA), and 1% Penicillin/Streptomycin (Pen/Strep; ThermoFisher Scientific, USA). HEK 293 cells were maintained in a 25 cm<sup>2</sup> rectangular canted neck cell culture flask at 37°C under humidified and 5% CO<sub>2</sub> atmospheric conditions. All mammalian cell culture procedures were performed in a laminar-flow hood to provide aseptic conditions, and all reagents and equipment were stored in a manner that maintained their sterility. As HEK 293 cells reached the 80-90% confluency, twice a week, they were subcultured. The complete medium on confluent cells was aspirated, and cells were briefly rinsed with pre-warmed 3 ml of 1X Dulbecco's Phosphate Buffered Saline (DPBS, Biological Industries, Israel). Cells were detached from the bottom of the flask using pre-warmed 1 ml of 1X TrypLE™ Express enzyme (ThermoFisher Scientific, USA), and incubation at 37°C for 5 minutes. The flask was observed under ZEISS Axio Vert.A1 inverted microscope (Zeiss, Germany) until the cell layer dispersed. Cells were harvested in 4 ml of fresh pre-warmed complete medium to dilute the TrypLE™ Express enzyme and aspirated by gently pipetting. Aspirated cells were transferred into a 50 ml conical bottom tube (Greiner Bio-One, Austria) and spun down at 900 rpm for 3 minutes to remove the enzyme. The supernatant was carefully discarded, and the cell pellet was dissociated by gently tapping the tube. Cells were resuspended in 5 ml of fresh pre-warmed complete medium. The total number of cells and percent viability were determined using a hemocytometer, cell counter, and Trypan Blue. 20 µl of a sample from cell stock was mixed with 20 µl of Trypan Blue and incubated for 1-2 minutes. Then, 10 µl of Trypan Blue treated cells were loaded in the hemocytometer; then live and dead (blue) cells were counted in the selected 4 sets of 16 corners. The total cell number was calculated using the following formula:

$$\text{Total cells/ml} = \frac{\text{Total live cell counted} \times \text{Dilution factor} \times 10^4}{\text{Number of squares counted}}$$

Cell viability was calculated as follows:

$$\text{Cell viability (\%)} = \frac{\text{Average live cell counted}}{\text{Average live cell counted} + \text{Average dead cell counted}} \times 100$$

An appropriate volume of resuspended cells was transferred to a new 25 cm<sup>2</sup> culture flask as a subculture and appropriate culture vessel for subsequent transfection containing fresh pre-warmed complete medium. The seeding density for vessels used in this work is given in Table 2.12. The flask and vessel were rocked back-and-forth then side-to-side several times to distribute cells evenly. Cells were incubated at 37°C under humidified and 5% CO<sub>2</sub> atmospheric conditions.

Table 2.12. HEK 293 seeding density into cell culture vessels used.

<b>Culture vessels</b>	<b>Seeding density</b>	<b>Final volume</b>
T-25	0.50 x 10 <sup>6</sup>	5 ml
35-mm dish	0.25 x 10 <sup>6</sup> or 0.50 x 10 <sup>6</sup>	2 ml
24-well plate	0.20 x 10 <sup>6</sup>	0.5 ml
96-well plate	0.01 x 10 <sup>6</sup>	0.1 or 0.075 ml

### **2.3.2 Transient plasmid transfection of HEK 293 cells**

The transient transfection was carried out using Invitrogen™ Lipofectamine™ LTX Reagent with PLUS™ Reagent. The appropriate amount of DNA was diluted in Gibco™ Opti-MEM™ Reduced Serum Medium with phenol red, and PLUS™ Reagent was added. Into another tube, Lipofectamine™ LTX Reagent was also diluted in Opti-MEM™. The amount of the reagents for each culture vessel is given as follows:

Table 2.13. Reagents used in transient transfection of HEK 293 cells according to culture vessels.

<b>Culture vessels</b>	<b>DNA (ng/μl)</b>	<b>Opti-MEM in mix (μl)</b>	<b>PLUS™ (μl)</b>	<b>LTX (μl)</b>	<b>Opti-MEM onto cells (μl)</b>	<b>Complete medium (μl)</b>
35-mm	500	100	4	4	1000	1000
24-well	200	50	2	2	100	300
96-well	100	9.75	0.25	0.25	30	50

The Opti-MEM – LTX mixture was added to the Opti-MEM – DNA – PLUS™ mixture and the total mixture was incubated at room temperature for 30 minutes. Meanwhile, the culture medium on top of the cells was removed, and cells were rinsed with pre-warmed 1X PBS once; then, pre-warmed Opti-MEM was added onto the cells. The mixture, including the plasmid DNA, was gently dropwise added to the cells. The culture vessel was placed in the CO<sub>2</sub> incubator and left for 3 hours. The complete medium was added onto the transfected cells, and they were incubated in the CO<sub>2</sub> incubator for 48 hours.

#### **2.4 Laser scanning confocal imaging**

Constructs with correct sequence were imaged using Zeiss LSM880 Laser Scanning Confocal Microscope equipped with Zeiss 63x/1.4 Plan Apochrome Oil DIC objective (Stem Cell Institute, Ankara University, Turkey) to verify their membrane localization and expression in HEK 293; cells were seeded into 35-mm glass-bottom dishes ( $0.25 \times 10^6$  cells/dish). The imaging of cells expressing EGFP tagged ADGRG1 was carried out using a 488 nm laser for excitation, and emitted light was collected between 493 – 586 nm.

## **2.5 Western blotting**

HEK 293 cells were seeded into a 35-mm culture dish ( $0.50 \times 10^6$  cells/dish) and transfected with ADGRG1 constructs followed by incubation for 48 hours in a CO<sub>2</sub> incubator (see Section 2.2.1 and 2.2.2).

### **2.5.1 Sample preparation: cell lysis and protein harvesting**

35-mm dishes were placed on ice, and culture medium was discarded. The cells were washed with 500  $\mu$ l of ice-cold 1X PBS and lysed using a cell scraper and ice-cold 1X Radioimmunoprecipitation (RIPA) buffer (see Appendix B). Cell lysates were transferred into pre-chilled microcentrifuge tubes and incubated on ice for 30 minutes. During incubation, the tube contents were agitated by vortexing every 5 minutes. Tubes were centrifuged at 16000 g for 20 minutes at 4°C. Supernatants were transferred to new pre-chilled tubes, and the total protein concentration was calculated using Pierce™ BCA Assay Kit (Thermo Fisher Scientific, USA).

### **2.5.2 Cell loading and running**

Cell lysates were diluted in 4X Laemmli buffer (Appendix B). 20  $\mu$ g of protein were loaded into wells, along with molecular weight marker. Bio-Rad Mini-PROTEAN TGX Stain-free Precast was run at 300 V until the dye front reached the reference line. At the end of the run, the gel was gently removed from the cassette and soaked into Mili-Q® ultrapure water, then imaged using Bio-Rad ChemiDoc MP Imaging System.

### **2.5.3 Protein transfer**

A transfer pack including filter papers, PVDF membrane, and gel was prepared. Filter papers (ion reservoir stack) were rinsed with Bio-Rad 10X Tris/Glycine

transfer buffer. PVDF membrane was activated in methanol and washed with transfer buffer. The transfer pack was layered and placed in the transfer cassette depicted in Figure 2.8.

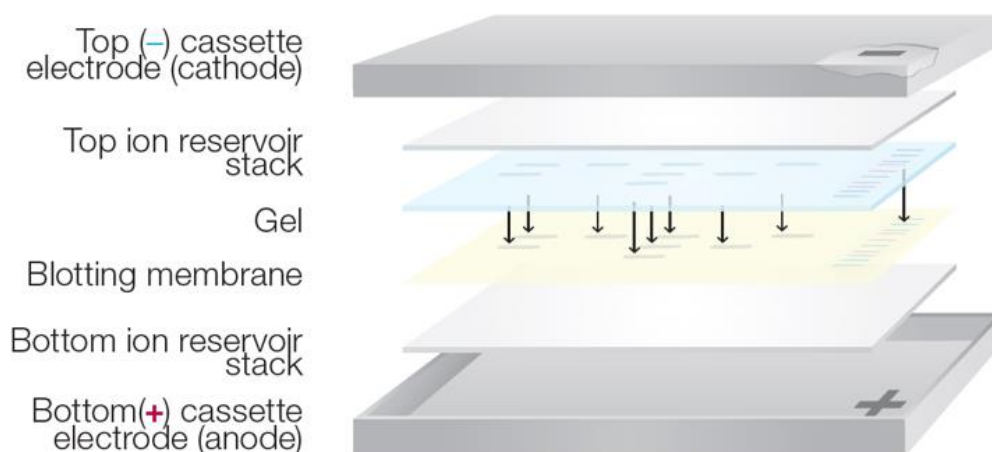


Figure 2.7. Assembly of a protein transfer pack. Adapted from Bio-Rad.com.

The excess transfer buffer and air bubbles between the components were removed using the blot roller before placing the cassette lid. Transfer cassette was inserted into the Bio-Rad Trans-blot® TurboTurbo™ Rapid Transfer system, and transfer protocol was run at 25 V for 30 min. The blotting sandwich was disassembled carefully, and the membrane and the blot were soaked in 1X TBST (Appendix B). Both were imaged using Bio-Rad ChemiDoc MP imaging system.

#### 2.5.4 Blocking and antibody probing

Membranes were soaked in a blocking solution containing 5% non-fat dry milk in 1X TBST and incubated for 1 hour at room temperature with constant gentle shaking. After blocking, the membranes were rinsed with 1X TBST and probed with 1:500 dilution of ADGRG1 primary antibody (Santa Cruz Biotechnology, USA) overnight in a cold room with constant shaking. The following day, membranes were incubated in blocking solution for 5 minutes at room temperature with constant shaking. Then, the blocking solution was discarded, and this step was repeated three times.

Membranes were rinsed with 1X TBST and incubated in 1:7500 dilution of secondary antibody conjugated to Horseradish Peroxide for 1 hour at room temperature with constant shaking. For signal development, membranes were incubated in SuperSignal™ West Pico PLUS Chemiluminescent Substrate for 5 minutes at room temperature in the dark and imaged using Bio-Rad ChemiDoc MP imaging system.

## 2.6 Serum Response Element (SRE)-dual-luciferase reporter assay

HEK 293 cells seeded into a 24-well plate were co-transfected with pmirGLO plasmid containing Serum Response Element and ADGRG1 constructs in pcDNA3.1(+) plasmid according to the protocol given in Section 2.3.1 and 2.3.2. SRE in the pmirGLO plasmid map presented in Figure 2.7. The plasmid is a kind gift from Dr. Demet Araç (University of Chicago).

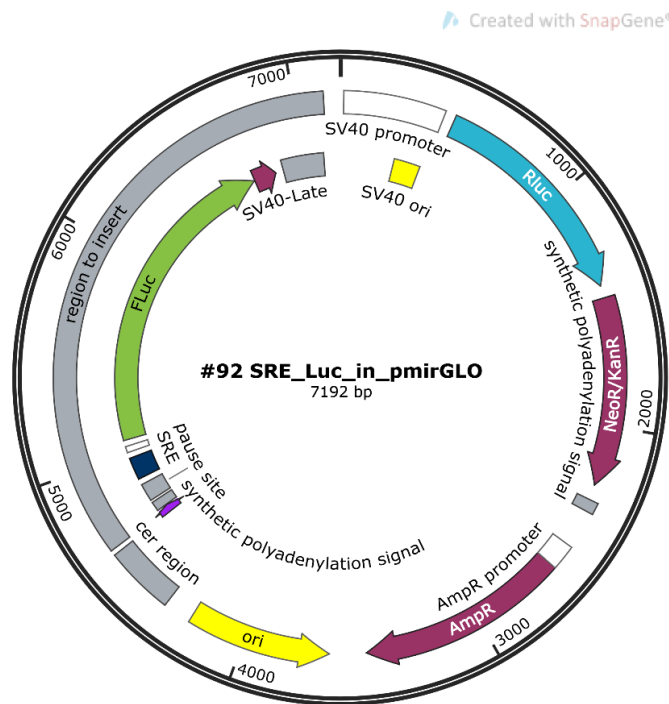


Figure 2.8. Serum Response Element (SRE) in pmirGLO plasmid. SRE is located upstream of FLuc, which is the experimental reporter. RLuc is constitutively expressed and acts as a control reporter.

On the assay day, a 24-well plate was removed from the incubator, and the culture medium was removed. The cells were harvested by the addition of pre-warmed 100  $\mu$ l of TrypLE™ to each well. The enzyme was diluted with 300  $\mu$ l of pre-warmed complete media, and cell layers were dispersed via pipetting up and down. Each well co-transfected with pmirGLO and one of the EGFP tagged ADGRG1 construct were transferred into separate microcentrifuge tubes. The cells were centrifuged at 900 rpm for 3 minutes, and the supernatant was aspirated carefully. The pellet was resuspended gently in 750  $\mu$ l of pre-warmed Gibco™ Opti-MEM™ Reduced Serum Medium without phenol red (hereafter refer to as Opti-MEM<sup>-</sup>). The 75  $\mu$ l of each co-transfected cell was dispensed as triplicate into a white, F-bottom 96-well microplate and allowed to equilibrate at room temperature. Meanwhile, Coelenteraine-400a and Pierce™ D-Luciferin, monopotassium salt working solution (WS) was prepared. 15 ml of 200X stock solutions were diluted to 4X in 750  $\mu$ l of Opti-MEM<sup>-</sup> and 4X Coelenteraine-400a and D-Luciferin solutions were mixed to make 2X WS. 75  $\mu$ l of 2X WS was added to each well to make the final concentration 1X (Table 2.14). The RLuc and FLuc activities were measured using Mithras<sup>2</sup> LB 943 Multimode Microplate Reader (Berthold Technologies, Germany) and MicroWin 2010. 410m80 filter for RLuc and 610lp filter for FLuc were used during measurement.

Table 2.14. Substrate preparation for luciferase reporter assay.

	<b>D-Luciferin</b>	<b>Coleneteraine-400a</b>
<b>Solvent volume</b>	3.33 ml of H <sub>2</sub> O	2.56 ml of EtOH
<b>Aliquot (Stock) volume</b>	15 $\mu$ l	15 $\mu$ l
<b>Aliquot (Stock) conc.</b>	30 mg/ml (200X)	1000 $\mu$ M (200X)
<b>Final conc. (in a well)</b>	471 $\mu$ M (1X)	5 $\mu$ M (1X)

## 2.7 NanoBRET assay

HEK 293 cells were seeded in a white 96-well microplate and co-transfected with 100 ng NLuc tagged ADGRG1 as BRET donor and 100 ng EGFP tagged ADGRG1 as BRET acceptor according to transfection protocol in Section 2.3.2. On the assay day, the working solution was prepared by diluting one volume of Furimazine

(Promega, USA) in 100 volumes of Opti-MEM<sup>+</sup> per well. Medium on the cells was discarded, and the working solution was immediately added onto cells; then NanoBRET was directly measured using Mithras<sup>2</sup> LB 943 Multimode Microplate Reader (Berthold Technologies, Germany), and data were acquired with MicroWin 2010. 460m70 filter for NLuc emission and 515m40 filter for EGFP emission were used during measurement.

## **2.8 BRET saturation assay**

HEK 293 cells were seeded in a white 96-well microplate and co-transfected with a constant amount of NLuc tagged ADGRG1 as BRET donor (10 ng) both in the absence and presence of increasing amounts of EGFP tagged ADGRG1 as BRET acceptor (0, 10, 20, 50, 200, 500 ng) according to transfection protocol in Section 2.3.2. 48 hours after transfection, Furimazine (Promega, USA) working solution was prepared by diluting one volume of the substrate in 100 volumes of Opti-MEM<sup>+</sup> per well. Media on the wells were discarded, and a working solution was immediately added onto cells. NanoBRET was directly measured using Mithras<sup>2</sup> LB 943 Multimode Microplate Reader (Berthold Technologies, Germany) and MicroWin 2010. 460m70 filter for NLuc and 515m40 filter for EGFP were used during measurement.

## CHAPTER 3

### RESULTS

#### 3.1 Construction of fluorescent or bioluminescent-tagged receptors

EGFP or NLuc tagged ADGRG1 receptors were constructed via insertional PCR method explained in detail in 2.1.2. Using the products from the first PCR (see Table 2.2), ADGRG1 constructs tagged with EGFP or NLuc on various positions on the C-terminal domain were made using insertional PCR (see Table 2.3 for details and conditions). The PCR products were then digested with the DpnI enzyme and used directly in *E. coli* transformation. Three colonies for each PCR condition were inoculated in LB broth, grown for 16 hours, and plasmids were isolated. For choosing ADGRG1 cDNAs with the correct insert size, plasmids were digested with KpnI and XbaI and then loaded in 1% agarose gel (Figure 3.1 and 3.2).

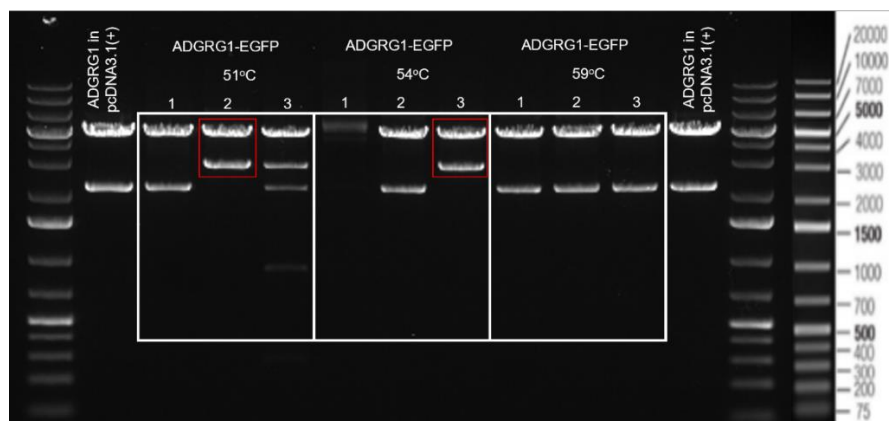


Figure 3.1. Agarose gel image of insertional PCR products after restriction enzyme (KpnI-XbaI) digestion to control the size of the EGFP tagged ADGRG1 on C-terminus. The size of EGFP tagged ADGRG1 cDNAs is 2799 bp. Red boxes indicate the plasmid and insert with the correct size. DNA ladder is Invitrogen™ 1 kb Plus DNA Ladder.

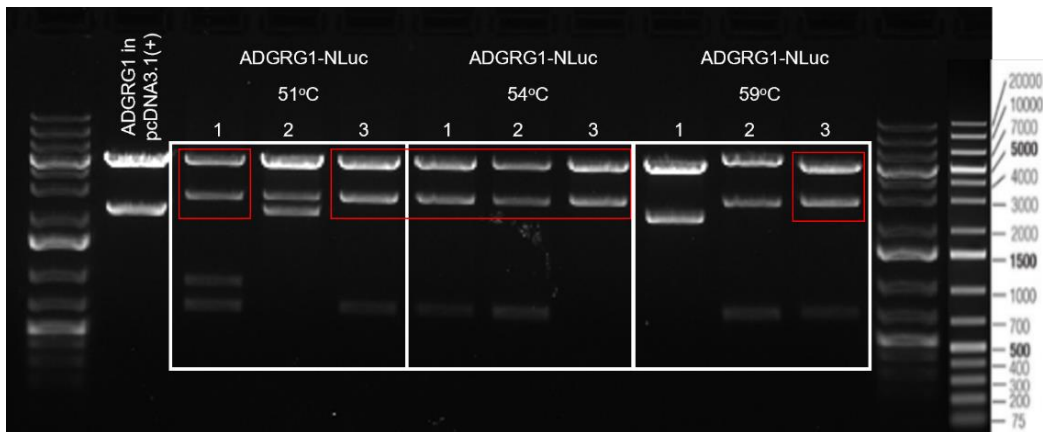


Figure 3.2. Agarose gel image of insertional PCR products after restriction enzyme (KpnI-XbaI) digestion to control the size of the NLuc tagged ADGRG1 on C-terminus. The size of NLuc tagged ADGRG1 cDNAs is 2595 bp. Red boxes indicate the plasmid and insert with the correct size. DNA ladder is Invitrogen™ 1 kb Plus DNA Ladder.

For ADGRG1-L-EGFP, ADGRG1-L-NLuc, ADGRG1-667-EGFP, and ADGRG1-667-NLuc, colony PCR (Table 2.6) was run to identify positive colonies before plasmid isolation. PCR products were loaded on 1% agarose gel (Figure 3.3 and 3.4).

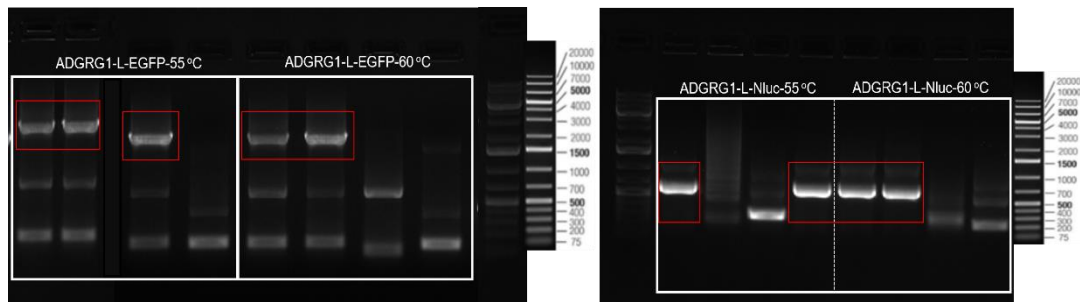


Figure 3.3. Agarose gel electrophoresis image of colony PCR for C-terminally tagged ADGRG1 cDNAs with EGFP carrying linker (2811 bp) or NLuc carrying linker (2607 bp). Red boxes indicate the plasmid and insert with the correct size. DNA ladder is Invitrogen™ 1 kb Plus DNA Ladder.

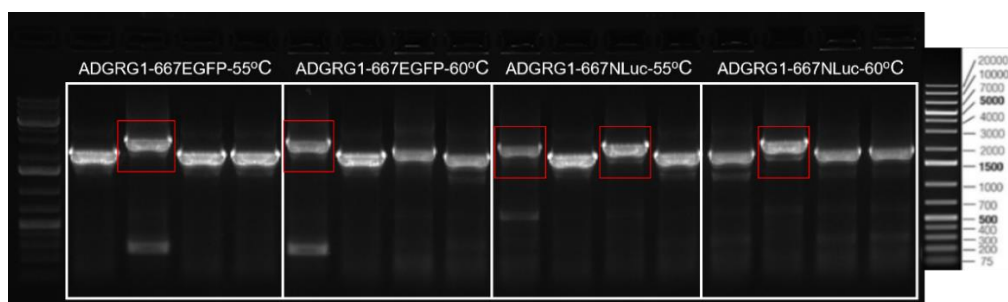


Figure 3.4. Agarose gel electrophoresis image of colony PCR for ADGRG1 cDNAs tagged with EGFP carrying linker (2799 bp) or NLuc carrying linker (2595 bp) between amino acids 667-668. Red boxes indicate the plasmid and insert with the correct size. DNA ladder is Invitrogen™ 1 kb Plus DNA Ladder.

The plasmids with the correct insert were isolated from the remaining colonies and digested with KpnI and XbaI restriction enzymes to control the size of the inserts. Digestion products loaded in 1% agarose gel.

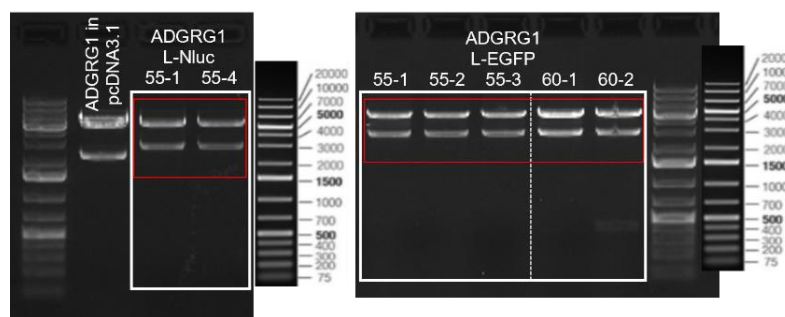


Figure 3.5. Agarose gel image of restriction enzyme (KpnI-XbaI) digestion products of the NLuc with linker or EGFP with linker tagged ADGRG1 on C-terminus. Red boxes indicate the plasmid and insert with the correct size. DNA ladder is Invitrogen™ 1 kb Plus DNA Ladder.

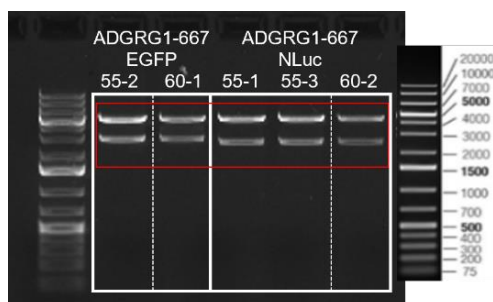


Figure 3.6. Agarose gel image of restriction enzyme (KpnI-XbaI) digestion products of the NLuc with linker or EGFP with linker tagged ADGRG1 on C-terminus. Red

boxes indicate the plasmid and insert with the correct size. DNA ladder is Invitrogen™ 1 kb Plus DNA Ladder.

Plasmids were verified by Sanger sequencing, and the constructs with correct sequences were imaged using a confocal microscope.

### 3.2 Truncation of ADGRG1

Truncated ADGRG1 receptor was constructed via the ligation method. The PCR protocol (see Table 2.9) was conducted to truncate ADGRG1 cDNA using ADGRG1-WT in pcDNA3.1(+). PCR products were purified via GeneJET PCR Purification Kit (ThermoFisher Scientific, USA). These double-stranded fragments carrying KpnI and XbaI restriction sites and vector were then digested with these restriction enzymes and loaded on an agarose gel to obtain pure insert and linearized vector. The ligation reaction was set up, and products were used directly in *E. coli* transformation. Isolated plasmids were digested with KpnI and XbaI restriction enzymes to control insert size, then loaded in 1% agarose gel (Figure 3.7).

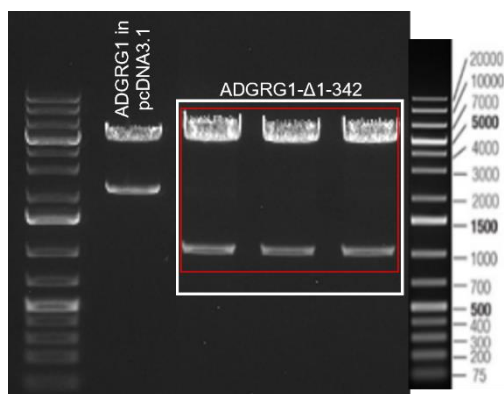


Figure 3.7. Agarose gel image of restriction enzyme (KpnI-XbaI) digestion products of the truncated ADGRG1 (1062 bp). Red box indicates the plasmid and inserts with the correct size. DNA ladder is Invitrogen™ 1 kb Plus DNA Ladder. FlhGPR56, full-length human GPR56 (ADGRG1).

Plasmids were sent for Sanger sequencing, and the constructs with correct sequences were used in the SRE-dual luciferase reporter assay.

### 3.3 Laser scanning confocal microscopy

Confocal imaging offers reduced background signal, which significantly improves resolution and image contrast in thin samples because confocal microscopes can eliminate the signals away from the focal plane with the help of a pinhole [180]. (Figure 3.8)

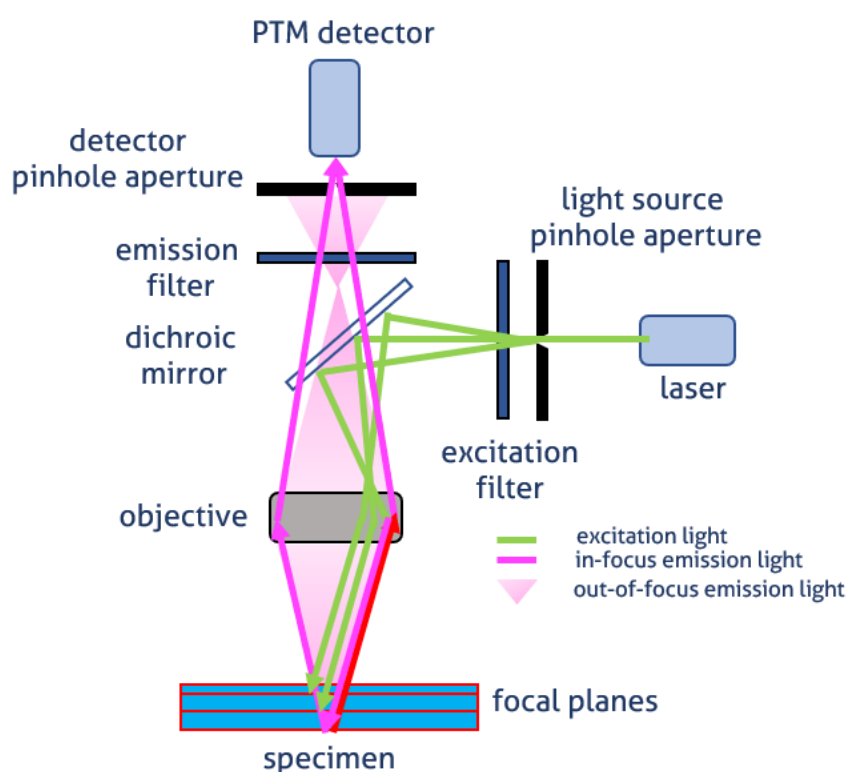


Figure 3.8. Schematic illustration of image generation in a confocal microscope. Adapted from ptglab.com.

Cells expressing ADGRG1 constructs were imaged using a laser scanning confocal microscope. HEK 293 cells were grown in 35-mm glass-bottom dishes, transfected with ADGRG1-EGFP, ADGRG1-L-EGFP, or ADGRG1-667-EGFP constructs, and imaged after 48 hours (Figure 3.9). Live cells imaging was done in a CO<sub>2</sub> incubation chamber (PeCon, Germany) using Zeiss 63x/1.4 Plan Apochrome Oil DIC objective. The images were acquired using an excitation laser beam at 488 nm, and EGFP emission was collected between 493 - 586 nm.

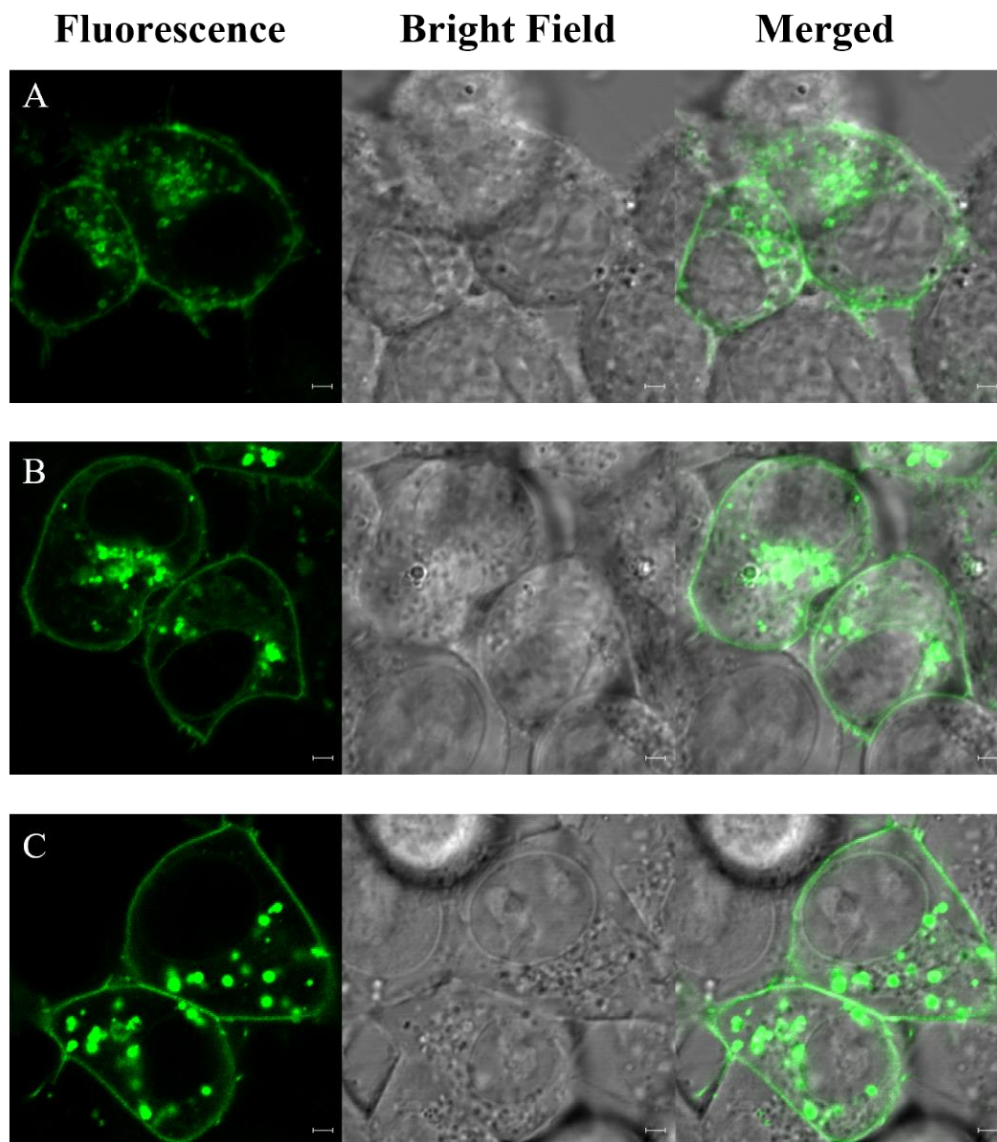


Figure 3.9. Laser scanning confocal images of ADGRG1-EGFP (A), ADGRG1-L-EGFP (B), and ADGRG1-667-EGFP (C). Scale bar corresponds to 2  $\mu$ m.

### 3.4 Western blotting

HEK 293 cells were transfected with C-terminally tagged ADGRG1 constructs in pcDDNA3.1(+) and WT ADGRG1 in pcDDNA3.1(+). Transformants were harvested for total protein extraction. 20 mg protein was loaded on each well and resolved on commercial precast SDS-PAGE. The stain-free gel image is given in Figure 3.10.

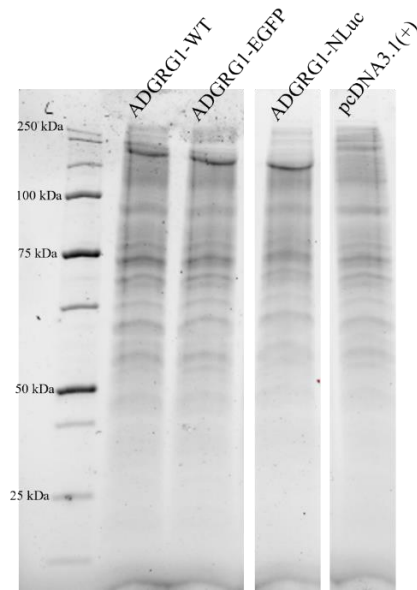


Figure 3.10. Before transfer, stain-free precast SDS gel image. The size of ADGRG-WT is 77.7 kDa; ADGRG1-CtE is 104.6 kDa; ADGRG1-CtN is 96.8 kDa. Precision Plus Protein™ Unstained Protein standard (Bio-Rad, USA) was used as a protein ladder.

The proteins on SDS gel were transferred to the PVDF membrane by a semi-dry blotting system. Figure 3.11 shows the gel image after transfer and the membrane image.

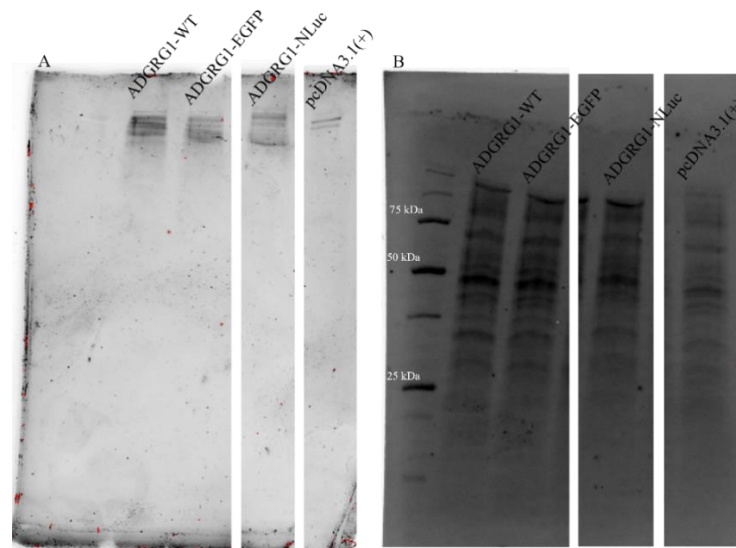


Figure 3.11. After transfer, stain-free precast SDS gel image (A) and PVDF membrane image (B).

The blot was probed with primary GPR56 Antibody (G-6) 200  $\mu\text{g}/\text{ml}$  (Santa Cruz Biotechnology, USA) following the blocking step. Then, IgGK BP-HRP (200  $\mu\text{g}/0.5\text{ ml}$ ) (Santa Cruz Biotechnology, USA) was used as the secondary antibody, and the blot was incubated with SuperSignal™ West Pico PLUS Chemiluminescent Substrate.

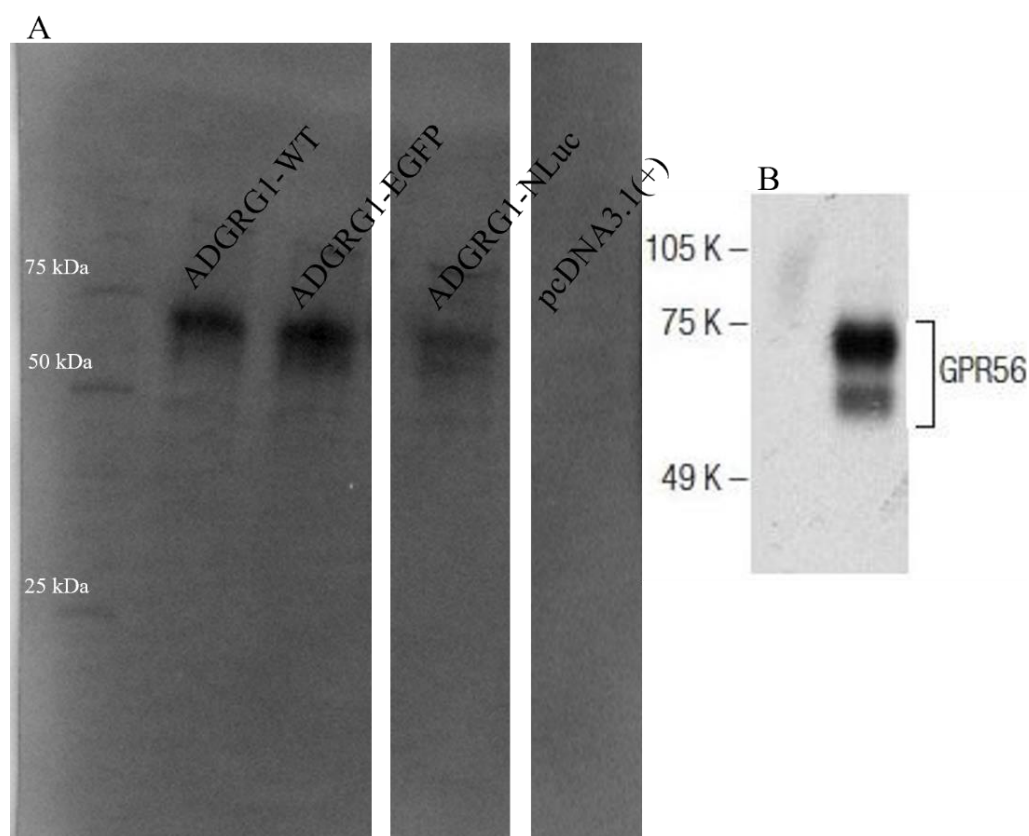


Figure 3.12. The immunoblot image. (A) The size of ADGRG1-WT is 77.7 kDa; ADGRG1-Ct-E is 104.6 kDa; ADGRG1-Ct-N is 96.8 kDa. (B) The immunoblot image of ADGRG1 (GPR56) detected by GPR56 Antibody (G-6) 200  $\mu\text{g}/\text{ml}$  was taken from Santa Cruz Biotechnology.

### 3.5 SRE-dual luciferase reporter assay

HEK 293 cells were co-transfected with SRE in pmirGLO plasmid and EGFP tagged ADGRG1 fusion proteins. Coelenterazine 400a and D-Luciferin as a mixture were used to obtain the bioluminescent signal, resulting from substrate oxidation by FLuc

and RLuc. Luciferases. Background signal obtained from cells transfected with empty plasmid subtracted from measured intensities of both FLuc and RLuc. Background-subtracted FLuc intensities normalized to background-subtracted RLuc intensities (experimental reporter/control reporter). Luciferase activity (%) calculated as follows:

$$\text{Luciferase activity (\%)} = \frac{\text{tagged ADGRG1}_N - \text{NC}_N}{\text{PC}_N - \text{NC}_N} \times 100$$

Where tagged ADGRG1<sub>N</sub> is the normalized ratio of fusion protein intensities, NC<sub>N</sub> is the normalizing ratio of intensities from cells transfected with only SRE plasmid, PC<sub>N</sub> is the normalizing ratio of ADGRG1-WT protein intensities. In other words, the activity of ADGRG1 constructs normalized to ADGRG-WT.

The data from triplicate samples and three separate readings were averaged and analyzed using two-way ANOVA with Bonferroni correction in GraphPad Prism 8 (Figure 3. 13).

The G protein signaling activity of ADGRG1 constructs was compared to ADGRG1-WT signaling activity using the SRE dual luciferase assay. The reporter luciferase (FLuc) activity was significantly increased in ADGRG1-Δ1-342 [55], supporting the literature. ADGRG1-EGFP had a similar effect with ADGRG1-WT on SRE activity. ADGRG1-L-EGFP and ADGRG1-667-EGFP also led to an increased SRE activity. It is noteworthy to mention that we did not observe any bleed-through from the cells treated with only D-luciferin in 410m80 filter or from cells treated only with coelenterazine 400a in the 610lp filter. These results suggested that all ADGRG1 constructs made in this study are functional.

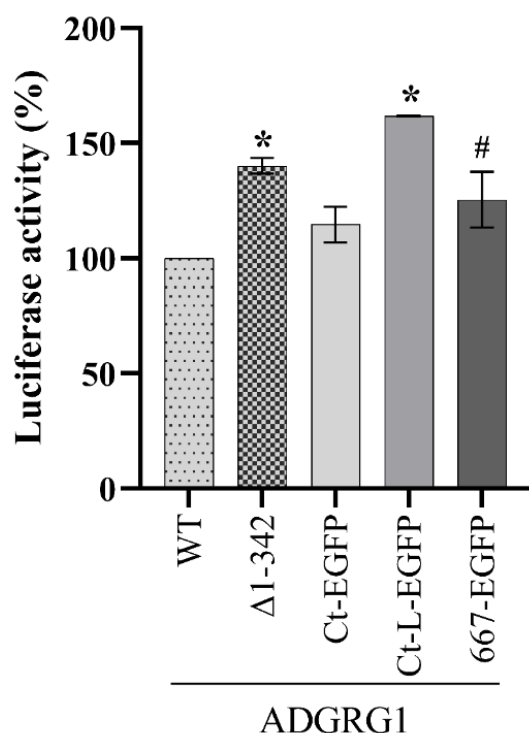


Figure 3.13. Dual Luciferase reporter assay in HEK 293 cells. The bars indicate ADGR1-WT, ADGRG1-Δ1-342, ADGRG1-EGFP, ADGRG1-L-EGFP, and ADGRG1-667-EGFP, respectively. Error bars denote the standard deviation among readings. # p<0.05. \* p<0.001. n=3.

### 3.6 NanoBRET assay

In the NanoBRET assay, NLuc tagged ADGRG1 receptors were used as a BRET donor, while EGFP tagged ADGRG1 receptors act as a BRET acceptor. HEK 293 cells were transfected with donor and acceptor pair tagged on C-terminal (ADGRG1-EGFP and ADGRG1-NLuc), fused via linker from C-terminal (ADGRG1-L-EGFP and ADGRG1-L-NLuc), or inserted between amino acid 667-668 (ADGRG1-667-EGFP and ADGRG1-667-NLuc). Furimazine as a substrate for NLuc was added onto cells, and energy transfer was measured as a fluorescence signal. The BRET ratio calculation is given in the following formula:

$$BRET\ ratio = \frac{SI_{EGFP} - BI_{EGFP}}{SI_{NLuc} - BI_{NLuc}}$$

where  $SI_{EGFP}$  is the intensity of sample (ADGRG1 construct) measured by EGFP (acceptor) emission filter,  $SI_{NLuc}$  is the intensity of sample measured by NLuc (donor) emission filter,  $BI_{EGFP}$  is the intensity of cells transfected with empty vector, measured by EGFP emission filter and,  $BI_{NLuc}$  is the intensity of cells transfected with empty vector, measured by NLuc emission filter.

The overlap of the NLuc emission spectrum at EGFP emission wavelength generates the background signal from the cells expressing only the donor. Thus, the ratio was corrected for the background signal by subtracting the background BRET ratio from the BRET ratio of the sample obtained from cells expressing the BRET pair. This calculation gives the net BRET ratio formulized as follows:

$$Net\ BRET\ ratio = \frac{SI_{EGFP} - BI_{EGFP}}{SI_{NLuc} - BI_{NLuc}} - cf$$

Where  $cf$  is the correction factor corresponding to the BRET ratio of the background signal measured from the cells expressing only the donor in the same experiment.

The data from triplicate samples and three separate readings were averaged and analyzed by using two-way ANOVA with Bonferroni correction in GraphPad Prism 8 (Figure 3. 14).

The bleed-through of the NLuc signal from the EGFP filter was calculated as 0.28. The net BRET ratio was 0.09, 0.22, and 0.23 for ADGRG1-EGFP & ADGRG1-NLuc, ADGRG1-L-EGFP & ADGRG1-L-NLuc, and ADGRG1-667-EGFP & ADGRG1-667-NLuc, respectively. According to the net BRET results, it can be concluded that ADGRG1 receptors tagged on C-terminus were shown to dimerize.

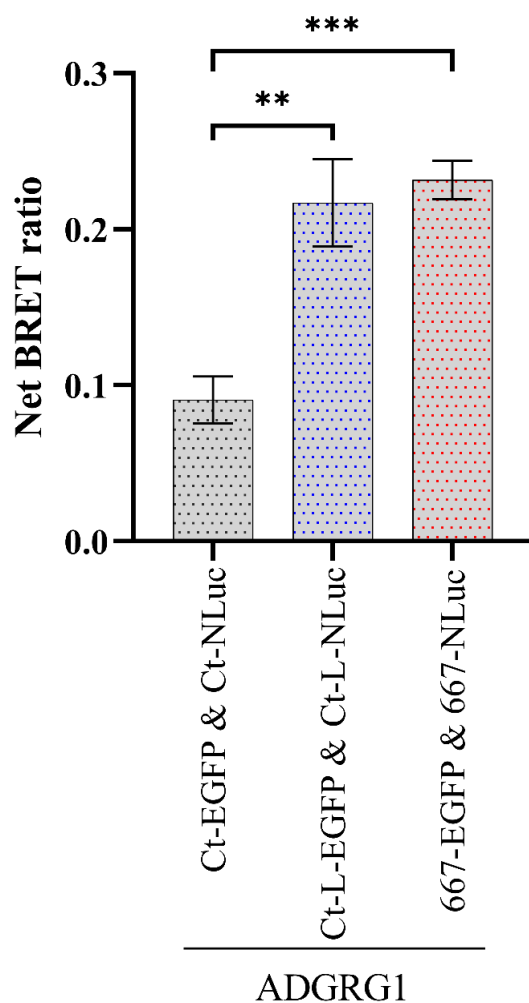


Figure 3.14. The net BRET ratio of ADGRG1 fusion proteins, including ADGRG1-EGFP and ADGRG1-NLuc; ADGRG1-Ct-L-EGFP and ADGRG1-L-NLuc; ADGRG1-667-EGFP and ADGRG1-NLuc. Error bars denote the standard deviation among readings.  $p < 0.05$ .  $n = 3$ .

### 3.7 BRET saturation assay

In saturation assay, a constant amount of NLuc (donor) and an increasing amount of EGFP (acceptor) were co-expressed in HEK 293 cells to eliminate the bystander BRET. The BRET ratio was calculated as described in Section 3.6. The data from triplicate samples and three separate readings were averaged, and the saturation curve was plotted as a function of the acceptor/donor ratio using GraphPad Prism 8 Figure 3.15.

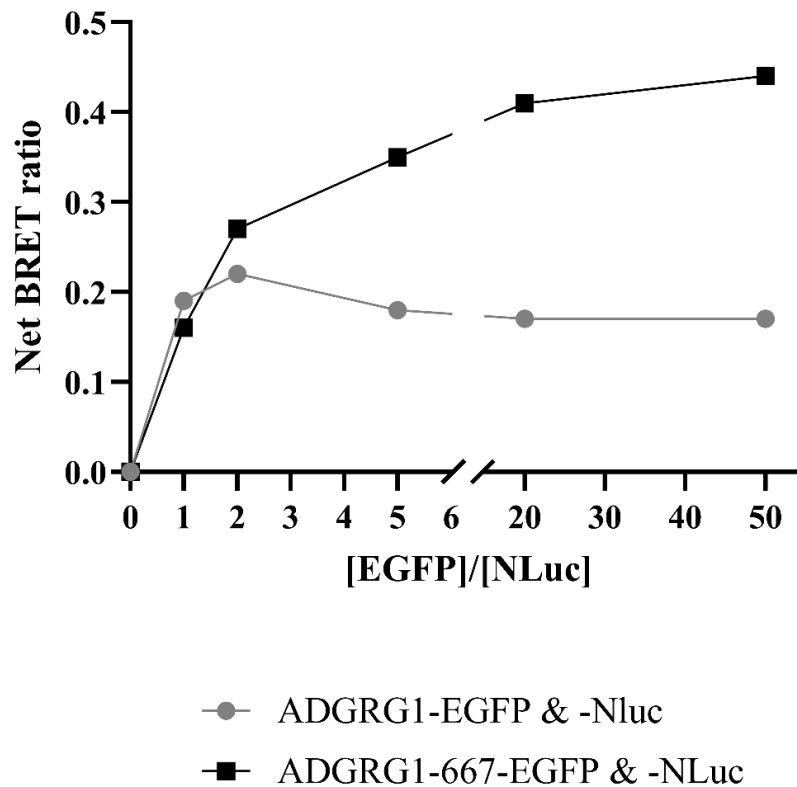


Figure 3.15. BRET saturation assay for ADGRG1 constructs. The ratio of EGFP tagged ADGRG1 receptor concentration to NLuc tagged ADGRG1 receptor concentration ( $[EGFP]/[NLuc]$ ) is 0, 1, 2, 5, 20, 50, respectively.

In this assay, ADGRG1-L-EGFP and ADGRG1-L-NLuc were not included since the only difference between these fusion proteins and tagged ADGRG1 on C-terminus is a four amino acid long linker. Saturation assay suggested the specificity of BRET for ADGRG1 because the saturation curve fits the theoretical curve and did not give a linear increase with the increased acceptor concentration, expected in the case of the bystander BRET. At higher ratios of  $[EGFP]/[NLuc]$ , the BRET ratio reached a plateau, revealing the saturable interaction between EGFP or NLuc tagged ADGRG1.



## CHAPTER 4

### DISCUSSION

#### 4.1 Construction of fluorescent or bioluminescent-tagged receptors

The critical part of tagged protein construction is deciding on the tagging position since the receptor's trafficking, localization, and signaling should be preserved after the fluorescent or bioluminescent protein insertion. To monitor the oligomerization of receptors, the extracellular N-terminus (Nt) and extracellular loop can be considered a position for inserting the tags. However, N-terminal tagging may disturb the membrane localization due to the size of the tag and most GPCRs have a membrane target signal on their N-terminus [181]. In extracellular loop tagging, large fluorophores may disrupt the receptor's conformation, resulting in improper signaling. Different studies have indicated that GPCR - GPCR dimerization are mainly found through the receptors' cytosolic carboxy end (C-terminus, Ct) [182-184]. Thus, the C-terminal tagging of the GPCRs is the most straightforward method for investigating receptor oligomerization by maintaining the receptors' function and localization. In addition, direct fusion of protein tags without a linker may interfere with the structure of protein domains, resulting in impaired bioactivity [185], low yield in protein synthesis [186], or protein misfolding [187]. Therefore, in this study Gly-Ser-Ser-Gly linker sequence was preferred in addition to direct fusion since it is flexible and composed of small non-polar (Gly) and polar (Ser) amino acids which allow for mobility and appropriate separation [188]. Also, an alternative position nearby the C-terminus after the 7-TM, between the amino acids 667-668, was also determined, considering the secondary structure of the region.

## **4.2 Truncation of ADGRG1**

ADGRG1 is characterized by a large N-terminus unlike the canonical GPCRs [20] and cleaved at the GPS motif in the GAIN domain located in NTF by autocatalytic reaction during receptor processing [27], but remains non-covalently bound to the CTF [25]. Many different studies revealed that the NTF of the ADGRG1 regulates the receptor function [20, 55]. In general, N-terminally truncated GPCRs do not show increased activity. Truncation of NTF can result in alterations in ligand binding properties or receptor trafficking [189-191]. Interestingly, N-terminally truncated ADGRG1 receptors, especially at position 342, show robust activity when compared to the full-length (WT) receptor [55]. Based on this finding, the truncated ADGRG1 receptor was constructed to be used as a control in the SRE-dual luciferase reporter assay.

## **4.3 Laser scanning confocal microscopy**

ADGRG1 fusion proteins were successfully constructed, and HEK 293 cells were transfected with EGFP tagged ADGRG1 constructs for live-cell imaging. The images were acquired using an excitation laser beam at 488 nm, and EGFP emission was collected between 493 - 586 nm. All EGFP constructs were localized mainly on the plasma membrane, as expected. Additionally, ADGRG1 constructs were seen in subcellular localizations in vesicle-like structures. This observation is expected due to the ongoing trafficking, protein synthesis, and endocytosis during live-cell imaging.

Bioluminescence imaging is not as straightforward as fluorescence imaging, and the confocal microscopes in general are not equipped for bioluminescence imaging. However, it is expected that ADGRG1 NLuc constructs would give a similar cellular localization as the EGFP tagged constructs on the same positions.

#### **4.4 Western blotting**

As seen in Figure 3.11, almost all proteins were transferred to the immunoblot. In Figure 3.12.A, all constructs were in the same size as the WT receptor and had 2 bands around 75 kDa, compatible with the ADGRG1 Ab probing image from Santa Cruz Biotechnology in Figure 3.12.B. However, the size of ADGRG1-EGFP is approximately 105 kDa, and ADGRG1-NLuc is approximately 97 kDa. The ADGRG1 primary antibody is against amino acids 289-381, corresponding to the NTF of the receptor. Autoproteolysis at the GAIN domain of ADGRG1 between the end of the NTF and the beginning of the 7-TM region is a known phenomenon [16], however the NTF and CTF still remain bound together by non-covalent interactions [25]. After the membrane probing, only NTF of the tagged and WT receptors was detected on the immunoblot, possibly due to the dissociation of CTF of ADGRG1 in SDS-PAGE. This finding also is also further evidence for the self-cleavage of the ADGRG1 receptor.

#### **4.5 SRE-dual luciferase reporter assay**

The assay is based on the downstream Serum Response Element activity of ADGRG1 constructs, and FLuc in pmirGLO plasmid acts as a reporter under the control of the target SRE promoter, while RLuc is called a control reporter since its expression is constitutive in the transfected cells.

We did not follow the commercial assay protocols for this assay because commercial protocols suggest cell lysis before the addition of bioluminescent substrates. We did not get reproducible results using this lytic method and decided to optimize the protocol without lysing the cells (data not shown). Bioluminescent substrates can pass through cellular membrane; thus, we prepared substrate mixture and added it directly to the harvested cells to measure the bioluminescence signal inside the cell.

Overexpression of ADGRG1 is known to stimulate SRE-mediated transcription through  $G\alpha_{12/13}$  and Rho [57, 59] and truncated ADGRG1 from amino acid 342

(ADGRG1- $\Delta$ 1-342) has an increased SRE activity compared to WT [55]. The WT-ADGRG1 activity was considered as 100% and compared to each construct. Accordingly, the truncated receptor showed increased activity, corresponding with the previous literature [55]. According to the results, all ADGRG1 constructs made in this study were functional. NLuc-tagged ADGRG1 receptors could not be tested for the function using this method since both NLuc and RLuc oxidize coelenterazine. However, NLuc constructs were assumed to be functional because the tagging position was the same, and NLuc is smaller in size compared to EGFP. We are also in the process of constructing fluorescence-based pmirGLO plasmid to test the functionality of the NLuc tagged ADGRG1 constructs.

We used an overexpression vector (pcDNA3.1(+)) in this study and the overexpression of proteins can trigger non-specific events in cells. To eliminate this possibility, Kim *et al.* co-expressed shRNA, which specifically blocks the human ADGRG1 expression in HEK293T cells, and revealed that SRE activity driven by ADGRG1 dramatically decreased [57]. This finding proves that SRE activity depends on ADGRG1 and is independent of overexpression. So, in this study the SRE activity of the ADGRG1 constructs is not due to overexpression in our experimental conditions.

#### **4.6 NanoBRET assay**

Optical filters are used to separate two signals from the donor and the acceptor in BRET measurements. The light passes through the filters, and bandpass barriers refine the light before it reaches the detector [192]. Thus, filter characteristics determine the quality of the separation of donor and acceptor emissions. We chose our filter set to achieve the optimal separation both in BRET and SRE assay.

According to the results reported herein, all the C-terminally tagged ADGRG1 receptors were shown form dimers using our BRET assay. Additionally, all the BRET pairs were measured to be different, hence we can claim that the interaction

between ADGRG1 receptors was specific. We would have expected a same net BRET in the case of non-specific interactions due to the random collisions. The addition of linker (GSSG) or tagging from a more interior position, 667, improved the BRET ratio. Direct insertion of EGFP to the ADGRG1 C-terminus may have interfered with the receptor function, and we might not have been able to detect this effect using an SRE-based functional assay. Thus, we are in the process of confirming the functionality of ADGRG1 constructs using the Nuclear Factor of Activated T-cells Response Element (NFAT-RE)-Dual Luciferase Reporter Assay. ADGRG1 downstream signaling also includes the activation of NFAT-RE [87]. As a summary, these results give us a clue about the specific interaction between ADGRG1 constructs.

#### **4.7 BRET saturation assay**

BRET-based studies used for showing receptor-receptor interactions require some controls to eliminate the false-positive signals because this method is known to be affected by protein expression levels and sample handling. BRET assays with one particular donor-to-acceptor ratio are considered qualitative. BRET saturation assay has been applied to prove the specificity of basic BRET experiments and provide additional information as a quantitative assay. A constant amount of BRET donor (NLuc) was titrated with the increasing amounts of BRET acceptor (EGFP) to saturate the donor. The BRET saturation curve in Figure 3.15 fitted the theoretical curve in which the BRET signal increases in a hyperbolic manner and reaches a plateau when all donors have occupied with acceptor molecules. So, the saturation curves plotted in this study prove that the interaction between ADGRG1 receptors in live cells are specific and independent of the receptor overexpression.



## CHAPTER 5

### CONCLUSION

Biochemical and physiological methods have proved the existence of GPCR oligomers both *in vitro* and *in vivo*. The hypothesis of this study was “ADGRG1 a model aGPCR, as numerous other GPCRs family members, can form receptor dimers”. Understanding their functional role and therapeutic potential is one of the most important questions to be answered. Powerful and straightforward methods, like BRET, have been utilized to reveal the receptor-receptor interactions. In this study, the dimerization of ADGRG1, a model aGPCR, was investigated using NanoBRET.

ADGRG1 fusion proteins were constructed tagging with NLuc or EGFP at various positions at receptor C-terminal domain. The plasma membrane localization, expression, and functionality of these constructs were assessed. All constructs were localized on the plasma membrane with some intracellular puncta, possibly due to the biosynthesis, trafficking, and endocytosis. The expressions of ADGRG1 constructs in HEK 293 cells were shown by Western blotting. The ADGRG1 constructs were also shown to activate SRE-mediated transcription through  $G\alpha_{12/13}$  in accordance with the previous literature [59]. The dimerization ADGRG1 constructs were determined by NanoBRET. However, the BRET assays could give “background” energy transfer when the signal from the crowded cell membrane reaches a remarkable level. Thus, the possibility of bystander BRET was eliminated with BRET saturation assay. For monomeric proteins, net BRET is in a linear relationship with increasing acceptor concentration. On the other hand, the hyperbolic relationship is expected for real oligomers.

Until this study, there was no definitive information on the dimerization of any member of aGPCR families in the literature, and our study hypothesized that aGPCRs also form dimers as numerous other GPCRs. This study is the first to show the *in vivo* homodimerization in the aGPCR family. The BRET method developed herein provided us an ADGRG1 dimerization assay and will open the path for investigating the effect of receptor dimerization on the activation mechanisms of ADGRG1; the effect of large N-terminal domain on receptor dimerization and finally the effect of *BFPP* mutations on this dimerization.

## Future Work

The formation of oligomeric assemblies in the endoplasmic reticulum (ER) has been reported as an essential step in ER quality control for many proteins [193]. Proteins in oligomeric complexes could be able to escape the ER quality control system since their hydrophobic parts or retention signals are masked during the interaction. Oligomerization is also important for membrane localization of GPCRs [194]. Several different studies using FRET and BRET methods have shown that the GPCR dimerization starts in the ER [195, 196]. Combining these data and our imaging results, we will investigate the ADGRG1 oligomerization using organelle markers and a fluorescence-based method termed Bimolecular Fluorescence Complementation (BiFC) in ER and other subcellular localizations. Additionally, the imaging of NLuc tagged ADGRG1 constructs combining the EGFP tagged constructs colocalization will be optimized.

In the Western blot technique, to detect CTF, we are in search of antibody. Moreover, Western blot optimization with anti-EGFP antibody is still in optimization for detecting ADGRG1-EGFP, ADGRG1-L-EGFP and ADGRG1-667-EGFP. We are also planning to use a recently released anti-NLuc antibody (Promega, USA) for the verification of ADGRG1-NLuc, ADGRG1-L-NLuc and ADGRG1-667-NLuc.

The fluorescence-based SRE and NFAT reporter assay plasmids are currently under construction to be used for NLuc tagged ADGRG1 constructs in Dual-Luciferase Reporter Assay. For this, FLuc and RLuc cDNAs in the pmirGLO plasmid are being replaced with EGFP and mCherry fluorescent proteins.

In BRET and saturation assays, the oligomerization deficient-mutants of ADGRG1 receptor will be identified. Additionally, linkage and pedigree analysis have reported at least 20 mutations in ADGRG1 leading to *BFPP*, which is an autosomal recessively inherited human developmental disorder [197]. However, the effects of these mutations on receptor activation and signaling through oligomerization still

mostly remain unknown. Thus, the relationship between *BFPP* mutations and ADGRG1 oligomerization will be studied. Moreover, the synthetic ECD binding proteins for ADGRG1 were engineered in 2017 by Dr. Demet Araç and her colleagues [54]. The ADGRG1 oligomerization upon *Stachel*-independent activation will be studied using these proteins. The long extracellular N-terminus of ADGRG1 includes several regions and domains, like PLL, GAIN, and serine-threonine proline (STP) segment [197, 198]. The effect of these domains on ADGRG1 oligomerization will be investigated using various truncated receptor constructs.

## REFERENCES

1. Henderson, R. and P.N.T. Unwin, *Three-dimensional model of purple membrane obtained by electron microscopy*. Nature, 1975. **257**(5521): p. 28-32.
2. Baldwin, J.M., *Structure and function of receptors coupled to G proteins*. Curr Opin Cell Biol, 1994. **6**(2): p. 180-90.
3. Schonenbach, N.S., S. Hussain, and M.A. O'Malley, *Structure and function of G protein-coupled receptor oligomers: implications for drug discovery*. Wiley Interdiscip Rev Nanomed Nanobiotechnol, 2015. **7**(3): p. 408-27.
4. Latek, D., et al., *G protein-coupled receptors--recent advances*. Acta Biochim Pol, 2012. **59**(4): p. 515-29.
5. Lefkowitz, R.J., *The superfamily of heptahelical receptors*. Nat Cell Biol, 2000. **2**(7): p. E133-6.
6. Hopkins, A.L. and C.R. Groom, *The druggable genome*. Nat Rev Drug Discov, 2002. **1**(9): p. 727-30.
7. Bockaert, J. and J.P. Pin, *Molecular tinkering of G protein-coupled receptors: an evolutionary success*. Embo j, 1999. **18**(7): p. 1723-9.
8. Lagerström, M.C. and H.B. Schiöth, *Structural diversity of G protein-coupled receptors and significance for drug discovery*. Nat Rev Drug Discov, 2008. **7**(4): p. 339-57.
9. Alexander, S.P., et al., *THE CONCISE GUIDE TO PHARMACOLOGY 2017/18: G protein-coupled receptors*. Br J Pharmacol, 2017. **174** Suppl 1(Suppl Suppl 1): p. S17-s129.

10. Basith, S., et al., *Exploring G Protein-Coupled Receptors (GPCRs) Ligand Space via Cheminformatics Approaches: Impact on Rational Drug Design*. *Frontiers in Pharmacology*, 2018. **9**(128).
11. Ghosh, E., et al., *Methodological advances: the unsung heroes of the GPCR structural revolution*. *Nat Rev Mol Cell Biol*, 2015. **16**(2): p. 69-81.
12. Schiöth, H.B. and R. Fredriksson, *The GRAFS classification system of G-protein coupled receptors in comparative perspective*. *Gen Comp Endocrinol*, 2005. **142**(1-2): p. 94-101.
13. Fredriksson, R., et al., *The G-protein-coupled receptors in the human genome form five main families. Phylogenetic analysis, paralogon groups, and fingerprints*. *Mol Pharmacol*, 2003. **63**(6): p. 1256-72.
14. Nordstrom, K.J., et al., *The Secretin GPCRs descended from the family of Adhesion GPCRs*. *Mol Biol Evol*, 2009. **26**(1): p. 71-84.
15. Bjarnadottir, T.K., et al., *The human and mouse repertoire of the adhesion family of G-protein-coupled receptors*. *Genomics*, 2004. **84**(1): p. 23-33.
16. Langenhan, T., G. Aust, and J. Hamann, *Sticky Signaling—Adhesion Class G Protein-Coupled Receptors Take the Stage*. *Science Signaling*, 2013. **6**(276): p. re3-re3.
17. Hamann, J., et al., *International Union of Basic and Clinical Pharmacology. XCIV. Adhesion G protein-coupled receptors*. *Pharmacol Rev*, 2015. **67**(2): p. 338-67.
18. Wilde, C., et al., *The constitutive activity of the adhesion GPCR GPR114/ADGRG5 is mediated by its tethered agonist*. *FASEB J*, 2016. **30**(2): p. 666-73.
19. Bjarnadottir, T.K., et al., *Identification of novel splice variants of Adhesion G protein-coupled receptors*. *Gene*, 2007. **387**(1-2): p. 38-48.

20. Salzman, G.S., et al., *Structural Basis for Regulation of GPR56/ADGRG1 by Its Alternatively Spliced Extracellular Domains*. Neuron, 2016. **91**(6): p. 1292-1304.
21. Aust, G., et al., *Detection of alternatively spliced EMR2 mRNAs in colorectal tumor cell lines but rare expression of the molecule in colorectal adenocarcinomas*. Virchows Arch, 2003. **443**(1): p. 32-7.
22. Matsushita, H., V.G. Lelianaova, and Y.A. Ushkaryov, *The latrophilin family: multiply spliced G protein-coupled receptors with differential tissue distribution*. FEBS Lett, 1999. **443**(3): p. 348-52.
23. Rothe, J., et al., *Involvement of the Adhesion GPCRs Latrophilins in the Regulation of Insulin Release*. Cell Rep, 2019. **26**(6): p. 1573-1584 e5.
24. Boucard, A.A., S. Maxeiner, and T.C. Sudhof, *Latrophilins function as heterophilic cell-adhesion molecules by binding to teneurins: regulation by alternative splicing*. J Biol Chem, 2014. **289**(1): p. 387-402.
25. Yona, S., et al., *Adhesion-GPCRs: emerging roles for novel receptors*. Trends Biochem Sci, 2008. **33**(10): p. 491-500.
26. Arac, D., et al., *A novel evolutionarily conserved domain of cell-adhesion GPCRs mediates autoprolysis*. EMBO J, 2012. **31**(6): p. 1364-78.
27. Krasnoperov, V., et al., *Structural requirements for alpha-latrotoxin binding and alpha-latrotoxin-stimulated secretion. A study with calcium-independent receptor of alpha-latrotoxin (CIRL) deletion mutants*. J Biol Chem, 1999. **274**(6): p. 3590-6.
28. Krasnoperov, V.G., et al., *alpha-Latrotoxin stimulates exocytosis by the interaction with a neuronal G-protein-coupled receptor*. Neuron, 1997. **18**(6): p. 925-37.
29. Krasnoperov, V., et al., *Post-translational proteolytic processing of the calcium-independent receptor of alpha-latrotoxin (CIRL), a natural chimera of the cell adhesion protein and the G protein-coupled receptor. Role of the G protein-coupled receptor proteolysis site (GPS) motif*. J Biol Chem, 2002. **277**(48): p. 46518-26.

30. Lin, H.H., et al., *Autocatalytic cleavage of the EMR2 receptor occurs at a conserved G protein-coupled receptor proteolytic site motif*. J Biol Chem, 2004. **279**(30): p. 31823-32.
31. Fredriksson, R., et al., *Novel human G protein-coupled receptors with long N-terminals containing GPS domains and Ser/Thr-rich regions*. FEBS Lett, 2002. **531**(3): p. 407-14.
32. Stacey, M., et al., *EMR4, a novel epidermal growth factor (EGF)-TM7 molecule up-regulated in activated mouse macrophages, binds to a putative cellular ligand on B lymphoma cell line A20*. J Biol Chem, 2002. **277**(32): p. 29283-93.
33. Liebscher, I., et al., *A tethered agonist within the ectodomain activates the adhesion G protein-coupled receptors GPR126 and GPR133*. Cell Rep, 2014. **9**(6): p. 2018-26.
34. Kishore, A. and R.A. Hall, *Versatile Signaling Activity of Adhesion GPCRs*, in *Adhesion G Protein-coupled Receptors: Molecular, Physiological and Pharmacological Principles in Health and Disease*, T. Langenhan and T. Schöneberg, Editors. 2016, Springer International Publishing: Cham. p. 127-146.
35. Demberg, L.M., et al., *Identification of the tethered peptide agonist of the adhesion G protein-coupled receptor GPR64/ADGRG2*. Biochem Biophys Res Commun, 2015. **464**(3): p. 743-7.
36. Petersen, S.C., et al., *The adhesion GPCR GPR126 has distinct, domain-dependent functions in Schwann cell development mediated by interaction with laminin-211*. Neuron, 2015. **85**(4): p. 755-69.
37. Scholz, N., et al., *The adhesion GPCR latrophilin/CIRL shapes mechanosensation*. Cell Rep, 2015. **11**(6): p. 866-874.
38. Stoveken, H.M., et al., *Adhesion G protein-coupled receptors are activated by exposure of a cryptic tethered agonist*. Proc Natl Acad Sci U S A, 2015. **112**(19): p. 6194-9.

39. Kishore, A., et al., *Stalk-dependent and Stalk-independent Signaling by the Adhesion G Protein-coupled Receptors GPR56 (ADGRG1) and BAI1 (ADGRB1)*. J Biol Chem, 2016. **291**(7): p. 3385-94.
40. Promel, S., T. Langenhan, and D. Arac, *Matching structure with function: the GAIN domain of adhesion-GPCR and PKD1-like proteins*. Trends Pharmacol Sci, 2013. **34**(8): p. 470-8.
41. Lin, H.-H., et al., *GPS Proteolytic Cleavage of Adhesion-GPCRs*, in *Adhesion-GPCRs: Structure to Function*, S. Yona and M. Stacey, Editors. 2010, Springer US: Boston, MA. p. 49-58.
42. Davies, T., R. Mariani, and R. Latif, *The TSH receptor reveals itself*. Journal of Clinical Investigation, 2002. **110**(2): p. 161-164.
43. Hsiao, C.C., et al., *Site-specific N-glycosylation regulates the GPS auto-proteolysis of CD97*. FEBS Lett, 2009. **583**(19): p. 3285-90.
44. Gray, J.X., et al., *CD97 is a processed, seven-transmembrane, heterodimeric receptor associated with inflammation*. J Immunol, 1996. **157**(12): p. 5438-47.
45. Jin, Z., et al., *Disease-associated mutations affect GPR56 protein trafficking and cell surface expression*. Hum Mol Genet, 2007. **16**(16): p. 1972-85.
46. Chang, G.-W., et al., *Proteolytic cleavage of the EMR2 receptor requires both the extracellular stalk and the GPS motif*. FEBS Letters, 2003. **547**(1-3): p. 145-150.
47. Qian, F., et al., *Cleavage of polycystin-1 requires the receptor for egg jelly domain and is disrupted by human autosomal-dominant polycystic kidney disease 1-associated mutations*. Proc Natl Acad Sci U S A, 2002. **99**(26): p. 16981-6.
48. Promel, S., et al., *The GPS motif is a molecular switch for bimodal activities of adhesion class G protein-coupled receptors*. Cell Rep, 2012. **2**(2): p. 321-31.

49. Audet, M. and M. Bouvier, *Restructuring G-protein-coupled receptor activation*. Cell, 2012. **151**(1): p. 14-23.
50. Bortolato, A., et al., *Structure of Class B GPCRs: new horizons for drug discovery*. Br J Pharmacol, 2014. **171**(13): p. 3132-45.
51. de Graaf, C., et al., *Extending the Structural View of Class B GPCRs*. Trends Biochem Sci, 2017. **42**(12): p. 946-960.
52. Zhu, B., et al., *GAIN domain-mediated cleavage is required for activation of G protein-coupled receptor 56 (GPR56) by its natural ligands and a small-molecule agonist*. J Biol Chem, 2019. **294**(50): p. 19246-19254.
53. Kishore, A. and R.A. Hall, *Disease-associated extracellular loop mutations in the adhesion G protein-coupled receptor G1 (ADGRG1; GPR56) differentially regulate downstream signaling*. J Biol Chem, 2017. **292**(23): p. 9711-9720.
54. Salzman, G.S., et al., *Stachel-independent modulation of GPR56/ADGRG1 signaling by synthetic ligands directed to its extracellular region*. Proc Natl Acad Sci U S A, 2017. **114**(38): p. 10095-10100.
55. Paavola, K.J., et al., *The N terminus of the adhesion G protein-coupled receptor GPR56 controls receptor signaling activity*. J Biol Chem, 2011. **286**(33): p. 28914-21.
56. Promel, S., et al., *Characterization and functional study of a cluster of four highly conserved orphan adhesion-GPCR in mouse*. Dev Dyn, 2012. **241**(10): p. 1591-602.
57. Kim, J.E., et al., *Splicing variants of the orphan G-protein-coupled receptor GPR56 regulate the activity of transcription factors associated with tumorigenesis*. J Cancer Res Clin Oncol, 2010. **136**(1): p. 47-53.
58. Bae, B.I., et al., *Evolutionarily dynamic alternative splicing of GPR56 regulates regional cerebral cortical patterning*. Science, 2014. **343**(6172): p. 764-8.

59. Iguchi, T., et al., *Orphan G protein-coupled receptor GPR56 regulates neural progenitor cell migration via a G alpha 12/13 and Rho pathway*. J Biol Chem, 2008. **283**(21): p. 14469-78.
60. Chiang, N.Y., et al., *GPR56/ADGRG1 Activation Promotes Melanoma Cell Migration via NTF Dissociation and CTF-Mediated Galpha12/13/RhoA Signaling*. J Invest Dermatol, 2017. **137**(3): p. 727-736.
61. Stoveken, H.M., et al., *Gedunin- and Khivorin-Derivatives Are Small-Molecule Partial Agonists for Adhesion G Protein-Coupled Receptors GPR56/ADGRG1 and GPR114/ADGRG5*. Mol Pharmacol, 2018. **93**(5): p. 477-488.
62. Piao, X., et al., *G protein-coupled receptor-dependent development of human frontal cortex*. Science, 2004. **303**(5666): p. 2033-6.
63. Piao, X. and C.A. Walsh, *A novel signaling mechanism in brain development*. Pediatr Res, 2004. **56**(3): p. 309-10.
64. Bai, Y., et al., *GPR56 is highly expressed in neural stem cells but downregulated during differentiation*. Neuroreport, 2009. **20**(10): p. 918-22.
65. Jeong, S.J., et al., *Characterization of G protein-coupled receptor 56 protein expression in the mouse developing neocortex*. J Comp Neurol, 2012. **520**(13): p. 2930-40.
66. Murayama, A.Y., et al., *The polymicrogyria-associated GPR56 promoter preferentially drives gene expression in developing GABAergic neurons in common marmosets*. Sci Rep, 2020. **10**(1): p. 21516.
67. Chang, B.S., et al., *Bilateral frontoparietal polymicrogyria: clinical and radiological features in 10 families with linkage to chromosome 16*. Ann Neurol, 2003. **53**(5): p. 596-606.
68. Koirala, S., et al., *GPR56-regulated granule cell adhesion is essential for rostral cerebellar development*. J Neurosci, 2009. **29**(23): p. 7439-49.

69. Luo, R., et al., *G protein-coupled receptor 56 and collagen III, a receptor-ligand pair, regulates cortical development and lamination*. Proc Natl Acad Sci U S A, 2011. **108**(31): p. 12925-30.
70. Chiang, N.Y., et al., *Disease-associated GPR56 mutations cause bilateral frontoparietal polymicrogyria via multiple mechanisms*. J Biol Chem, 2011. **286**(16): p. 14215-25.
71. Luo, R., et al., *Mechanism for adhesion G protein-coupled receptor GPR56-mediated RhoA activation induced by collagen III stimulation*. PLoS One, 2014. **9**(6): p. e100043.
72. Zhang, D., et al., *Niche-derived laminin-511 promotes midbrain dopaminergic neuron survival and differentiation through YAP*. Sci Signal, 2017. **10**(493).
73. Jeong, S.J., et al., *GPR56 functions together with alpha3beta1 integrin in regulating cerebral cortical development*. PLoS One, 2013. **8**(7): p. e68781.
74. Bahi-Buisson, N. and R. Guerrini, *Diffuse malformations of cortical development*. Handb Clin Neurol, 2013. **111**: p. 653-65.
75. Piao, X., et al., *Genotype-phenotype analysis of human frontoparietal polymicrogyria syndromes*. Ann Neurol, 2005. **58**(5): p. 680-7.
76. Colognato, H. and I.D. Tzvetanova, *Glia unglued: how signals from the extracellular matrix regulate the development of myelinating glia*. Dev Neurobiol, 2011. **71**(11): p. 924-55.
77. Chun, S.J., et al., *Integrin-linked kinase is required for laminin-2-induced oligodendrocyte cell spreading and CNS myelination*. J Cell Biol, 2003. **163**(2): p. 397-408.
78. Relucio, J., et al., *Laminin regulates postnatal oligodendrocyte production by promoting oligodendrocyte progenitor survival in the subventricular zone*. Glia, 2012. **60**(10): p. 1451-67.

79. Arai, K. and E.H. Lo, *Astrocytes protect oligodendrocyte precursor cells via MEK/ERK and PI3K/Akt signaling*. J Neurosci Res, 2010. **88**(4): p. 758-63.
80. Domingues, H.S., et al., *Oligodendrocyte, Astrocyte, and Microglia Crosstalk in Myelin Development, Damage, and Repair*. Front Cell Dev Biol, 2016. **4**: p. 71.
81. Hagemeyer, N., et al., *Microglia contribute to normal myelinogenesis and to oligodendrocyte progenitor maintenance during adulthood*. Acta Neuropathol, 2017. **134**(3): p. 441-458.
82. Giera, S., et al., *The adhesion G protein-coupled receptor GPR56 is a cell-autonomous regulator of oligodendrocyte development*. Nat Commun, 2015. **6**: p. 6121.
83. Ackerman, S.D., et al., *The adhesion GPCR Gpr56 regulates oligodendrocyte development via interactions with Galpha12/13 and RhoA*. Nat Commun, 2015. **6**: p. 6122.
84. Traiffort, E., et al., *Astrocytes and Microglia as Major Players of Myelin Production in Normal and Pathological Conditions*. Front Cell Neurosci, 2020. **14**: p. 79.
85. Giera, S., et al., *Microglial transglutaminase-2 drives myelination and myelin repair via GPR56/ADGRG1 in oligodendrocyte precursor cells*. Elife, 2018. **7**.
86. Ackerman, S.D., et al., *GPR56/ADGRG1 regulates development and maintenance of peripheral myelin*. J Exp Med, 2018. **215**(3): p. 941-961.
87. Singh, A.K. and H.-H. Lin, *The role of GPR56/ADGRG1 in health and disease*. Biomedical Journal, 2021.
88. van der Poel, M., et al., *Transcriptional profiling of human microglia reveals grey-white matter heterogeneity and multiple sclerosis-associated changes*. Nat Commun, 2019. **10**(1): p. 1139.

89. Belzeaux, R., et al., *GPR56/ADGRG1 is associated with response to antidepressant treatment*. Nat Commun, 2020. **11**(1): p. 1635.
90. Wu, M.P., et al., *G-protein coupled receptor 56 promotes myoblast fusion through serum response factor- and nuclear factor of activated T-cell-mediated signalling but is not essential for muscle development in vivo*. Febs j, 2013. **280**(23): p. 6097-113.
91. White, J.P., et al., *G protein-coupled receptor 56 regulates mechanical overload-induced muscle hypertrophy*. Proc Natl Acad Sci U S A, 2014. **111**(44): p. 15756-61.
92. Jang, Y.J., et al., *Apigenin enhances skeletal muscle hypertrophy and myoblast differentiation by regulating Prmt7*. Oncotarget, 2017. **8**(45).
93. Zhang, Y., et al., *The RNA-binding protein PCBP2 inhibits Ang II-induced hypertrophy of cardiomyocytes through promoting GPR56 mRNA degeneration*. Biochem Biophys Res Commun, 2015. **464**(3): p. 679-84.
94. Kitakaze, T., et al., *Extracellular transglutaminase 2 induces myotube hypertrophy through G protein-coupled receptor 56*. Biochim Biophys Acta Mol Cell Res, 2020. **1867**(2): p. 118563.
95. Chen, G., et al., *GPR56 is essential for testis development and male fertility in mice*. Dev Dyn, 2010. **239**(12): p. 3358-67.
96. Ayers, K.L., et al., *Identification of candidate gonadal sex differentiation genes in the chicken embryo using RNA-seq*. BMC Genomics, 2015. **16**: p. 704.
97. Roly, Z.Y., et al., *Adhesion G-protein-coupled receptor, GPR56, is required for Mullerian duct development in the chick*. J Endocrinol, 2020. **244**(2): p. 395-413.
98. Della Chiesa, M., et al., *GPR56 as a novel marker identifying the CD56dull CD16+ NK cell subset both in blood stream and in inflamed peripheral tissues*. Int Immunol, 2010. **22**(2): p. 91-100.

99. Nijmeijer, S., H.F. Vischer, and R. Leurs, *Adhesion GPCRs in immunology*. *Biochem Pharmacol*, 2016. **114**: p. 88-102.
100. Peng, Y.M., et al., *Specific expression of GPR56 by human cytotoxic lymphocytes*. *J Leukoc Biol*, 2011. **90**(4): p. 735-40.
101. Chang, G.W., et al., *The Adhesion G Protein-Coupled Receptor GPR56/ADGRG1 Is an Inhibitory Receptor on Human NK Cells*. *Cell Rep*, 2016. **15**(8): p. 1757-70.
102. Yeung, J., et al., *GPR56/ADGRG1 is a platelet collagen-responsive GPCR and hemostatic sensor of shear force*. *Proc Natl Acad Sci U S A*, 2020. **117**(45): p. 28275-28286.
103. Truong, K.L., et al., *Killer-like receptors and GPR56 progressive expression defines cytokine production of human CD4(+) memory T cells*. *Nat Commun*, 2019. **10**(1): p. 2263.
104. Zhang, S., et al., *GPR56 Drives Colorectal Tumor Growth and Promotes Drug Resistance through Upregulation of MDR1 Expression via a RhoA-Mediated Mechanism*. *Mol Cancer Res*, 2019. **17**(11): p. 2196-2207.
105. Gad, A.A. and N. Balenga, *The Emerging Role of Adhesion GPCRs in Cancer*. *ACS Pharmacol Transl Sci*, 2020. **3**(1): p. 29-42.
106. Ji, B., et al., *GPR56 promotes proliferation of colorectal cancer cells and enhances metastasis via epithelialmesenchymal transition through PI3K/AKT signaling activation*. *Oncol Rep*, 2018. **40**(4): p. 1885-1896.
107. Jin, G., et al., *The G-protein coupled receptor 56, expressed in colonic stem and cancer cells, binds progastrin to promote proliferation and carcinogenesis*. *Oncotarget*, 2017. **8**(25): p. 40606-40619.
108. Liu, Z., et al., *Expression of orphan GPR56 correlates with tumor progression in human epithelial ovarian cancer*. *Neoplasma*, 2017. **64**(1): p. 32-39.

109. Zendman, A.J., et al., *TM7XN1, a novel human EGF-TM7-like cDNA, detected with mRNA differential display using human melanoma cell lines with different metastatic potential.* FEBS Lett, 1999. **446**(2-3): p. 292-8.
110. Yang, L., et al., *GPR56 Regulates VEGF production and angiogenesis during melanoma progression.* Cancer Res, 2011. **71**(16): p. 5558-68.
111. Millar, M.W., N. Corson, and L. Xu, *The Adhesion G-Protein-Coupled Receptor, GPR56/ADGRG1, Inhibits Cell-Extracellular Matrix Signaling to Prevent Metastatic Melanoma Growth.* Front Oncol, 2018. **8**: p. 8.
112. Yang, L., et al., *GPR56 inhibits melanoma growth by internalizing and degrading its ligand TG2.* Cancer Res, 2014. **74**(4): p. 1022-31.
113. Huang, K.Y. and H.H. Lin, *The Activation and Signaling Mechanisms of GPR56/ADGRG1 in Melanoma Cell.* Front Oncol, 2018. **8**: p. 304.
114. Chiang, N.Y., et al., *Heparin interacts with the adhesion GPCR GPR56, reduces receptor shedding, and promotes cell adhesion and motility.* J Cell Sci, 2016. **129**(11): p. 2156-69.
115. Saito, Y., et al., *Maintenance of the hematopoietic stem cell pool in bone marrow niches by EVII-regulated GPR56.* Leukemia, 2013. **27**(8): p. 1637-49.
116. Daria, D., et al., *GPR56 contributes to the development of acute myeloid leukemia in mice.* Leukemia, 2016. **30**(8): p. 1734-41.
117. Daga, S., et al., *High GPR56 surface expression correlates with a leukemic stem cell gene signature in CD34-positive AML.* Cancer Med, 2019. **8**(4): p. 1771-1778.
118. Bargal, S.A., et al., *Genome-wide association analysis identifies SNPs predictive of in vitro leukemic cell sensitivity to cytarabine in pediatric AML.* Oncotarget, 2018. **9**(79): p. 34859-34875.
119. Shashidhar, S., et al., *GPR56 is a GPCR that is overexpressed in gliomas and functions in tumor cell adhesion.* Oncogene, 2005. **24**(10): p. 1673-1682.

120. Ohta, S., et al., *Agonistic antibodies reveal the function of GPR56 in human glioma U87-MG cells*. Biol Pharm Bull, 2015. **38**(4): p. 594-600.
121. Moreno, M., et al., *GPR56/ADGRG1 Inhibits Mesenchymal Differentiation and Radioresistance in Glioblastoma*. Cell Rep, 2017. **21**(8): p. 2183-2197.
122. Ng, S.Y., L.T. Lee, and B.K. Chow, *Receptor oligomerization: from early evidence to current understanding in class B GPCRs*. Front Endocrinol (Lausanne), 2012. **3**: p. 175.
123. Angers, S., A. Salahpour, and M. Bouvier, *Dimerization: An Emerging Concept for G Protein–Coupled Receptor Ontogeny and Function*. Annual Review of Pharmacology and Toxicology, 2002. **42**(1): p. 409-435.
124. Doumazane, E., et al., *A new approach to analyze cell surface protein complexes reveals specific heterodimeric metabotropic glutamate receptors*. FASEB J, 2011. **25**(1): p. 66-77.
125. Levitz, J., et al., *Mechanism of Assembly and Cooperativity of Homomeric and Heteromeric Metabotropic Glutamate Receptors*. Neuron, 2016. **92**(1): p. 143-159.
126. Whorton, M.R., et al., *A monomeric G protein-coupled receptor isolated in a high-density lipoprotein particle efficiently activates its G protein*. Proceedings of the National Academy of Sciences, 2007. **104**(18): p. 7682-7687.
127. Ferre, S., et al., *G protein-coupled receptor oligomerization revisited: functional and pharmacological perspectives*. Pharmacol Rev, 2014. **66**(2): p. 413-34.
128. Ding, W.-Q., et al., *Silencing of Secretin Receptor Function by Dimerization with a Misspliced Variant Secretin Receptor in Ductal Pancreatic Adenocarcinoma*. Cancer Research, 2002. **62**(18): p. 5223-5229.
129. White, J.H., et al., *Heterodimerization is required for the formation of a functional GABA(B) receptor*. Nature, 1998. **396**(6712): p. 679-82.

130. Hague, C., et al., *Cell surface expression of alpha1D-adrenergic receptors is controlled by heterodimerization with alpha1B-adrenergic receptors*. J Biol Chem, 2004. **279**(15): p. 15541-9.
131. Uberti, M.A., et al., *Heterodimerization with  $\beta$ <sup>2</sup>-Adrenergic Receptors Promotes Surface Expression and Functional Activity of  $\alpha$ <sup>1D</sup>-Adrenergic Receptors*. Journal of Pharmacology and Experimental Therapeutics, 2005. **313**(1): p. 16-23.
132. Kaupmann, K., et al., *GABA(B)-receptor subtypes assemble into functional heteromeric complexes*. Nature, 1998. **396**(6712): p. 683-7.
133. Jones, K.A., et al., *GABA(B) receptors function as a heteromeric assembly of the subunits GABA(B)R1 and GABA(B)R2*. Nature, 1998. **396**(6712): p. 674-9.
134. Fotiadis, D., et al., *Structure of the rhodopsin dimer: a working model for G-protein-coupled receptors*. Curr Opin Struct Biol, 2006. **16**(2): p. 252-9.
135. Baneres, J.L., et al., *Structure-based analysis of GPCR function: conformational adaptation of both agonist and receptor upon leukotriene B4 binding to recombinant BLT1*. J Mol Biol, 2003. **329**(4): p. 801-14.
136. Harikumar, K.G., et al., *Glucagon-like peptide-1 receptor dimerization differentially regulates agonist signaling but does not affect small molecule allostery*. Proceedings of the National Academy of Sciences, 2012. **109**(45): p. 18607-18612.
137. Dupre, D.J., et al., *Seven transmembrane receptor core signaling complexes are assembled prior to plasma membrane trafficking*. J Biol Chem, 2006. **281**(45): p. 34561-73.
138. Pétrin, D. and T.E. Hébert, *The Functional Size of GPCRs – Monomers, Dimers or Tetramers?*, in *GPCR Signalling Complexes – Synthesis, Assembly, Trafficking and Specificity*, D.J. Dupré, T.E. Hébert, and R. Jockers, Editors. 2012, Springer Netherlands: Dordrecht. p. 67-81.

139. Ge, B., et al., *Single-molecule imaging reveals dimerization/oligomerization of CXCR4 on plasma membrane closely related to its function*. *Sci Rep*, 2017. **7**(1): p. 16873.
140. Sleno, R. and T.E. Hebert, *The Dynamics of GPCR Oligomerization and Their Functional Consequences*. *Int Rev Cell Mol Biol*, 2018. **338**: p. 141-171.
141. Jastrzebska, B., et al., *Disruption of Rhodopsin Dimerization with Synthetic Peptides Targeting an Interaction Interface*. *J Biol Chem*, 2015. **290**(42): p. 25728-44.
142. Rabon, E.C., et al., *Radiation inactivation analysis of oligomeric structure of the H,K-ATPase*. *Journal of Biological Chemistry*, 1988. **263**(31): p. 16189-16194.
143. Morizumi, T., et al., *X-ray Crystallographic Structure and Oligomerization of Gloeobacter Rhodopsin*. *Sci Rep*, 2019. **9**(1): p. 11283.
144. Bonjack, M. and D. Avnir, *The near-symmetry of protein oligomers: NMR-derived structures*. *Sci Rep*, 2020. **10**(1): p. 8367.
145. Heckmeier, P.J., et al., *Determining the Stoichiometry of Small Protein Oligomers Using Steady-State Fluorescence Anisotropy*. *Biophysical Journal*, 2020. **119**(1): p. 99-114.
146. Li, F., et al., *Studying Homo-oligomerization and Hetero-oligomerization of MDMX and MDM2 Proteins in Single Living Cells by Using In Situ Fluorescence Correlation Spectroscopy*. *Biochemistry*, 2021. **60**(19): p. 1498-1505.
147. Gao, Y., et al., *Live Cell FRET Imaging Reveals Amyloid  $\beta$ -Peptide Oligomerization in Hippocampal Neurons*. *Int J Mol Sci*, 2021. **22**(9).
148. Dorsch, S., et al., *Analysis of receptor oligomerization by FRAP microscopy*. *Nat Methods*, 2009. **6**(3): p. 225-30.

149. Baiula, M., *Monitoring Opioid Receptor Interaction in Living Cells by Bioluminescence Resonance Energy Transfer (BRET)*, in *Opioid Receptors: Methods and Protocols*, S.M. Spampinato, Editor. 2021, Springer US: New York, NY. p. 35-43.
150. Wu, P. and L. Brand, *Resonance energy transfer: methods and applications*. Anal Biochem, 1994. **218**(1): p. 1-13.
151. Ward, W.W. and M.J. Cormier, *ENERGY TRANSFER VIA PROTEIN-PROTEIN INTERACTION IN RENILLA BIOLUMINESCENCE*. Photochemistry and Photobiology, 1978. **27**(4): p. 389-396.
152. Xia, Z. and J. Rao, *Biosensing and imaging based on bioluminescence resonance energy transfer*. Curr Opin Biotechnol, 2009. **20**(1): p. 37-44.
153. Baldwin, T.O., *Firefly luciferase: the structure is known, but the mystery remains*. Structure, 1996. **4**(3): p. 223-8.
154. Hall, M.P., et al., *Engineered Luciferase Reporter from a Deep Sea Shrimp Utilizing a Novel Imidazopyrazinone Substrate*. ACS Chemical Biology, 2012. **7**(11): p. 1848-1857.
155. Dale, N.C., et al., *NanoBRET: The Bright Future of Proximity-Based Assays*. Front Bioeng Biotechnol, 2019. **7**: p. 56.
156. Arpino, J.A., P.J. Rizkallah, and D.D. Jones, *Crystal structure of enhanced green fluorescent protein to 1.35 Å resolution reveals alternative conformations for Glu222*. PLoS One, 2012. **7**(10): p. e47132.
157. Pakhomov, A.A. and V.I. Martynov, *GFP family: structural insights into spectral tuning*. Chem Biol, 2008. **15**(8): p. 755-64.
158. Xu, Y., D.W. Piston, and C.H. Johnson, *A bioluminescence resonance energy transfer (BRET) system: Application to interacting circadian clock proteins*. Proceedings of the National Academy of Sciences, 1999. **96**(1): p. 151-156.

159. Borroto-Escuela, D.O., et al., *Bioluminescence resonance energy transfer methods to study G protein-coupled receptor-receptor tyrosine kinase heteroreceptor complexes*. *Methods Cell Biol*, 2013. **117**: p. 141-64.
160. Kocan, M., et al., *Demonstration of improvements to the bioluminescence resonance energy transfer (BRET) technology for the monitoring of G protein-coupled receptors in live cells*. *J Biomol Screen*, 2008. **13**(9): p. 888-98.
161. Bacart, J., et al., *The BRET technology and its application to screening assays*. *Biotechnol J*, 2008. **3**(3): p. 311-24.
162. Xing, Y., et al., *Improved QD-BRET conjugates for detection and imaging*. *Biochem Biophys Res Commun*, 2008. **372**(3): p. 388-94.
163. Pflieger, K.D.G. and K.A. Eidne, *Illuminating insights into protein-protein interactions using bioluminescence resonance energy transfer (BRET)*. *Nature Methods*, 2006. **3**(3): p. 165-174.
164. Sekar, R.B. and A. Periasamy, *Fluorescence resonance energy transfer (FRET) microscopy imaging of live cell protein localizations*. *J Cell Biol*, 2003. **160**(5): p. 629-33.
165. Mo, X.L. and H. Fu, *BRET: NanoLuc-Based Bioluminescence Resonance Energy Transfer Platform to Monitor Protein-Protein Interactions in Live Cells*. *Methods Mol Biol*, 2016. **1439**: p. 263-71.
166. Breton, B., et al., *Multiplexing of multicolor bioluminescence resonance energy transfer*. *Biophys J*, 2010. **99**(12): p. 4037-46.
167. Drinovec, L., et al., *Mathematical models for quantitative assessment of bioluminescence resonance energy transfer: application to seven transmembrane receptors oligomerization*. *Front Endocrinol (Lausanne)*, 2012. **3**: p. 104.
168. Mercier, J.F., et al., *Quantitative assessment of beta 1- and beta 2-adrenergic receptor homo- and heterodimerization by bioluminescence resonance energy transfer*. *J Biol Chem*, 2002. **277**(47): p. 44925-31.

169. Förster, T., *Transfer mechanisms of electronic excitation*. Discussions of the Faraday Society, 1959. **27**(0): p. 7-17.
170. Veatch, W. and L. Stryer, *The dimeric nature of the gramicidin A transmembrane channel: Conductance and fluorescence energy transfer studies of hybrid channels*. Journal of Molecular Biology, 1977. **113**(1): p. 89-102.
171. Inouye, S., et al., *Secretional luciferase of the luminous shrimp *Oplophorus gracilirostris*: cDNA cloning of a novel imidazopyrazinone luciferase(1)*. FEBS Lett, 2000. **481**(1): p. 19-25.
172. Angers, S., et al., *Detection of beta 2-adrenergic receptor dimerization in living cells using bioluminescence resonance energy transfer (BRET)*. Proc Natl Acad Sci U S A, 2000. **97**(7): p. 3684-9.
173. Ayoub, M.A., et al., *Monitoring of ligand-independent dimerization and ligand-induced conformational changes of melatonin receptors in living cells by bioluminescence resonance energy transfer*. J Biol Chem, 2002. **277**(24): p. 21522-8.
174. Devost, D. and H.H. Zingg, *Homo- and hetero-dimeric complex formations of the human oxytocin receptor*. J Neuroendocrinol, 2004. **16**(4): p. 372-7.
175. Vrecl, M., et al., *Opsin oligomerization in a heterologous cell system*. J Recept Signal Transduct Res, 2006. **26**(5-6): p. 505-26.
176. Ayoub, M.A. and K.D. Pflieger, *Recent advances in bioluminescence resonance energy transfer technologies to study GPCR heteromerization*. Curr Opin Pharmacol, 2010. **10**(1): p. 44-52.
177. Achour, L., et al., *Using quantitative BRET to assess G protein-coupled receptor homo- and heterodimerization*. Methods Mol Biol, 2011. **756**: p. 183-200.
178. Ayoub, M.A., et al., *Preferential formation of MT1/MT2 melatonin receptor heterodimers with distinct ligand interaction properties compared with MT2 homodimers*. Mol Pharmacol, 2004. **66**(2): p. 312-21.

179. Goin, J.C. and N.M. Nathanson, *Quantitative analysis of muscarinic acetylcholine receptor homo- and heterodimerization in live cells: regulation of receptor down-regulation by heterodimerization*. J Biol Chem, 2006. **281**(9): p. 5416-25.
180. St Croix, C.M., S.H. Shand, and S.C. Watkins, *Confocal microscopy: comparisons, applications, and problems*. Biotechniques, 2005. **39**(6 Suppl): p. S2-5.
181. Schoneberg, T., et al., *Mutant G-protein-coupled receptors as a cause of human diseases*. Pharmacol Ther, 2004. **104**(3): p. 173-206.
182. Schonenbach, N.S., et al., *Adenosine A2a receptors form distinct oligomers in protein detergent complexes*. FEBS Lett, 2016. **590**(18): p. 3295-306.
183. Cvejic, S. and L.A. Devi, *Dimerization of the delta opioid receptor: implication for a role in receptor internalization*. J Biol Chem, 1997. **272**(43): p. 26959-64.
184. Nguyen, K.D.Q., et al., *Oligomerization of the Human Adenosine A<sub>2A</sub> Receptor is Driven by the Intrinsically Disordered C-terminus*. bioRxiv, 2020: p. 2020.12.21.423144.
185. Bai, Y. and W.C. Shen, *Improving the oral efficacy of recombinant granulocyte colony-stimulating factor and transferrin fusion protein by spacer optimization*. Pharm Res, 2006. **23**(9): p. 2116-21.
186. Amet, N., H.F. Lee, and W.C. Shen, *Insertion of the designed helical linker led to increased expression of tf-based fusion proteins*. Pharm Res, 2009. **26**(3): p. 523-8.
187. Zhao, H.L., et al., *Increasing the homogeneity, stability and activity of human serum albumin and interferon- $\alpha$ 2b fusion protein by linker engineering*. Protein Expression and Purification, 2008. **61**(1): p. 73-77.
188. Chen, X., J.L. Zaro, and W.C. Shen, *Fusion protein linkers: property, design and functionality*. Adv Drug Deliv Rev, 2013. **65**(10): p. 1357-69.

189. Hague, C., et al., *The N Terminus of the Human  $\alpha 1D$ -Adrenergic Receptor Prevents Cell Surface Expression*. Journal of Pharmacology and Experimental Therapeutics, 2004. **309**(1): p. 388-397.
190. Andersson, H., et al., *Membrane assembly of the cannabinoid receptor 1: impact of a long N-terminal tail*. Mol Pharmacol, 2003. **64**(3): p. 570-7.
191. Muller, I., et al., *The N-terminal end truncated mu-opioid receptor: from expression to circular dichroism analysis*. Appl Biochem Biotechnol, 2010. **160**(7): p. 2175-86.
192. Dell, E.J., *Improving upon Monochromator Technology*. Genetic Engineering & Biotechnology News, 2014. **34**(2): p. 22-22.
193. Reddy, P.S. and R.B. Corley, *Assembly, sorting, and exit of oligomeric proteins from the endoplasmic reticulum*. Bioessays, 1998. **20**(7): p. 546-54.
194. Marshall, F.H., et al., *GABAB receptors - the first 7TM heterodimers*. Trends Pharmacol Sci, 1999. **20**(10): p. 396-9.
195. Terrillon, S., et al., *Oxytocin and vasopressin V1a and V2 receptors form constitutive homo- and heterodimers during biosynthesis*. Mol Endocrinol, 2003. **17**(4): p. 677-91.
196. Floyd, D.H., et al., *C5a receptor oligomerization. II. Fluorescence resonance energy transfer studies of a human G protein-coupled receptor expressed in yeast*. J Biol Chem, 2003. **278**(37): p. 35354-61.
197. Singer, K., et al., *GPR56 and the developing cerebral cortex: cells, matrix, and neuronal migration*. Mol Neurobiol, 2013. **47**(1): p. 186-96.
198. Araç, D. and K. Leon, *Structure, function and therapeutic potential of adhesion GPCRs*, in *GPCRs*. 2020. p. 23-41.

## APPENDICES

### A. Bacterial medium preparation

#### Luria-Bertani (LB) broth

Table A. 1. Components of Luria-Bertani broth for 1 liter.

Component	Amount
Tryptone	10 g
Yeast extract	5 g
NaCl	10 g

LB components are resolved in water followed by autoclave sterilization at 121°C for 20 minutes.

Luria-Bertani (LB) broth with agar is prepared with the addition of 20 g/L Agar to the mixture. Then, the final mixture is sterilized via autoclave. Just before pouring the mixture into plates, Ampicillin is added.

#### Super Optimum Broth with catabolite repression (SOC)

Table A. 2. Components of SOC for 1 liter.

Component	Amount
Tryptone	20 g
Yeast extract	5 g
1M NaCl	10 ml
1M KCl	2.5 ml
Autoclave and add	
1M MgCl <sub>2</sub> .6H <sub>2</sub> O, 1M MgSO <sub>4</sub> .7H <sub>2</sub> O	10 ml
2M Glucose	10 ml

## B. Solutions and buffers for Western blotting

### Radioimmunoprecipitation assay (RIPA) buffer

Table B. 1. Components of 5X RIPA buffer.

Components	Amount
1M Tris-HCl (pH 8.0)	5 ml
1 M NaCl	1.5 ml
NP-40	1 ml
SDS	0.1 g
Sodium deoxycholate	0.5 g

The volume is completed to 20 ml with water and sterilized using a filter with 0.22  $\mu\text{m}$  pore size under aseptic conditions. Just before use, protease inhibitors are added according to the following table:

Table B. 2. RIPA buffer with protease inhibitors.

Components	Amount
5X RIPA	1 ml
1 M DTT	5 $\mu\text{l}$
100 mM PMSF	25 $\mu\text{l}$
1 M Na $\beta$ -glycerophosphate	250 $\mu\text{l}$
cOmplete™ ULTRA Tablets, Mini, EDTA-free, EASYpack Protease Inhibitor Cocktail (Roche, Switzerland)	1/2

The volume is completed to 5 ml with water.

### Laemmli (Sample) buffer

Table B. 3. Components of 4X Laemmli buffer.

Components	Amount
SDS	0.8 g
1M Tris-HCl (pH 6.8)	2.5 ml
0.1% Bromophenol Blue	0.8 ml
Glycerol	4 ml
0.5 M EDTA	0.5 ml
$\beta$ -mercaptoethanol	2 ml

### **Running buffer**

Table B. 4. Components of 10X running buffer for 1 liter.

<b>Components</b>	<b>Amount</b>
Tris Base	30.3 g
Glycine	144.1 g
SDS	10.0 g

The volume is completed to 5 ml with water, and pH is adjusted to 8.3.

### **Tris-buffered saline (TBS)**

Table B. 5. Components of 10X TBS for 1 liter.

<b>Components</b>	<b>Amount</b>
Tris-HCl	24 g
Tris base	5.6 g
NaCl	88 g
H <sub>2</sub> O	800 ml

The volume is completed to 1 liter with water, and pH is adjusted to 7.6.

250 ml of 1X TBS with Tween® 20 detergent (TBST) is prepared by mixing 250 ml of 1X TBS with 250 µl of Tween® 20.

### C. Coding sequences of ADGRG1 constructs

#### kozak-ADGRG1-WT:

gccaccATGACTCCCCAGTCGCTGCTGCAGACGACACTGTTCCCTGCTGAGTCTGC  
TCTTCCCTGGTCCAAGGTGCCACGGCAGGGGCCACAGGGAAGACTTTTCGCTTCTG  
CAGCCAGCGGAACCAGACACACAGGAGCAGCCTCCACTACAAACCCACACCAGAC  
CTGCGCATCTCCATCGAGAACTCCGAAGAGGCCCTCACAGTCCATGCCCTTTCC  
CTGCAGCCCACCCTGCTTCCCGATCCTTCCCTGACCCAGGGGCTCTACCACTT  
CTGCCTCTACTGGAACCGACATGCTGGGAGATTACATCTTCTCTATGGCAAGCGT  
GACTTCTTGCTGAGTGACAAAGCCTCTAGCCTCCTCTGCTTCCAGCACCAGGAGG  
AGAGCCTGGCTCAGGGCCCCCGCTGTTAGCCACTTCTGTCACCTCCTGGTGGAG  
CCCTCAGAACATCAGCCTGCCAGTGCCGCCAGCTTCACCTTCTCCTTCCACAGT  
CCTCCCCACACGGCCGCTCACAATGCCTCGGTGGACATGTGCGAGCTCAAAGGG  
ACCTCCAGCTGCTCAGCCAGTTCTGAAGCATCCCCAGAAGGCCCTCAAGGAGGCC  
CTCGGCTGCCCCGCCAGCCAGCAGTTGCAGAGCCTGGAGTCGAAACTGACCTCT  
GTGAGATTTCATGGGGGACATGGTGTCTTCGAGGAGGACCGGATCAACGCCACGG  
TGTGGAAGCTCCAGCCCACAGCCGGCCTCCAGGACCTGCACATCCACTCCCGGCA  
GGAGGAGGAGCAGAGCGAGATCATGGAGTACTCGGTGCTGCTGCCTCGAACACTC  
TTCCAGAGGACGAAAGGCCGGAGCGGGGAGGCTGAGAAGAGACTCCTCCTGGTGG  
ACTTCAGCAGCCAAGCCCTGTTCCAGGACAAGAATTCCAGCCACGTCTGGGTGA  
GAAGGTCTTGGGGATTGTGGTACAGAACACCAAAGTAGCCAACCTCACGGAGCCC  
GTGGTGCTCACCTTCCAGCACCAGCTACAGCCGAAGAATGTGACTCTGCAATGTG  
TGTTCTGGGTTGAAGACCCACATTGAGCAGCCCGGGGCATTGGAGCAGTGTGG  
GTGTGAGACCGTCAGGAGAGAAACCCAAACATCCTGCTTCTGCAACCACTTGACC  
TACTTTGCAGTGCTGATGGTCTCCTCGGTGGAGGTGGACGCCGTGCACAAGCACT  
ACCTGAGCCTCCTCTCCTACGTGGGCTGTGTGCTCTCTGCCCTGGCCTGCCTTGT  
CACCATTGCCGCCTACCTCTGCTCCAGGGTGCCCTGCCGTGCAGGAGGAAACCT  
CGGGACTACACCATCAAGGTGCACATGAACCTGCTGCTGGCCGTCTTCCCTGCTGG  
ACACGAGCTTCCCTGCTCAGCGAGCCGGTGGCCCTGACAGGCTCTGAGGCTGGCTG  
CCGAGCCAGTGCCATCTTCCCTGCACTTCTCCCTGCTCACCTGCCCTTCCCTGGATG  
GGCCTCGAGGGGTACAACCTCTACCGACTCGTGGTGGAGGTCTTTGGCACCTATG  
TCCCTGGCTACCTACTCAAGCTGAGCGCCATGGGCTGGGGCTTCCCCATCTTTCT  
GGTGACGCTGGTGGCCCTGGTGGATGTGGACAACTATGGCCCCATCATCTTGGCT  
GTGCATAGGACTCCAGAGGGCGTCATCTACCCTTCCATGTGCTGGATCCGGGACT  
CCCTGGTCAGCTACATACCAACCTGGGCCTCTTCAGCCTGGTGTCTTCTGTTCAA  
CATGGCCATGCTAGCCACCATGGTGGTGCAGATCCTGCGGCTGCGCCCCACACC  
CAAAGTGGTCACATGTGCTGACACTGCTGGGCCTCAGCCTGGTCTTGGCCTGC  
CCTGGGCCTTGATCTTCTTCTCCTTTGCTTCTGGCACCTTCCAGCTTGTGCTCCT  
CTACCTTTTCAGCATCATCACCTCCTTCCAAGGCTTCCCTCATCTTCATCTGGTAC  
TGGTCCATGCGGCTGCAGGCCCGGGGTGGCCCTCCCCTCTGAAGAGCAACTCAG  
ACAGCGCCAGGCTCCCCATCAGCTCGGGCAGCACCTCGTCCAGCCGCATCTAG

**kozak-ADGRG1-Δ1-342:**

gccaccACTCTGCAATGTGTGTTCTGGGTTGAAGACCCACATTGAGCAGCCCGG  
GGCATTGGAGCAGTGCTGGGTGTGAGACCGTCAGGAGAGAAACCCAAACATCCTG  
CTTCTGCAACCACTTGACCTACTTTGCAGTGCTGATGGTCTCCTCGGTGGAGGTG  
GACGCCGTGCACAAGCACTACCTGAGCCTCCTCTCCTACGTGGGCTGTGTCGTCT  
CTGCCCTGGCCTGCCTTGTACCATTGCCGCCTACCTCTGCTCCAGGGTGCCCT  
GCCGTGCAGGAGGAAACCTCGGGACTACACCATCAAGGTGCACATGAACCTGCTG  
CTGGCCGTCTTCCTGCTGGACACGAGCTTCCTGCTCAGCGAGCCGGTGGCCCTGA  
CAGGCTCTGAGGCTGGCTGCCGAGCCAGTGCCATCTTCCTGCACTTCTCCCTGCT  
CACCTGCCTTTCTGGATGGGCCTCGAGGGGTACAACCTCTACCGACTCGTGGTG  
GAGGTCTTTGGCACCTATGTCCCTGGCTACCTACTCAAGCTGAGCGCCATGGGCT  
GGGGCTTCCCCATCTTTCTGGTGACGCTGGTGGCCCTGGTGGATGTGGACAATA  
TGGCCCCATCATCTTGGCTGTGCATAGGACTCCAGAGGGCGTCATCTACCCTTCC  
ATGTGCTGGATCCGGGACTCCCTGGTCAGCTACATCACCAACCTGGGCCTCTTCA  
GCCTGGTGTTTTCTGTTCAACATGGCCATGCTAGCCACCATGGTGGTGCAGATCCT  
GCGGCTGCGCCCCACACCCAAAAGTGGTCACATGTGCTGACACTGCTGGGCCTC  
AGCCTGGTCCTTGGCCTGCCCTGGGCCTTGATCTTCTTCTCCTTTGCTTCTGGCA  
CCTTCCAGCTTGTGCTCCTCTACCTTTTTCAGCATCATCACCTCCTTCCAAGGCTT  
CCTCATCTTCATCTGGTACTGGTCCATGCGGCTGCAGGCCCGGGGTGGCCCTCC  
CCTCTGAAGAGCAACTCAGACAGCGCCAGGCTCCCCATCAGCTCGGGCAGCACCT  
CGTCCAGCCGCATCTAG

**kozak-ADGRG1-egfp:**

gccaccATGACTCCCCAGTCGCTGCTGCAGACGACACTGTTCCCTGCTGAGTCTGC  
TCTTCCCTGGTCCAAGGTGCCACGGCAGGGGCCACAGGGAAGACTTTCGCTTCTG  
CAGCCAGCGGAACCAGACACACAGGAGCAGCCTCCACTACAAACCCACACCAGAC  
CTGCGCATCTCCATCGAGAACTCCGAAGAGGCCCTCACAGTCCATGCCCTTTTCC  
CTGCAGCCCACCCTGCTTCCCAGATCCTTCCCTGACCCCAGGGGCCTCTACCACTT  
CTGCCTCTACTGGAACCGACATGCTGGGAGATTACATCTTCTCTATGGCAAGCGT  
GACTTCTTGCTGAGTGACAAAGCCTCTAGCCTCCTCTGCTTCCAGCACCAGGAGG  
AGAGCCTGGCTCAGGGCCCCCGCTGTTAGCCACTTCTGTCACCTCCTGGTGGAG  
CCCTCAGAACATCAGCCTGCCAGTGCCGCCAGCTTACCTTCTCCTTCCACAGT  
CCTCCCCACACGGCCGCTCACAATGCCTCGGTGGACATGTGCGAGCTCAAAAGGG  
ACCTCCAGCTGCTCAGCCAGTTCCTGAAGCATCCCCAGAAGGCCCTCAAGGAGGCC  
CTCGGCTGCCCCCGCCAGCCAGCAGTTGCAGAGCCTGGAGTCGAACTGACCTCT  
GTGAGATTCATGGGGGACATGGTGTCTTCGAGGAGGACCGGATCAACGCCACGG  
TGTGGAAGCTCCAGCCCACAGCCGGCCTCCAGGACCTGCACATCCACTCCCGGCA  
GGAGGAGGAGCAGAGCGAGATCATGGAGTACTCGGTGCTGCTGCCTCGAACACTC

TTCCAGAGGACGAAAGGCCGGAGCGGGGAGGCTGAGAAGAGACTCCTCCTGGTGG  
ACTTCAGCAGCCAAGCCCTGTTCCAGGACAAGAATTCCAGCCACGTCCTGGGTGA  
GAAGGTCTTGGGGATTGTGGTACAGAACACCAAAGTAGCCAACCTCACGGAGCCC  
GTGGTGCTCACCTTCCAGCACCAGCTACAGCCGAAGAATGTGACTCTGCAATGTG  
TGTTCTGGGTTGAAGACCCACATTGAGCAGCCCCGGGCATTGGAGCAGTGTGG  
GTGTGAGACCGTCAGGAGAGAAACCCAAACATCCTGCTTCTGCAACCACTTGACC  
TACTTTGCAGTGCTGATGGTCTCCTCGGTGGAGGTGGACGCCGTGCACAAGCACT  
ACCTGAGCCTCCTCTCCTACGTGGGCTGTGTGCTCTCTGCCCTGGCCTGCCTTGT  
CACCATTGCCGCCTACCTCTGCTCCAGGGTGCCCTGCCGTGCAGGAGGAAACCT  
CGGGACTACACCATCAAGGTGCACATGAACCTGCTGCTGGCCGTCTTCTGCTGG  
ACACGAGCTTCTGCTCAGCGAGCCGGTGGCCCTGACAGGCTCTGAGGCTGGCTG  
CCGAGCCAGTGCCATCTTCCCTGCACTTCTCCCTGCTCACCTGCCTTTCTGGATG  
GGCCTCGAGGGGTACAACCTTACCGACTCGTGGTGGAGGTCTTTGGCACCTATG  
TCCCTGGCTACCTACTCAAGCTGAGCGCCATGGGCTGGGGCTTCCCCTCTTTCT  
GGTGACGCTGGTGGCCCTGGTGGATGTGGACAACCTATGGCCCCATCATCTTGGCT  
GTGCATAGGACTCCAGAGGGCGTCATCTACCCTTCCATGTGCTGGATCCGGGACT  
CCCTGGTCAGCTACATACCAACCTGGGCCTCTTCAGCCTGGTGTCTTCTGTTCAA  
CATGGCCATGCTAGCCACCATGGTGGTGCAGATCCTGCGGCTGCGCCCCACACC  
CAAAGTGGTCACATGTGCTGACACTGCTGGGCCTCAGCCTGGTCCTTGGCCTGC  
CCTGGGCCTTGATCTTCTTCTCCTTTGCTTCTGGCACCTTCCAGCTTGTGCTCCT  
CTACCTTTTCAGCATCATCACCTCCTTCCAAGGCTTCCCTCATCTTCATCTGGTAC  
TGGTCCATGCGGCTGCAGGCCCGGGGTGGCCCTCCCCTCTGAAGAGCAACTCAG  
ACAGCGCCAGGCTCCCCATCAGCTCGGGCAGCACCTCGTCCAGCCGCATCgtgag  
caagggcgaggagctggtcaccggggtggtgcccacccctggctcgagctggacggc  
gacgtaaaccggccacaagttcagcgtgtccggcgagggcgagggcgatgccacct  
acggcaagctgaccctgaagttcatctgcaccaccggcaagctgcccgtgcccctg  
gcccaccctcgtgaccaccctgacctacggcgtgcagtgcttcagccgctacccc  
gaccacatgaagcagcagcacttcttcaagtccgccaatgcccgaaggctacgtcc  
aggagcgcaccatcttcttcaaggacgacggcaactacaagaccgcgcccaggt  
gaagttcgagggcgacaccctggtgaaccgcatcgagctgaagggcatcgacttc  
aaggagacggcaacatcctggggcacaagctggagtacaactacaacagccaca  
acgtctatatcatggccgacaagcagaagaacggcatcaaggtgaacttcaagat  
ccgccacaacatcgaggacggcagcgtgcagctcgccgaccactaccagcagaac  
acccccatcgggcagcggccccgtgctgctgcccgacaaccactacctgagcacc  
agtccaagcttagcaaagatcccaacgagaagcgcgatcacatggtcctgctgga  
gttcgtgaccgcccgggatcactctcggcatggacgagctgtacaagTAG

**kozak-ADGRG1-nluc:**

gccaccATGACTCCCCAGTCGCTGCTGCAGACGACACTGTTCCCTGCTGAGTCTGC  
TCTTCTGGTCCAAGGTGCCACGGCAGGGGCCACAGGGAAGACTTTCGCTTCTG  
CAGCCAGCGGAACCAGACACACAGGAGCAGCCTCCACTACAAACCCACACCAGAC

CTGCGCATCTCCATCGAGAACTCCGAAGAGGCCCTCACAGTCCATGCCCCCTTTCC  
CTGCAGCCCACCCTGCTTCCCGATCCTTCCCTGACCCCAGGGGCCTCTACCACTT  
CTGCCTCTACTGGAACCGACATGCTGGGAGATTACATCTTCTCTATGGCAAGCGT  
GACTTCTTGCTGAGTGACAAAGCCTCTAGCCTCCTCTGCTTCCAGCACCAGGAGG  
AGAGCCTGGCTCAGGGCCCCCGCTGTTAGCCACTTCTGTACCTCCTGGTGGAG  
CCCTCAGAACATCAGCCTGCCAGTGCCGCCAGCTTACCTTCTCCTTCCACAGT  
CCTCCCCACACGGCCGCTCACAATGCCTCGGTGGACATGTGCGAGCTCAAAAGGG  
ACCTCCAGCTGCTCAGCCAGTTCCCTGAAGCATCCCCAGAAGGCCCTCAAGGAGGCC  
CTCGGCTGCCCCCGCCAGCCAGCAGTTGCAGAGCCTGGAGTCGAAACTGACCTCT  
GTGAGATTTCATGGGGGACATGGTGTCTTCGAGGAGGACCGGATCAACGCCACGG  
TGTGGAAGCTCCAGCCCACAGCCGGCCTCCAGGACCTGCACATCCACTCCCGGCA  
GGAGGAGGAGCAGAGCGAGATCATGGAGTACTCGGTGCTGCTGCCTCGAACACTC  
TTCCAGAGGACGAAAGGCCGGAGCGGGGAGGCTGAGAAGAGACTCCTCCTGGTGG  
ACTTCAGCAGCCAAGCCCTGTTCCAGGACAAGAATTCCAGCCACGTCTGGGTGA  
GAAGGTCTTGGGGATTGTGGTACAGAACACCAAAGTAGCCAACCTCACGGAGCCC  
GTGGTGCTCACCTTCCAGCACCAGCTACAGCCGAAGAATGTGACTCTGCAATGTG  
TGTTCTGGGTTGAAGACCCACATTGAGCAGCCCGGGCATTGGAGCAGTGCTGG  
GTGTGAGACCGTCAGGAGAGAAACCCAAACATCCTGCTTCTGCAACCACTTGACC  
TACTTTGCAGTGCTGATGGTCTCCTCGGTGGAGGTGGACGCCGTGCACAAGCACT  
ACCTGAGCCTCCTCTCCTACGTGGGCTGTGTCTCTGCCCTGGCCTGCCTTGT  
CACCATTGCCGCCTACCTCTGCTCCAGGGTGCCCTGCCGTGCAGGAGGAAACCT  
CGGGACTACACCATCAAGGTGCACATGAACCTGCTGCTGGCCGTCTTCTGCTGG  
ACACGAGCTTCTGCTCAGCGAGCCGGTGGCCCTGACAGGCTCTGAGGCTGGCTG  
CCGAGCCAGTGCCATCTTCCCTGCACTTCTCCCTGCTCACCTGCCTTTCTGGATG  
GGCCTCGAGGGGTACAACCTCTACCGACTCGTGGTGGAGGTCTTTGGCACCTATG  
TCCCTGGCTACCTACTCAAGCTGAGCGCCATGGGCTGGGGCTTCCCCATCTTTCT  
GGTGACGCTGGTGGCCCTGGTGGATGTGGACAACCTATGGCCCCATCATCTTGGCT  
GTGCATAGGACTCCAGAGGGCGTCATCTACCCTTCCATGTGCTGGATCCGGGACT  
CCCTGGTCAGCTACATACCAACCTGGGCCTTTCAGCCTGGTGTCTTCTGTTCAA  
CATGGCCATGCTAGCCACCATGGTGGTGCAGATCCTGCGGCTGCGCCCCACACC  
CAAAAGTGGTCACATGTGCTGACACTGCTGGGCCTCAGCCTGGTCTTGGCCTGC  
CCTGGGCCTTGATCTTCTTCTCCTTTGCTTCTGGCACCTTCCAGCTTGTCTCTCT  
CTACCTTTTCAGCATCATCACCTCCTTCCAAGGCTTCTCATCTTCATCTGGTAC  
TGGTCCATGCGGCTGCAGGCCCGGGGTGGCCCTCCCCTCTGAAGAGCAACTCAG  
ACAGCGCCAGGCTCCCCATCAGCTCGGGCAGCACCTCGTCCAGCCGCATCgtctt  
cacactcgaagatctcgttggggactggcgacagacagccggctacaacctggac  
caagtccttgaacagggaggtgtgtccagtttgtttcagaatctcgggggtgtccg  
taactccgatccaaaggattgtcctgagcggtgaaaatgggctgaagatcgacat  
ccatgtcatcatcccgatgaaggtctgagcggcgaccaaagggccagatcgaa  
aaaatttttaaggtggtgtacctgtggatgatcatcactttaaggtgatcctgc  
actatggcacactggtaatcgacggggttacgcgaacatgatcgactatctcgg  
acggccgatgaaggcatcgccgtgttcgacggcaaaaagatcactgtaacaggg  
accctgtggaacggcaacaaaattatcgacgagcgcctgatcaaccccgacggct  
ccctgctgttccgagtaaccatcaacggagtgaccggctggcggctgtgcaacg  
cattctggcgTAG

**kozak-ADGRG1-L-egfp:**

gccaccATGACTCCCCAGTCGCTGCTGCAGACGACACTGTTCCCTGCTGAGTCTGC  
TCTTCCCTGGTCCAAGGTGCCACGGCAGGGGCCACAGGGAAGACTTTCGCTTCTG  
CAGCCAGCGGAACCAGACACACAGGAGCAGCCTCCACTACAAACCCACACCAGAC  
CTGCGCATCTCCATCGAGAACTCCGAAGAGGCCCTCACAGTCCATGCCCCTTTCC  
CTGCAGCCCACCCTGCTTCCCGATCCTTCCCTGACCCCAGGGGCCTCTACCACTT  
CTGCCTCTACTGGAACCGACATGCTGGGAGATTACATCTTCTCTATGGCAAGCGT  
GACTTCTTGCTGAGTGACAAAGCCTCTAGCCTCCTCTGCTTCCAGCACCAGGAGG  
AGAGCCTGGCTCAGGGCCCCCGCTGTTAGCCACTTCTGTACCTCCTGGTGGAG  
CCCTCAGAACATCAGCCTGCCAGTGCCGCCAGCTTACCTTCTCCTTCCACAGT  
CCTCCCCACACGGCCGCTCACAATGCCTCGGTGGACATGTGCGAGCTCAAAAGGG  
ACCTCCAGCTGCTCAGCCAGTTCCCTGAAGCATCCCCAGAAGGCCTCAAGGAGGCC  
CTCGGCTGCCCCGCCAGCCAGCAGTTGCAGAGCCTGGAGTCGAAACTGACCTCT  
GTGAGATTCATGGGGGACATGGTGTCTTCGAGGAGGACCGGATCAACGCCACGG  
TGTGGAAGCTCCAGCCCACAGCCGGCCTCCAGGACCTGCACATCCACTCCCGGCA  
GGAGGAGGAGCAGAGCGAGATCATGGAGTACTCGGTGCTGCTGCCTCGAACACTC  
TTCCAGAGGACGAAAGGCCGGAGCGGGGAGGCTGAGAAGAGACTCCTCCTGGTGG  
ACTTCAGCAGCCAAGCCCTGTTCCAGGACAAGAATTCCAGCCACGTCTGGGTGA  
GAAGGTCTTGGGGATTGTGGTACAGAACACCAAAGTAGCCAACCTCACGGAGCCC  
GTGGTGCTCACCTTCCAGCACCAGCTACAGCCGAAGAATGTGACTCTGCAATGTG  
TGTTCTGGGTGAAGACCCACATTGAGCAGCCCGGGCATTGGAGCAGTGTGG  
GTGTGAGACCGTCAGGAGAGAAACCCAAACATCCTGCTTCTGCAACCACTTGACC  
TACTTTGCAGTGCTGATGGTCTCCTCGGTGGAGGTGGACGCCGTGCACAAGCACT  
ACCTGAGCCTCCTCTCCTACGTGGGCTGTGTCTCTGCCCCTGGCCTGCCTTGT  
CACCATTGCCGCCTACCTCTGCTCCAGGGTGCCCTGCCGTGCAGGAGGAAACCT  
CGGGACTACACCATCAAGGTGCACATGAACCTGCTGCTGGCCGTCTTCTGCTGG  
ACACGAGCTTCCCTGCTCAGCGAGCCGGTGGCCCTGACAGGCTCTGAGGCTGGCTG  
CCGAGCCAGTGCCATCTTCCCTGCACTTCTCCCTGCTCACCTGCCTTTTCTGGATG  
GGCCTCGAGGGGTACAACCTCTACCGACTCGTGGTGGAGGTCTTTGGCACCTATG  
TCCCTGGCTACCTACTCAAGCTGAGCGCCATGGGCTGGGGCTTCCCCATCTTCT  
GGTGACGCTGGTGGCCCTGGTGGATGTGGACAACCTATGGCCCCATCATCTTGGCT  
GTGCATAGGACTCCAGAGGGCGTCATCTACCCTTCCATGTGCTGGATCCGGGACT  
CCCTGGTCAGCTACATACCAACCTGGGCCTCTTCCAGCCTGGTGTCTTCTGTTCAA  
CATGGCCATGCTAGCCACCATGGTGGTGCAGATCCTGCGGCTGCGCCCCACACC  
CAAAGTGGTCACATGTGCTGACACTGCTGGGCCTCAGCCTGGTCTTGGCCTGC  
CCTGGGCCTTGATCTTCTTCTCCTTTGCTTCTGGCACCTTCCAGCTTGTGTCCT  
CTACCTTTTCAGCATCATCACCTCCTTCCAAGGCTTCCCTCATCTTCATCTGGTAC  
TGGTCCATGCGGCTGCAGGCCCGGGGTGGCCCTCCCCTCTGAAGAGCAACTCAG  
ACAGCGCCAGGCTCCCCATCAGCTCGGGCAGCACCTCGTCCAGCCGCATCGGCAG  
CAGCGGCgtgagcaagggcgaggagctggtcaccgggggtggtgcccatcctggtc  
gagctggacggcgacgtaaacggccacaagttcagcgtgtccggcgagggcgagg  
gcatgccacctacggcaagctgacctgaagttcatctgcaccaccggcaagct  
gcccgtgccctggcccaccctcgtgaccaccctgacctacggcgtgcagtgcttc  
agccgctaccccgaccacatgaagcagcagcacttcttcaagtccgccaatgcccg  
aaggctacgtccaggagcgcaccatcttcttcaaggacgacggcaactacaagac

ccgcgcccaggtgaagtccgagggcgacaccctggtgaaccgcatcgagctgaag  
ggcatcgacttcaaggaggacggcaacatcctggggcacaagctggagtacaact  
acaacagccacaacgtctatatcatggccgacaagcagaagaacggcatcaaggt  
gaacttcaagatccgccacaacatcgaggacggcagcgtgcagctcgccgaccac  
taccagcagaacacccccatcggcgacggccccgtgctgctgcccgacaaccact  
acctgagcaccagtcgaagcttagcaaagatcccaacgagaagcgcgatccat  
ggtcctgctggagtccgtgaccgcccgggatcactctcggcgatggacgagctg  
tacaagTAG

**kozak-ADGRG1-L-nluc:**

gccaccATGACTCCCCAGTCGCTGCTGCAGACGACACTGTTCCCTGCTGAGTCTGC  
TCTTCCTGGTCCAAGGTGCCACGGCAGGGGCCACAGGGAAGACTTTCGCTTCTG  
CAGCCAGCGGAACCAGACACACAGGAGCAGCCTCCACTACAAACCCACACCAGAC  
CTGCGCATCTCCATCGAGAACTCCGAAGAGGCCCTCACAGTCCATGCCCTTTCC  
CTGCAGCCCACCCTGCTTCCCGATCCTTCCCTGACCCCAGGGGCCTCTACCACTT  
CTGCCTCTACTGGAACCGACATGCTGGGAGATTACATCTTCTCTATGGCAAGCGT  
GACTTCTTGCTGAGTGACAAAGCCTCTAGCCTCCTCTGCTTCCAGCACCAGGAGG  
AGAGCCTGGCTCAGGGCCCCCGCTGTTAGCCACTTCTGTCACCTCCTGGTGGAG  
CCCTCAGAACATCAGCCTGCCAGTGCCGCCAGCTTCACCTTCTCCTTCCACAGT  
CCTCCCCACACGGCCGCTCACAATGCCTCGGTGGACATGTGCGAGCTCAAAAGGG  
ACCTCCAGCTGCTCAGCCAGTTCCTGAAGCATCCCCAGAAGGCCCTCAAGGAGGCC  
CTCGGCTGCCCCCGCCAGCCAGCAGTTGCAGAGCCTGGAGTCGAAACTGACCTCT  
GTGAGATTTCATGGGGGACATGGTGTCTTCGAGGAGGACCGGATCAACGCCACGG  
TGTGGAAGCTCCAGCCCACAGCCGGCCTCCAGGACCTGCACATCCACTCCCGGCA  
GGAGGAGGAGCAGAGCGAGATCATGGAGTACTCGGTGCTGCTGCCTCGAACACTC  
TTCCAGAGGACGAAAGGCCGGAGCGGGGAGGCTGAGAAGAGACTCCTCCTGGTGG  
ACTTCAGCAGCCAAGCCCTGTTCCAGGACAAGAATTCCAGCCACGTCTGGGTGA  
GAAGGTCTTGGGGATTGTGGTACAGAACACCAAAGTAGCCAACCTCACGGAGCCC  
GTGGTGCTCACCTTCCAGCACCAGCTACAGCCGAAGAATGTGACTCTGCAATGTG  
TGTTCTGGGTTGAAGACCCACATTGAGCAGCCCGGGGCATTGGAGCAGTGCTGG  
GTGTGAGACCGTCAGGAGAGAAACCCAAACATCCTGCTTCTGCAACCACTTGACC  
TACTTTGCAGTGCTGATGGTCTCCTCGGTGGAGGTGGACGCCGTGCACAAGCACT  
ACCTGAGCCTCCTCTCCTACGTGGGCTGTGTGCTCTCTGCCCTGGCCTGCCTTGT  
CACCATTGCCGCCTACCTCTGCTCCAGGGTGCCCTGCCGTGCAGGAGGAAACCT  
CGGGACTACACCATCAAGGTGCACATGAACCTGCTGCTGGCCGTCTTCTGCTGG  
ACACGAGCTTCTGCTCAGCGAGCCGGTGGCCCTGACAGGCTCTGAGGCTGGCTG  
CCGAGCCAGTGCCATCTTCCCTGCACTTCTCCCTGCTCACCTGCCTTTCTGGATG  
GGCCTCGAGGGGTACAACCTCTACCGACTCGTGGTGGAGGTCTTTGGCACCTATG  
TCCCTGGCTACCTACTCAAGCTGAGCGCCATGGGCTGGGGCTTCCCATCTTTCT  
GGTGACGCTGGTGGCCCTGGTGGATGTGGACAACCTATGGCCCCATCATCTTGGCT  
GTGCATAGGACTCCAGAGGGCGTCATCTACCCTTCCATGTGCTGGATCCGGGACT  
CCCTGGTCAGCTACATACCAACCTGGGCCTCTTCAGCCTGGTGTCTTCTGTTCAA

CATGGCCATGCTAGCCACCATGGTGGTGCAGATCCTGCGGCTGCGCCCCACACC  
CAAAAGTGGTCACATGTGCTGACACTGCTGGGCCTCAGCCTGGTCCTTGGCCTGC  
CCTGGGCCTTGATCTTCTTCTCCTTTGCTTCTGGCACCTTCCAGCTTGTCTGCTCCT  
CTACCTTTTTCAGCATCATCACCTCCTTCCAAGGCTTCCATCTTCATCTGGTAC  
TGGTCCATGCGGCTGCAGGCCCGGGGTGGCCCCCTCCCCTCTGAAGAGCAACTCAG  
ACAGCGCCAGGCTCCCCATCAGCTCGGGCAGCACCTCGTCCAGCCGCATCGGCAG  
CAGCGGCgtcttcacactcgaagatttcggtggggactggcgacagacagccggc  
tacaacctggaccaagtccttgaacagggagggtgtgtccagtttgttcagaatc  
tcgggggtgtccgtaactccgatccaaaggattgtcctgagcggtgaaaatgggct  
gaagatcgacatccatgtcatcatcccgtatgaaggctctgagcggcgaccaaag  
ggccagatcgaaaaaatttttaaggtgggtgtaccctgtggatgatcatcacttta  
aggtgatcctgcactatggcacactggtaatcgacgggggttacgccgaacatgat  
cgactatttcggacggccgtatgaaggcatcgccgtgttcgacggcaaaaagatc  
actgtaacagggaccctgtggaacggcaacaaaattatcgacgagcgctgatca  
accccgacggctccctgctgttccgagtaacctcaacggagtgaccggctggcg  
gctgtgcaacgcattctggcgTAG

**kozak-ADGRG1-667-egfp:**

gccaccATGACTCCCCAGTCGCTGCTGCAGACGACACTGTTCCCTGCTGAGTCTGC  
TCTTCTGGTCCAAGGTGCCACGGCAGGGGCCACAGGGAAGACTTTCGCTTCTG  
CAGCCAGCGGAACCAGACACACAGGAGCAGCCTCCACTACAAACCCACACCAGAC  
CTGCGCATCTCCATCGAGAACTCCGAAGAGGCCCTCACAGTCCATGCCCTTTCC  
CTGCAGCCCACCCTGCTTCCCGATCCTTCCCTGACCCAGGGGCCTCTACCACTT  
CTGCCTCTACTGGAACCGACATGCTGGGAGATTACATCTTCTCTATGGCAAGCGT  
GACTTCTTGCTGAGTGACAAAGCCTCTAGCCTCCTCTGCTTCCAGCACCAGGAGG  
AGAGCCTGGCTCAGGGCCCCCGCTGTTAGCCACTTCTGTACCTCCTGGTGGAG  
CCCTCAGAACATCAGCCTGCCAGTGCCGCCAGCTTACCTTCTCCTTCCACAGT  
CCTCCCCACACGGCCGCTCACAATGCCTCGGTGGACATGTGCGAGCTCAAAGGG  
ACCTCCAGCTGCTCAGCCAGTTCCCTGAAGCATCCCCAGAAGGCCCTCAAGGAGGCC  
CTCGGCTGCCCCGCCAGCCAGCAGTTGCAGAGCCTGGAGTCGAAACTGACCTCT  
GTGAGATTATGGGGGACATGGTGTCTTTCGAGGAGGACCGGATCAACGCCACGG  
TGTGGAAGCTCCAGCCACAGCCGGCCTCCAGGACCTGCACATCCACTCCCGGCA  
GGAGGAGGAGCAGAGCGAGATCATGGAGTACTCGGTGCTGCTGCCTCGAACACTC  
TTCCAGAGGACGAAAGGCCCGGAGCGGGGAGGCTGAGAAGAGACTCCTCCTGGTGG  
ACTTCAGCAGCCAAGCCCTGTTCCAGGACAAGAATTCCAGCCACGTCTGGGTGA  
GAAGGTCTTGGGGATTGTGGTACAGAACACCAAAGTAGCCAACCTCACGGAGCCC  
GTGGTGCTCACCTTCCAGCACCAGCTACAGCCGAAGAATGTGACTCTGCAATGTG  
TGTTCTGGGTTGAAGACCCACATTGAGCAGCCCGGGGCATTGGAGCAGTGTGG  
GTGTGAGACCGTCAGGAGAGAAACCCAAACATCCTGCTTCTGCAACCACTTGACC  
TACTTTGCAGTGCTGATGGTCTCCTCGGTGGAGGTGGACGCCGTGCACAAGCACT  
ACCTGAGCCTCCTCTCCTACGTGGGCTGTGTCTGCTCTGCCCCTGGCCTGCCTTGT  
CACCATTGCCGCTACCTCTGCTCCAGGGTGCCCCCTGCCGTGCAGGAGGAAACCT

CGGGACTACACCATCAAGGTGCACATGAACCTGCTGCTGGCCGTCTTCCTGCTGG  
ACACGAGCTTCCTGCTCAGCGAGCCGGTGGCCCTGACAGGCTCTGAGGCTGGCTG  
CCGAGCCAGTGCCATCTTCCTGCACTTCTCCCTGCTCACCTGCCTTTCCTGGATG  
GGCCTCGAGGGGTACAACCTCTACCGACTCGTGGTGGAGGTCTTTGGCACCTATG  
TCCCTGGCTACCTACTCAAGCTGAGCGCCATGGGCTGGGGCTTCCCCATCTTTCT  
GGTGACGCTGGTGGCCCTGGTGGATGTGGACAACTATGGCCCCATCATCTTGGCT  
GTGCATAGGACTCCAGAGGGCGTCATCTACCCTTCCATGTGCTGGATCCGGGACT  
CCCTGGTCAGCTACATACCAACCTGGGCCTCTTCAGCCTGGTGTTCCTGTTCAA  
CATGGCCATGCTAGCCACCATGGTGGTGCAGATCCTGCGGCTGCGCCCCACACC  
CAAAGTGGTCACATGTGCTGACACTGCTGGGCCTCAGCCTGGTCTTGGCCTGC  
CCTGGGCCTTGATCTTCTTCTCCTTTGCTTCTGGCACCTTCCAGCTTGTGCTCCT  
CTACCTTTTCAGCATCATCACCTCCTTCCAAGGCTTCCCTCATCTTCATCTGGTAC  
TGGTCCATGCGGCTGCAGGCCGGGGTgtgagcaagggcgaggagctgttcaccg  
gggtggtgccccatcctggtcgagctggacggcgacgtaaaccggccacaagtccag  
cgtgtccggcgagggcgagggcgatgccacctacggcaagctgacctgaagttc  
atctgcaccaccggcaagctgcccgtgccctggcccaccctcgtgaccacctga  
cctacggcgtgcagtgttcagccgtaccccgaccacatgaagcagcagcactt  
cttcaagtccgcatgcccgaaggctacgtccaggagcgcaccatcttcttcaag  
gacgacggcaactacaagaccgcgcccaggtgaagttcgagggcgacaccctgg  
tgaaccgcatcgagctgaagggcatcgacttcaaggaggacggcaacatcctggg  
gcacaagctggagtacaactacaacagccacaacgtctatatcatggccgacaag  
cagaagaacggcatcaaggtgaacttcaagatccgccacaacatcgaggacggca  
gctgtcagctcgccgaccactaccagcagaacacccccatcggcgacggccccgt  
gctgctgcccgacaaccactacctgagcaccagtcctcaagcttagcaaagatccc  
aacgagaagcgcgatcacatggtcctgctggagttcgtgaccgcccggggatca  
ctctcggcatggacgagctgtacaagGGCCCCTCCCCTCTGAAGAGCAACTCAGA  
CAGCGCCAGGCTCCCCATCAGCTCGGGCAGCACCTCGTCCAGCCGCATCTAG

**kozak-ADGRG1-667-nluc:**

gccaccATGACTCCCCAGTCGCTGCTGCAGACGACACTGTTCCCTGCTGAGTCTGC  
TCTTCCTGGTCCAAGGTGCCACGGCAGGGGCCACAGGGAAGACTTTCGCTTCTG  
CAGCCAGCGGAACCAGACACACAGGAGCAGCCTCCACTACAAACCCACACCAGAC  
CTGCGCATCTCCATCGAGAACTCCGAAGAGGCCCTCACAGTCCATGCCCTTTCC  
CTGCAGCCCACCCTGCTTCCCGATCCTTCCCTGACCCCAGGGCCTCTACCACTT  
CTGCCTCTACTGGAACCGACATGCTGGGAGATTACATCTTCTCTATGGCAAGCGT  
GACTTCTTGCTGAGTGACAAAGCCTCTAGCCTCCTCTGCTTCCAGCACCAGGAGG  
AGAGCCTGGCTCAGGGCCCCCGCTGTTAGCCACTTCTGTCACCTCCTGGTGGAG  
CCCTCAGAACATCAGCCTGCCAGTGCCGCCAGCTTACCTTCTCCTTCCACAGT  
CCTCCCCACACGGCCGCTCACAATGCCTCGGTGGACATGTGCGAGCTCAAAAGGG  
ACCTCCAGCTGCTCAGCCAGTTCCTGAAGCATCCCCAGAAGGCCTCAAGGAGGCC  
CTCGGCTGCCCCCGCCAGCCAGCAGTTGCAGAGCCTGGAGTCGAACTGACCTCT  
GTGAGATTCATGGGGGACATGGTGTCTTCGAGGAGGACCGGATCAACGCCACGG

TGTGGAAGCTCCAGCCCACAGCCGGCCTCCAGGACCTGCACATCCACTCCCGGCA  
GGAGGAGGAGCAGAGCGAGATCATGGAGTACTCGGTGCTGCTGCCTCGAACACTC  
TTCCAGAGGACGAAAGGCCGGAGCGGGGAGGCTGAGAAGAGACTCCTCCTGGTGG  
ACTTCAGCAGCCAAGCCCTGTTCCAGGACAAGAATTCCAGCCACGTCTGGGTGA  
GAAGGTCTTGGGGATTGTGGTACAGAACACCAAAGTAGCCAACCTCACGGAGCCC  
GTGGTGCTCACCTTCCAGCACCAGCTACAGCCGAAGAATGTGACTCTGCAATGTG  
TGTTCTGGGTGAAGACCCACATTGAGCAGCCCGGGGCATTGGAGCAGTGCTGG  
GTGTGAGACCGTCAGGAGAGAAACCCAAACATCCTGCTTCTGCAACCACTTGACC  
TACTTTGCAGTGCTGATGGTCTCCTCGGTGGAGGTGGACGCCGTGCACAAGCACT  
ACCTGAGCCTCCTCTCCTACGTGGGCTGTGTGCTCTCTGCCCTGGCCTGCCTTGT  
CACCATTGCCGCCTACCTCTGCTCCAGGGTGCCCTGCCGTGCAGGAGGAAACCT  
CGGGACTACACCATCAAGGTGCACATGAACCTGCTGCTGGCCGTCTTCCCTGCTGG  
ACACGAGCTTCTGCTCAGCGAGCCGGTGGCCCTGACAGGCTCTGAGGCTGGCTG  
CCGAGCCAGTGCCATCTTCTGCACTTCTCCCTGCTCACCTGCCTTTCTGGATG  
GGCCTCGAGGGGTACAACCTCTACCGACTCGTGGTGGAGGTCTTTGGCACCTATG  
TCCCTGGCTACCTACTCAAGCTGAGCGCCATGGGCTGGGGCTTCCCCATCTTTCT  
GGTGACGCTGGTGGCCCTGGTGGATGTGGACAACTATGGCCCCATCATCTTGGCT  
GTGCATAGGACTCCAGAGGGCGTCATCTACCCTTCCATGTGCTGGATCCGGGACT  
CCCTGGTCAGCTACATACCAACCTGGGCCTCTTCAGCCTGGTGTCTTCTGTTCAA  
CATGGCCATGCTAGCCACCATGGTGGTGCAGATCCTGCGGCTGCGCCCCACACC  
CAAAGTGGTCACATGTGCTGACACTGCTGGGCCTCAGCCTGGTCCTTGGCCTGC  
CCTGGGCCTTGATCTTCTTCTCCTTTGCTTCTGGCACCTTCCAGCTTGTGCTCCT  
CTACCTTTTCAGCATCATCACCTCCTTCCAAGGCTTCTCATCTTCATCTGGTAC  
TGGTCCATGCGGCTGCAGGCCCGGGTgtcttcacactcgaagatttcggtggg  
actggcgacagacagccggctacaacctggaccaagtccttgaacagggaggtgt  
gtccagtttgtttcagaatctcggggtgtccgtaactccgatccaaaggattgtc  
ctgagcggtgaaaatgggctgaagatcgacatccatgtcatcatcccgtatgaag  
gtctgagcggcgaccaaagtggccagatcgaaaaatttttaaggtgggtgtacc  
tgtggatgatcatcactttaaggtgatcctgcactatggcacactggtaatcgac  
ggggttacgccgaacatgatcgactatctcgacggccggtatgaaggcatcgccg  
tgttcgacggcaaaaagatcactgtaacagggaccctgtggaacggcaaaaaat  
tatcgacgagcgcctgatcaaccccgacggctccctgctgttccgagtaaccatc  
aacggagtgaccggctggcggctgtgcaaacgcattctggcgGGCCCTCCCTC  
TGAAGAGCAACTCAGACAGCGCCAGGCTCCCCATCAGCTCGGGCAGCACCTCGTC  
CAGCCGCATCTAG